Experimental investigation and thermodynamic evaluation of the CsNO3-LiNO3-NaNO3 ternary system

Edouard Koffi Kouassi, Max Wedjers Manouan, Eulogne Zoro, David Boa, Pierre Benigni, Hmida Zamali, Jacques Rogez, Dalila Hellali

▶ **To cite this version:**

Edouard Koffi Kouassi, Max Wedjers Manouan, Eulogne Zoro, David Boa, Pierre Benigni, et al.. Experimental investigation and thermodynamic evaluation of the CsNO3-LiNO3-NaNO3 ternary system. Journal of Alloys and Compounds, 2021, 864, pp.158131. 10.1016/j.jallcom.2020.158131 . hal-03117360

HAL Id: hal-03117360
https://hal.science/hal-03117360

Submitted on 8 Mar 2022

HAL is a multi-disciplinary open access archive for the deposit and dissemination of scientific research documents, whether they are published or not. The documents may come from teaching and research institutions in France or abroad, or from public or private research centers.

L'archive ouverte pluridisciplinaire **HAL**, est destinée au dépôt et à la diffusion de documents scientifiques de niveau recherche, publiés ou non, émanant des établissements d'enseignement et de recherche français ou étrangers, des laboratoires publics ou privés.

Distributed under a Creative Commons Attribution - NonCommercial - NoDerivatives 4.0 International License

Experimental investigation and thermodynamic evaluation of the $CsNO_3$-$LiNO_3$-$NaNO_3$ ternary system

Edouard Koffi Kouassi[a], Max Wedjers Manouan[a,b], Eulogne Zoro[c], David Boa[a], Pierre Benigni[d], Hmida Zamali[e], Jacques Rogez[d], Dalila Hellali[e,*]

[a]*Université Nangui Abrogoua, UFR SFA, Laboratoire de Thermodynamique et de Physico-Chimie du Milieu, 02 BP 801 Abidjan 02, Côte d'Ivoire*
[b]*Université de Man, UFR ST, BP 20 Man, Côte d'Ivoire*
[c]*Ecole Normale Supérieure d'Abidjan, 08 BP 10 Abidjan 08, Côte d'Ivoire*
[d]*Aix Marseille Univ., Univ. Toulon, CNRS, IM2NP Marseille, France*
[e]*Université de Tunis El Manar, Faculté des Sciences de Tunis, LR15ES01 Laboratoire de Matériaux, Cristallochimie et Thermodynamique Appliquée, 2092, Tunis, Tunisie*

Abstract

The alkali nitrate mixtures are promising phase change materials (PCMs) in the temperature range (373-573) K for the development of thermal storage systems. In this context, their thermochemical properties and phase diagrams which provide useful thermal information are needed for their better use. In the present paper, the mixtures based on cesium nitrate, lithium nitrate, and sodium nitrate are studied by both experimental and optimization techniques. Thus, a critical analysis of thermodynamic data from literature sources of the phases in the $CsNO_3$-$LiNO_3$-$NaNO_3$ ternary system including the pure components is performed. Therefore, reliable phase change data (enthalpy and temperature) of pure nitrates $CsNO_3$, $LiNO_3$ and $NaNO_3$ are proposed. In addition, by means of differential thermal analysis (DTA), the binary $CsNO_3$-$LiNO_3$ system and two vertical sections (X_{CsNO_3} / X_{LiNO_3} = 1 and X_{NaNO_3} = 0.2) in the ternary $CsNO_3$-$LiNO_3$-$NaNO_3$ system are investigated. X-ray diffraction (XRD) technique is also used to analyze phases in the $CsNO_3$-$LiNO_3$ binary system at room temperature.

The $CsNO_3$-$LiNO_3$ binary system is characterized by a congruent equimolar compound $Cs_{0.5}Li_{0.5}NO_3$ which appears at (334 ± 2) K. Two eutectic reactions are found at (445 ± 2) K and (435 ± 2) K, respectively. The system exhibits also a plateau at (427 ± 2) K corresponding to the polymorphic transition of $CsNO_3$. The $CsNO_3$-$LiNO_3$-$NaNO_3$ ternary system shows two ternary eutectic reactions at (408 ± 2) K and (405 ± 2) K, respectively. Combining our results with experimental data available in the literature, an optimization of the thermodynamic parameters in the ternary system is performed with the help of Calphad approach. A reasonable agreement between the calculated results and the experimental data is obtained.

***Keywords*:** Phase diagram; DTA; XRD; Calphad; $CsNO_3$-$LiNO_3$-$NaNO_3$ ternary system.

*Corresponding author : Dalila HELLALI
E-mail address: dalilahlali@hotmail.fr

1. Introduction

Energy storage is a key element to improve the efficiency of thermal energy utilization in various branches of the industry (construction, electronic, biomedical, textile, automotive, etc.), as it allows the decoupling between production and demand of energy. In applications with intermittent energy generation, such as solar thermal systems or waste heat recovery, an appropriate thermal storage system is essential [1]. Among the different modes of thermal energy storage, latent heat storage (LHS) is particularly attractive due to the high energy storage density with a possible isothermal operation, lower costs and compactness [2-4]. LHS uses phase change materials (PCMs) as heat storage medium which absorb and release energy through phase change transitions at constant temperature [5-14]. According to the working temperature, PCMs can be divided into low temperature, medium temperature and high temperature. The temperature range associated to each group can vary depending on the applications [2, 13, 15-19]. It has been pointed out that PCMs with a melting temperature between 393 K and 573 K are of great interest in the industrial and domestic applications of solar thermal energy (drying, cooling, distillation, etc.) [17, 20, 21]. Because alkali nitrates seem to be potential solid-liquid PCMs in the temperature range (373-573) K [22], we have undertaken, for some years now, the development of multicomponent nitrate mixtures based on $NaNO_3$ which has been found as a proper PCM with respect to its heat of fusion and corrosiveness [23-25]. The purpose of our studies is to access the composition of mixtures having a lower congruent melting temperature ($T < 573$ K) through the phase diagram study.

One of the systems that draw our attention is the $AgNO_3$-$CsNO_3$-$LiNO_3$-$NaNO_3$ quaternary system. It is worth noting that the phase diagram determination of a multicomponent system based only on experimental methods is time consuming and expensive. Therefore, the prediction work using the numerical method along with the available data of lower order systems, becomes a necessity.

Except for $CsNO_3$-$LiNO_3$ system, all limiting binary systems of the $AgNO_3$-$CsNO_3$-$LiNO_3$-$NaNO_3$ quaternary system have been assessed thermodynamically and the parameters describing the Gibbs energy of all binary phases are well-known [23-26]. Two of the four ternary sub-systems of the quaternary system have been already evaluated in our previous works: $AgNO_3$-$LiNO_3$-$NaNO_3$ [23, 24] and $AgNO_3$-$CsNO_3$-$NaNO_3$ [25]. But up to now, no

thermodynamic modeling of the remaining two ($AgNO_3$-$CsNO_3$-$LiNO_3$ and $CsNO_3$-$LiNO_3$-$NaNO_3$) is available.

As a part of the investigation of the $AgNO_3$-$CsNO_3$-$LiNO_3$-$NaNO_3$ quaternary system, the present work is devoted to the thermodynamic evaluation of the $CsNO_3$-$LiNO_3$-$NaNO_3$ system. The main purpose is to provide the Gibbs free energy parameters of all the phases using Calphad method which has three keywords: critical review, modelisation and optimization. For a better understanding of phase equilibria in the $CsNO_3$-$LiNO_3$ and $CsNO_3$-$LiNO_3$-$NaNO_3$ systems especially at low temperature (298 K < T < 350 K), an experimental investigation was undertaken using X-ray diffraction and differential thermal analysis.

2. Critical review of literature information

2.1 General aspects

Since the 19th-century, the thermodynamic properties especially phase change properties of pure nitrates $CsNO_3$, $LiNO_3$, $NaNO_3$ and their mixtures have been reported by several authors. Most of data were reviewed, evaluated and compiled in many handbooks and publications [27-39]. Though these databanks provide easily useful data for different applications whether practically or in simulation techniques, sometimes they need to be updated taking into account new information. In the present work, a new critical review is proposed as an actualization of previous compilations. This task is based on a thermodynamic analysis associated to statistical evaluation.

The thermodynamic analysis is focused on salt sample characteristics (purity, mass, etc.) and experimental methods (apparatus, procedures, conditions, etc.) which are the two major elements affecting measurements. Phase change properties of salts can be investigated by different experimental methods. But, the most commonly techniques used are differential scanning calorimetry (DSC) and differential thermal analysis (DTA) which are recognized as the most accurate methods [7, 40-45]. However, some conditions must be fulfilled to get reliable data. For example, the phase transition process is affected by the combination of sample mass and heating rate [45, 46]. It was also showed that impurities of a sample affect the value of its thermochemical properties [40, 47, 48]. In addition, a good calibration of a device can be a guarantee for accurate measurements [49, 50]. When thermal properties of salts are measured, an appropriate crucible should be considered [40, 51, 52], and so on. Apart from experimental operations, the way the transition temperature and the latent heat are determined from DTA or DSC curves can be one of the greatest sources of error. Generally,

the temperature of the thermal effect is defined as the onset temperature *i.e*. the intersection point of the tangent from start edge inflexion point and the baseline [53]. Regarding the latent heat of transition, the challenge is the choice of an initial and final temperature marking before integrating the peak [54].

The statistical analysis is performed, in the present work, to define the scattering of data. For the statistical significance determination, one-way ANOVA (Analysis of Variance) is used (95% confidence level). When the ANOVA produces a statistically significant test, Duncan post-hoc test is carried out. At this stage, the uncertainty of the different measurements is a crucial parameter. Unfortunately, some of original papers do not report uncertainty. In this case, the highest value of uncertainty of different bibliographic sources is taken. All statistical analyses are made with IBM SPSS version 22 software.

Finally, it is important to notice that when data go through critical evaluation, the use of the original values is recommended in order to avoid propagation of errors. Thereby, smoothed numerical values and data from compilations (handbooks) are not taken into account.

2.2 Pure nitrates

2.2.1 Cesium nitrate ($CsNO_3$)

Most of $CsNO_3$ crystallographic data obtained prior to 1974 were compiled by Rao et al. [55]. They showed that $CsNO_3$ exhibits, between room temperature and its melting temperature, two stable crystalline forms at normal pressure. The low temperature form (phase II) is hexagonal $P3_1m$ with a = 10.87 Å and c = 7.76 Å. At high temperature, $CsNO_3$ has a cubic structure (phase I) with a = 4.499 Å. Results of later works [56-62] are in agreement with the number of crystallographic forms of $CsNO_3$ [55]. However the cell parameters and space groups are a little bit different from those reported by Rao et al. [55]. The recent paper of Somov et al. [63] pointed out a new $CsNO_3$ low temperature structure (monoclinic) with space group $P2_1/c$ and lattice parameters : a = 4.5699(9) Å, b = 11.1871(10) Å, c = 9.1484(18) Å, β = 131.24(3)°. This allotropic form, stable at room temperature, was prepared by crystallization of a mixture of water and dimethylsulfoxide C_2H_6OS (DMSO).

2.2.1.1 Heat capacity

• *Low-temperature phase: $CsNO_3$ (II)*

Low temperature heat capacity of $CsNO_3$ has been determined by different authors [32, 64-68]. All data are gathered in the same plot (Fig. 1a). Fig.1b presents an enlargement in the temperature range (300 – 425) K. The experimental techniques and relative uncertainties are given in brackets.

The scattering of the experimental data is within ± 3%, except for the results of Maeso and Largo [68]. Data of these authors, obtained by DSC, are about 6% lower than those of Jriri et al. [32] determined by the same method. As stated above, DSC is among the more suitable methods to determine heat capacity, but accurate measurements depend on several factors. The data of Jriri et al. [32] are considered as more reliable because a great care was taken during their experiments to overcome most of practical challenges (calibrations, heat capacity of the empty calorimeter, sample purity and masses, oxidation and corrosion of interior of the calorimeter, etc.). Therefore, heat capacity obtained by Maeso and Largo [68] is rejected. On the other hand, one can notice that the data of Flotow et al. [66] extrapolated from low temperature are consistent with those of Jriri et al. [32].

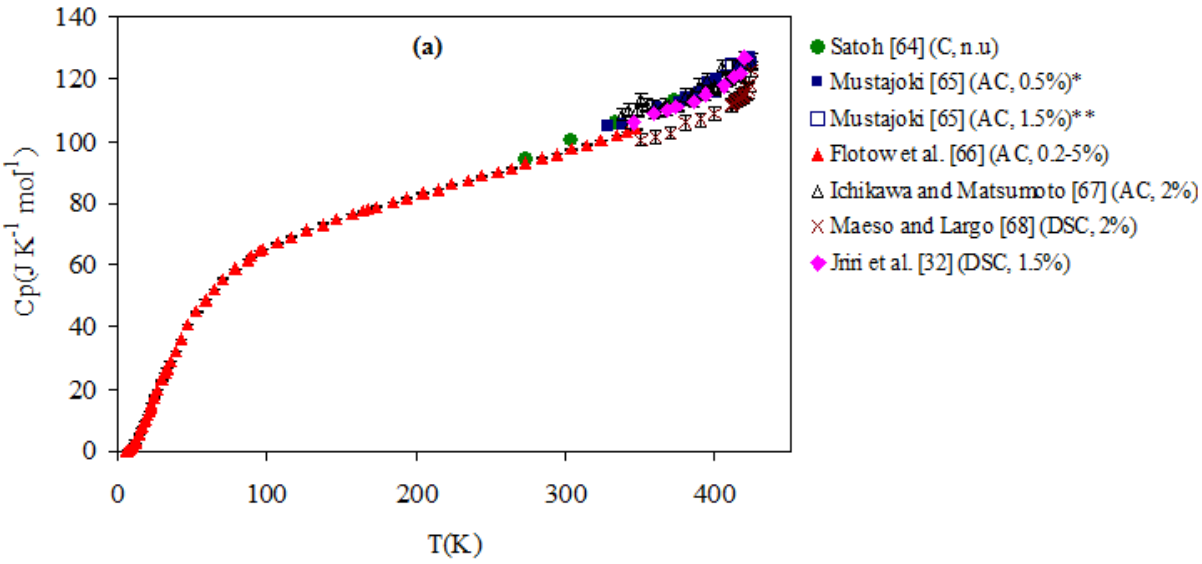

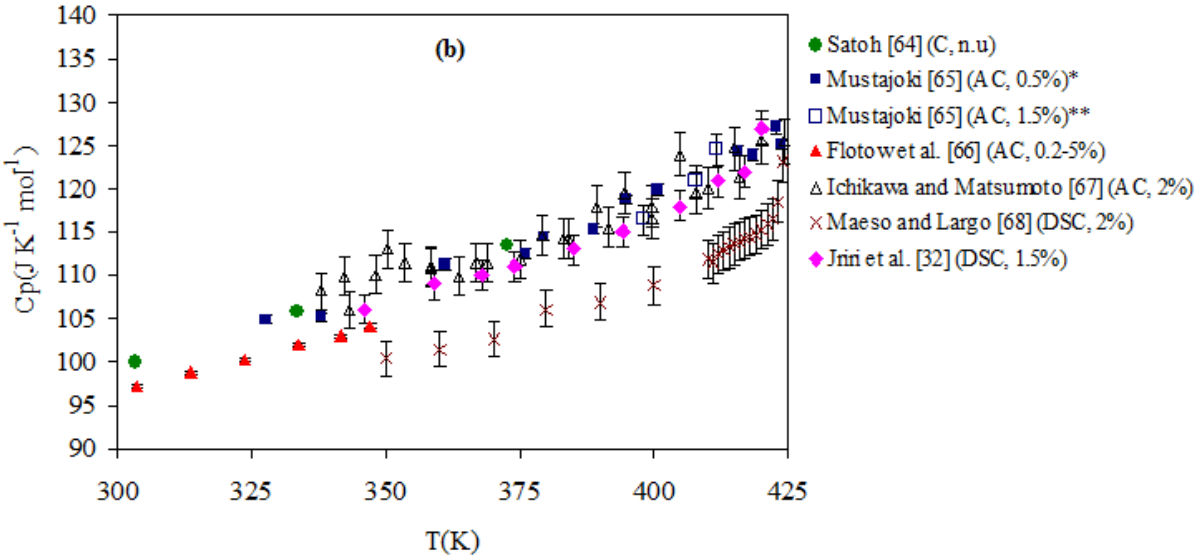

Fig. 1. Temperature dependence of the molar heat capacity of $CsNO_3$ (II) from different sources. (a) Temperature range (0 - 425) K. (b) Enlargement in the temperature range (300 – 425) K. Error bars represent the experimental uncertainties on Cp.
C : Calorimetry ; AC : Adiabatic Calorimetry ; DSC : Differential Scanning Calorimetry ; *Data obtained on heating ; **Data obtained on cooling ; n.u. : no uncertainty mentioned.

• *High-temperature phase: $CsNO_3$ (I)*

High-temperature heat capacities of $CsNO_3$ collected from literature data [32, 64, 65, 67, 68] are presented in Fig. 2. As it can be seen, the values of Ichikawa and Matsumoto [67] obtained by adiabatic calorimetry, agree satisfactorily with those of Jriri et al. [32] determined by DSC. The results found by Mustajoki [65] using an adiabatic calorimetric method, are also in agreement, in the temperature range (450 – 550) K, with these two sets of data [32, 67]. However, for T > 550 K, Mustajoki [65] reported higher values. For example, between 660 K and 680 K, the difference between his data and the above two sets of data is about 10%. The fact that the heat capacity increases drastically with an increase in the temperature may be attributed to a phase transition. As for $CsNO_3$ (II), the DSC results published by Maeso and Largo [68] are the lowest data in the temperature range (430 – 610) K. The heat capacity of $CsNO_3$ (I) determined by Satoh [64], using an ice calorimetric technique, is abnormally high compared to the other literature data. For lack of more experimental information, his data are considered inaccurate.

Based on sample characteristics and calorimeter operation, it is worthy to consider the data of Ichikawa and Matsumoto [67] and those of Jriri et al. [32] as the most reliable with uncertainty of ±2%.

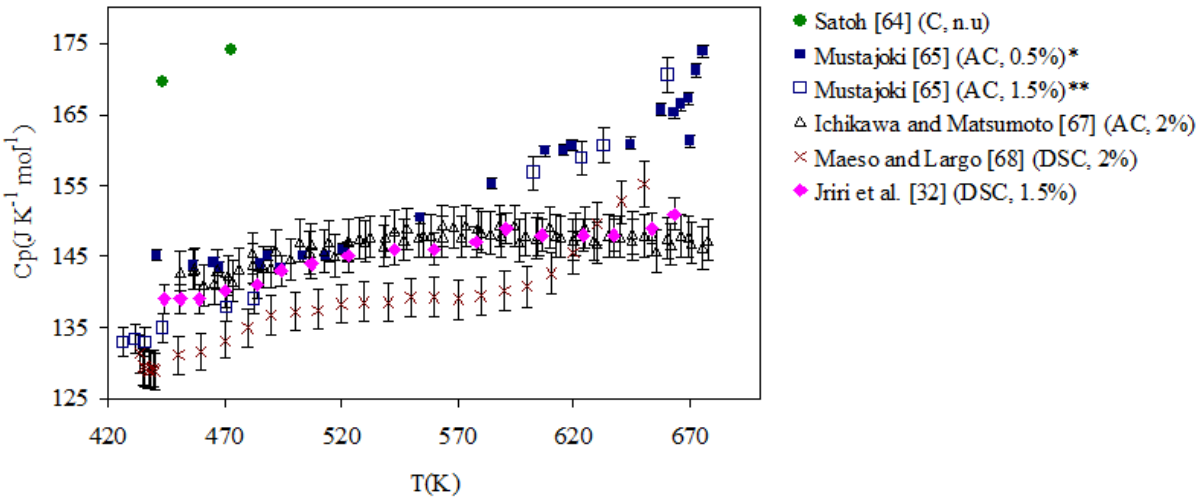

Fig. 2. Temperature dependence of the molar heat capacity of $CsNO_3$ (I) from different sources in the temperature range (425 – 678) K. Error bars represent the experimental uncertainties on Cp.
C : Calorimetry ; AC : Adiabatic Calorimetry ; DSC : Differential Scanning Calorimetry ; *Data obtained on heating ; **Data obtained on cooling ; n.u. : no uncertainty mentioned.

• *Liquid phase*

The heat capacities of $CsNO_3$ liquid phase from different authors [32, 65, 67, 68] are presented in Fig. 3. There is some scatter in the data. However, results obtained by Ichikawa and Matsumoto [67] and by Jriri et al. [32] agree satisfactorily within experimental uncertainties. The discrepancy between the data of Jriri et al. [32] and those of Maeso and Largo [68] who used the same experimental technique (DSC) is of the order of 26%. Maeso and Largo [68] have the highest values in contrast to those of the solid phases. The data of Mustajoki [65] are about 10% lower compared to those of Maeso and Largo [68] and about 18% higher than the data of Ichikawa and Matsumoto [67] and Jriri et al. [32].

For the reasons mentioned above, the data of Ichikawa and Matsumoto [65] and those of Jriri et al. [32] are considered as the most reliable with uncertainty of ±2%.

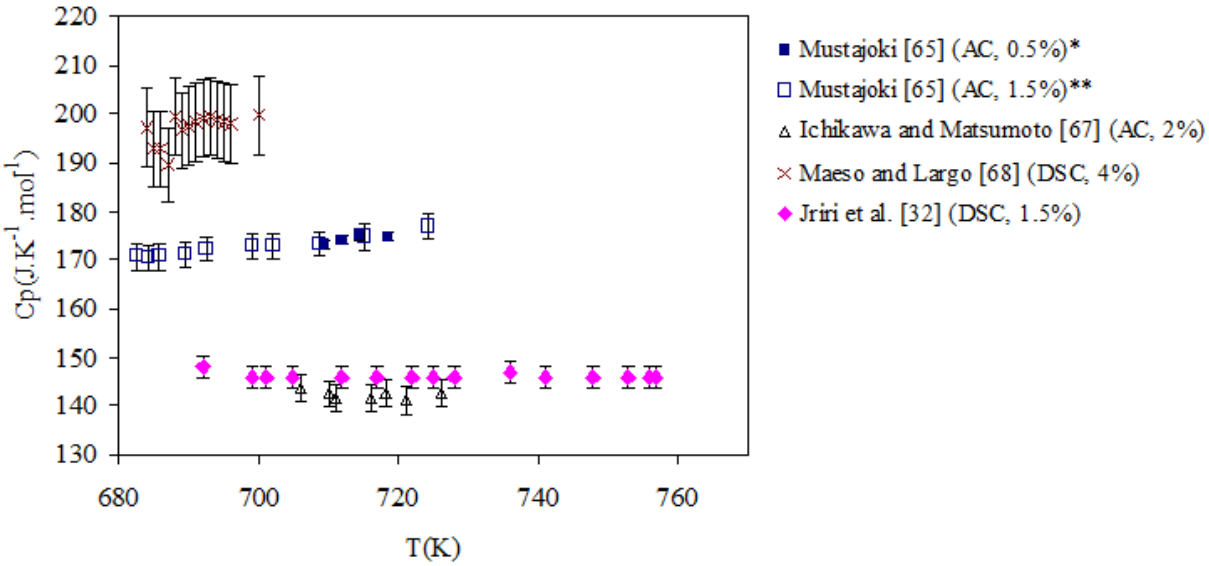

Fig. 3. Temperature dependence of the molar heat capacity of $CsNO_3$ liquid phase (T > 678 K) from different sources. Error bars represent the experimental uncertainties on Cp.
C: Calorimetry; AC: Adiabatic Calorimetry; DSC: Differential Scanning Calorimetry; *Data obtained on heating; **Data obtained on cooling.

2.2.1.2 Temperature and enthalpy of phase changes (solid-solid transition, melting)

Thermochemical properties (enthalpy and temperature) of solid-solid transition and melting of $CsNO_3$ have been reported by many authors [32, 38, 49, 60, 65-90]. The data gathered during the present work are presented in Table 1 altogether with the experimental techniques and the sample characteristics (purity and treatment before the use).

The data have been classified into four groups based on the used experimental method: (i) DSC (Differential Scanning Calorimetry); (ii) STA/DTA (Simultaneous Simple or Direct and Differential Thermal Analysis); (iii) Other calorimetry (e.g., drop calorimetry, adiabatic calorimetry, near adiabatic, and dissolution calorimetry); (iv) Chemical analysis and all other methods (e.g., electrochemical measurement, mixing method, volume discontinuity method, XRD, XPS, EMF, Raman spectroscopy).

• *Solid-solid transition temperature ($T_{II/I}$)*

The solid-solid transition temperatures ($T_{II/I}$) of $CsNO_3$ compiled from literature lie in the (423 – 434) K range [32, 38, 49, 60, 65-73, 77-79, 83-89] with a maximum uncertainty of ±2 K. The differences between values are statistically significant. Therefore, the Duncan post-hoc test is carried out to see where differences between values occur. The post-hoc test leads to five homogeneous subsets. The higher value (434 K) of Gordon and Campbell [70] stands alone, this means that “434 K” is significantly different from all the other temperature values. As mentioned in their paper, many experimental factors such as heating rate, geometry of

apparatus and especially the type of recording system influence the appearance of the DTA curves. DTA curves obtained by Gordon and Campbell [70] are not enough accurate. So, it seems justified to cast some doubts about the reliability of this transition temperature value. The lower value (423 K) obtained by Fermor and Kjekshus [78] using electrical measurements is questionable due to the limitations of the technique used. Indeed, this temperature determined from the curve of resistivity versus inverse of absolute temperature may be underestimated. For example, in their same work, a value of 425 K for $T_{II/I}$ is obtained from the curve of dielectric constant versus temperature on heating. The Duncan test without the result of Gordon and Campbell [70] and that of Fermor and Kjekshus [78] leads to three homogeneous subsets. Two values are considered to be problematic: 430.35 K (Ichikawa and Matsumoto [67], AC) and (424±1) K (Zamali and Jemal [83], DTA).

Ichikawa and Matsumoto [67] used a Pt-Rh thermocouple for the temperature measurements. This thermocouple was calibrated by a cryoscopic method for pure-grade recrystallized reagents KNO_3, K_2SO_4, Ag_2SO_4 and $KClO_4$. Although, the solid-solid transition temperature recorded for KNO_3 (402.95 K) seems reliable [32, 83], that obtained under the same experimental conditions for $RbNO_3$ (439.45 K, first solid-solid phase transition) is higher at least 2 K than most of published data [39]. Therefore, the solid-solid transition temperature of $CsNO_3$ obtained by Ichikawa and Matsumoto [67] may be considered as high.

The II/I phase transition temperature obtained by Zamali and Jemal [83] is lower than all those determined with the same method (DTA). Their value which was neither confirmed in the works from the same laboratory [84-86, 88, 89] is looked as less reliable. The data of Mustajoki [65] similar to that of Zamali and Jemal [83] is also considered as less reliable. The data of Chary et al. [60] and Bakes et al. [73] are ignored because of lack of information about the purity of salts used.

Finally, 7 [60, 65, 67, 70, 73, 78, 83] of the 24 determinations are rejected. Although two homogeneous subsets are obtained, the differences between the measurements are not statistically significant (*p-value* = 0.447 > 0.05). The mean value of 427.2735 K and standard deviation equal to 2.0113 K comparable to experimental uncertainty, are obtained.

The statistic analysis of solid-solid transition temperature of $CsNO_3$, which is an example for all other statistical analyses, is repoted in *Supplementary data section*.

Fig. 4 represents the mean value of solid-solid transition temperature with the experimental results collected from literature. Apart from the experimental values of Ichikawa

and Matsumoto [67] ((430.35±0.1) K), Gordon and Campbell [70] ((434±1) K) and, Fermor and Kjekshus [78] (423 K), all other published values are acceptable within the maximum experimental uncertainty of ±2 K. However, it is important to notice that the values of Zamali and Jemal [83] (424±1) K and Mustajoki [65] (424.5 K) are very close to the lower limit of acceptable values. Taking into account the experimental uncertainty, these values may be considered as acceptable.

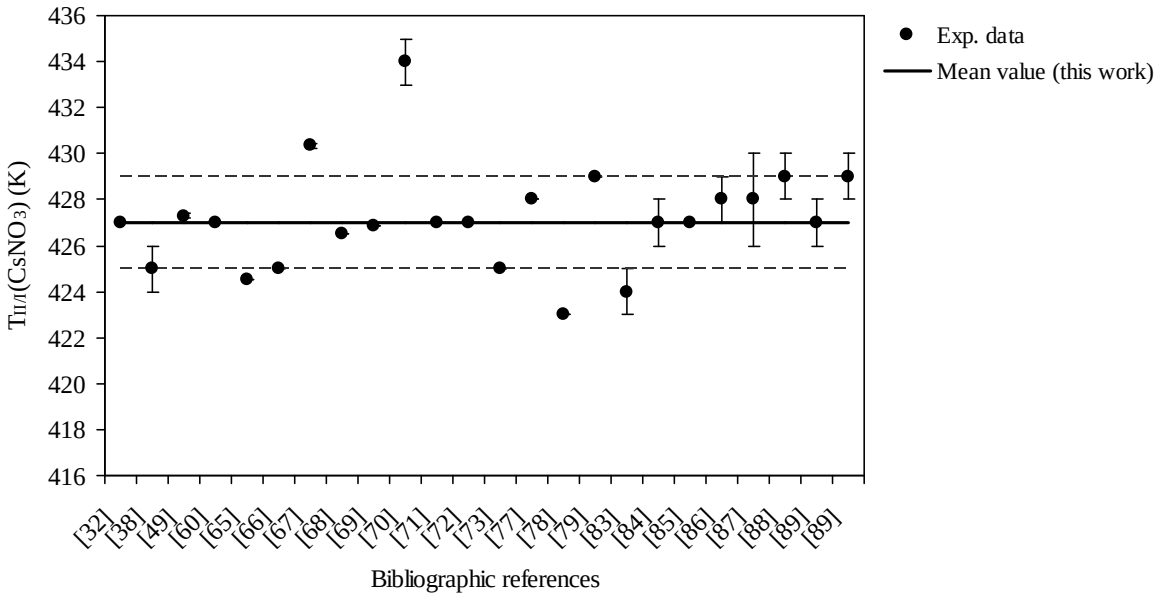

Fig. 4. Experimental solid-solid transition temperature of $CsNO_3$ from different sources compared with the mean value (this work). Error bars represent experimental uncertainties. Acceptable values are inside dashed lines.

Considering all acceptable data, the mean value is recalculated and the recommended value for the solid-solid transition temperature of $CsNO_3$ proposed in this work is (427±2) K.

• *Melting temperature (T_m)*

The compiled melting temperatures (T_m) of $CsNO_3$ vary from 677 K to 690 K [32, 38, 65-68, 70-76, 79-81, 83-90] with an experimental uncertainty of about ±2 K. Only Owens [76] claimed an uncertainty of ±5 K. Using volume discontinuity method, he found a melting temperature of 683 K. The temperature measurement was done with Chromel-Alumel thermocouple. For this type of thermocouple, the uncertainty does not exceed ±2.2 K [91]. So, the uncertainty obtained by Owens [76] is considered as very high. Due to less accurate experimental method used, the melting temperature proposed by Owens [76] is considered less reliable. The data of Bakes et al. [73], Diogenov and Sarapulova [75], and Shenkin [81]

are rejected because of lack of information about the purity of salts used. During the present analysis, an uncertainty of ±2 K is retained.

The 20 of the 25 determinations tested are statistically different. The post-hoc test leads to 4 homogeneous subsets.

Two values are totally incompatible: 690 K [74] and 677 K [38, 70, 72, 80]. The higher value (690 K) obtained by Kleppa and McCarty [74] using high-temperature reaction calorimetry can raise reasonable doubts. Indeed, the experimental method used is not accurate enough compared to DSC and ATD. For the same reason, the value of Plyuschev et al. [71] (687 K) is rejected.

By not considering the value of Kleppa and McCarty [74] and that of Plyuschev et al. [71], the subsets move from 4 to 2. The temperature determined by Ichikawa and Matsumoto [67] (684.85 K) stands alone. The melting temperature obtained under the same experimental conditions for $LiNO_3$ (529.65 K), $NaNO_3$ (583.35 K) and KNO_3 (609.45 K) [67] are higher than most of published data [32, 39]. Therefore, as already mentioned, the results of Ichikawa and Matsumoto [67] seem to be systematically high. The new statistical analysis taking into account 17 of the 25 experimental results shows that the values of 683 K [84, 86, 87] and 677 K [38, 70, 72, 80] are incompatible.

The melting temperature determined by Secco and Secco (683 K) [87] using DSC method is slightly higher than all those obtained by the same technique [32, 38, 68, 79, 89]. Though the method is accurate, some reasonable doubts may be exist about their value. Indeed, the melting temperature obtained under the same experimental conditions for $TlNO_3$ (483.15 K) [87] are higher than most of published data [89] obtained by DSC method. On the other hand, Bélaïd-Drira et al. [84, 86] obtained a slightly higher value of melting temperature of $CsNO_3$ (683 K) than that of Abdessattar et al. ((681±1) K) [89], although they worked under similar experimental conditions. The higher value, (683±1) K, seems less reliable.

Finally, 11 of the 25 determinations were rejected [67, 70, 73-76, 84, 86-88, 90]. The differences between the results considered are not statistically significant. One homogeneous subset is obtained with the mean value of 678.4500 K and standard deviation (SD) equal to 2.0894 K comparable to experimental uncertainty.

Comparison between the mean value for the melting temperature of $CsNO_3$ and the all experimental results is presented in Fig.5. One can notice that the results of Bélaïd-Drira et al. [84, 86] ((683±1) K), Secco and Secco [87] ((683±2) K) and Wacharine et al. [88] ((682±1) K), are consistent with each other and are just above the upper limit of acceptable values. The

data of Ichikawa and Matsumoto [67] ((684.85±0.10) K), Plyuschev et al. [71] (687 K), Kleppa and McCarty [74] (690 K) and Shenkin [81] (690 K) are far from the upper limit of acceptable values.

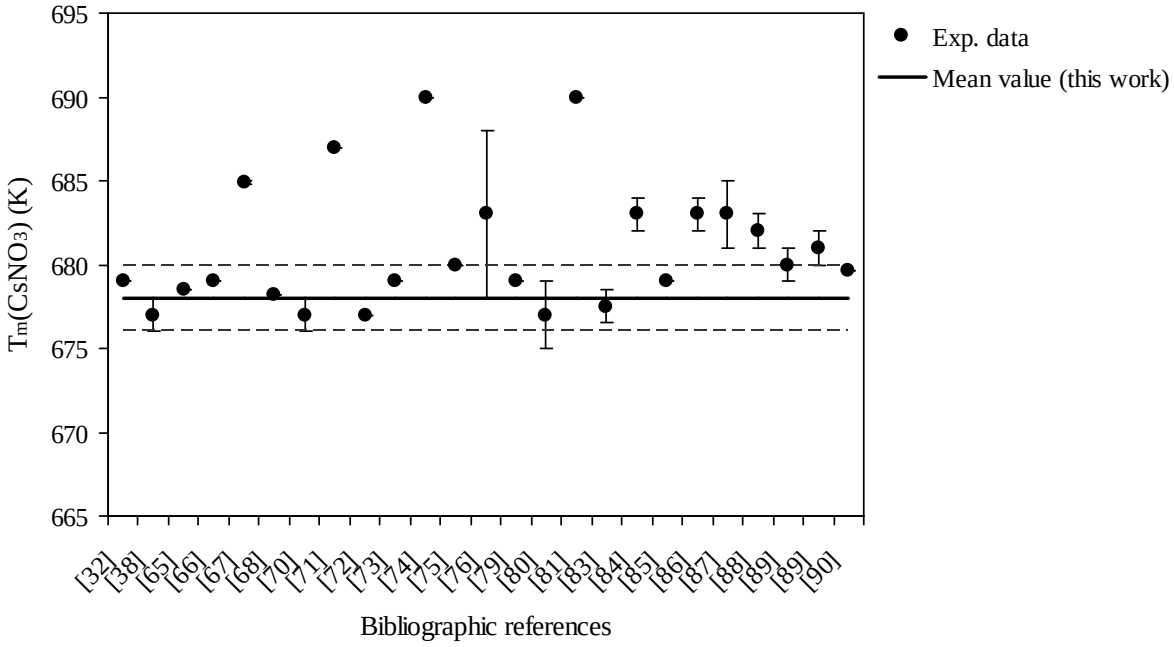

Fig. 5. Experimental melting temperature of $CsNO_3$ from different sources compared with the mean value (this work). Error bars represent experimental uncertainties. Acceptable values are inside dashed lines.

Considering all acceptable data, the mean value is recalculated and the recommended value for the melting temperature of $CsNO_3$ proposed in this work is (678±1) K.

• *Solid-solid transition enthalpy (*$\Delta_{II/I}H°$)

The values of solid-solid transition enthalpy of $CsNO_3$ *(*$\Delta_{II/I}H°$) collected from different sources are between 1464 J mol^{-1} and 5020 J mol^{-1} [32, 38, 49, 65, 68, 69, 77, 79, 87, 89]. The higher value found by Marchidan and Vasu [79] (5020 J mol^{-1}) using DSC method seems less reliable and is not taken into account in the present analysis. Indeed, this value is about 30% higher than the mean value of all data obtained by the same experimental method. Using DTA technique, Rao and Rao [77] gave the lowest value of solid-solid transition enthalpy (1464.4 J mol^{-1}) with a high uncertainty (±15%). They prepared $CsNO_3$ from the corresponding carbonate (Cs_2CO_3, analytical grade), but no details were given about the process or the purity. Impurities in the salt can explain the lower value of enthalpy. In addition, no indication was given about the working atmosphere (gas used) which is important

to protect salt from any pollution or contamination. Doubts about the reliability of the value may be raised. Therefore, the solid-solid enthalpy of Rao and Rao [77] is rejected.

Considering a maximum uncertainty of ±5%, it is found that the differences between the remaining values (8 of the 10 determinations) are statistically significant. The post-hoc test shows 2 homogeneous subsets. The value of Maeso and Largo [68] (3800 J mol^{-1}) and that of Secco and Secco [87] (3050 J mol^{-1}) are questioned. Both were obtained by DSC method. The data of Maeso and Largo [68] is the highest, while the value of Secco and Secco [87] is the lowest. Their data are not considered as reliable because of some deficiencies already identified in their works. The enthalpy given by Mustajoki [65] similar to that of Maeso and Largo [68] is also rejected. The remaining five data [32, 38, 49, 69, 89] lead to one homogeneous subset with the mean value of 3412.0000 J mol^{-1} and standard deviation equal to 153.8331 J mol^{-1}. This standard deviation corresponds to a relative uncertainty of 4.5 %.

Fig. 6 shows the comparison of the mean value with the published data. Solid-solid transition enthalpies published by Maeso and Largo [68] (3800 J mol^{-1}) and, Secco and Secco [87] ((3050±5%) J mol^{-1}) are close to the upper and lower limits of acceptable values, respectively. However, those mentioned by Rao and Rao [77] ((1464.4 ± 15%) J mol^{-1}) and, Marchidan and Vasu [79] (5020 J mol^{-1}) are very far from these limits.

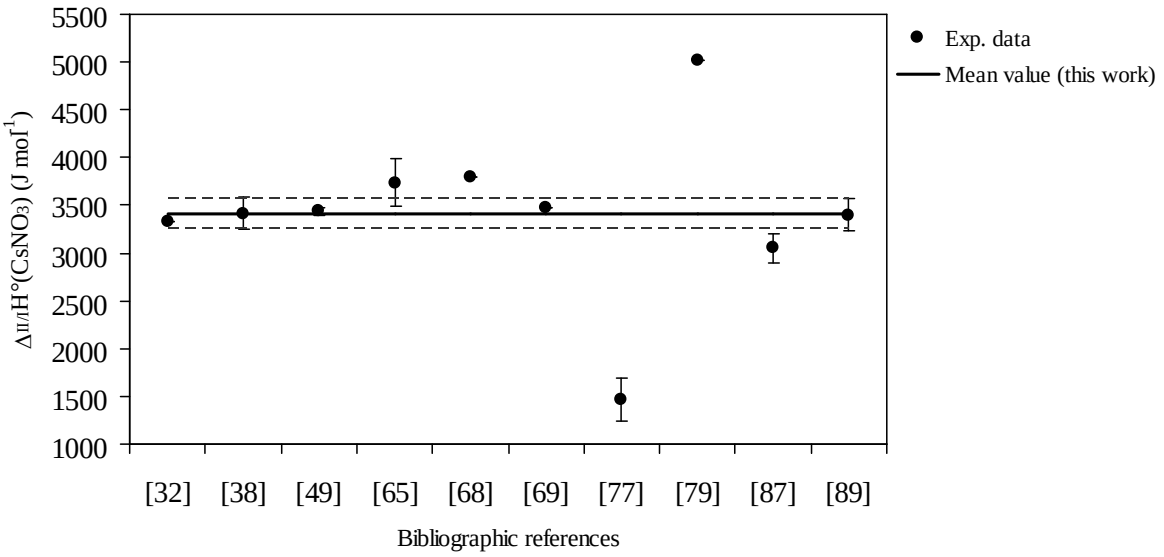

Fig. 6. Experimental solid-solid transition enthalpy of $CsNO_3$ from different sources compared with the mean value (this work). Error bars represent experimental uncertainties. Acceptable values are inside dashed lines.

Considering all acceptable data, the mean value is recalculated and the recommended value for the solid-solid transition enthalpy of $CsNO_3$ proposed in this work is (3466±142) J mol^{-1}.

• *Melting enthalpy* ($\Delta_m H°$)

The published melting enthalpies of $CsNO_3$ ($\Delta_m H°$) lie between 12100 J mol^{-1} and 15500 J mol^{-1} [32, 38, 65, 68, 73, 74, 82, 87, 89] with a maximum experimental uncertainty of ±5%.

First of all, the melting enthalpy of Bakes et al. [73] is rejected because of lack of information about the purity of the salt used. The higher value (15500 J mol^{-1}) obtained by Maeso and Largo [68] using DSC method, does not agree with any other value determined by the same experimental technique. This can be explained by the abnormally high value of heat capacity in the liquid phase. Accordingly, the melting enthalpy of Maeso and Largo [68] is considered unreliable. Using adiabatic calorimetry, Mustajoki [65] also gave a high melting enthalpy (14100 J mol^{-1}) related to the high heat capacity in the liquid phase. This value is considered less reliable. Indeed, the melting enthalpy obtained by integration of apparent heat capacity curves is subject to sources of significant experimental uncertainty. Besause the original paper of Trunin [82] could not be acquired during the present work, his data (13838 J mol^{-1}) is not taking into account.

The post-hoc test applied to the retained data [32, 38, 74, 87, 89] shows that the value of Kleppa and McCarty [74] (13443.2 J mol^{-1}) and that of Jriri et al. [32] (12100 J mol^{-1}) obtained by reaction calorimetry and DSC method, respectively, are questioned. Based on the most accurate method, the value of Jriri et al. [32] is kept and that of Kleppa and McCarty [74] is rejected.

Finally, one homogeneous subset [32, 38, 87, 89] with the mean value of 12545.0000 J mol^{-1} and standard deviation equal to 652.7565 J mol^{-1}, is obtained. The standard deviation corresponds to a relative uncertainty of 5.2 %.

Plot of experimental melting enthalpies of $CsNO_3$ from different sources compared with the mean value is shown in Fig. 7. The enthalpy value obtained by Bakes et al. [73] (13352 J mol^{-1}) and that of Kleppa and McCarty [74] ((13443.2±179.9) J mol^{-1}) are just above the upper limit of acceptable values. While, the data of Mustajoki [65] ((14100.08±125.52) J mol^{-1}), Maeso and Largo [68] (15500 J mol^{-1}) and Trunin [82] (13838 J mol^{-1}) are far from this limit.

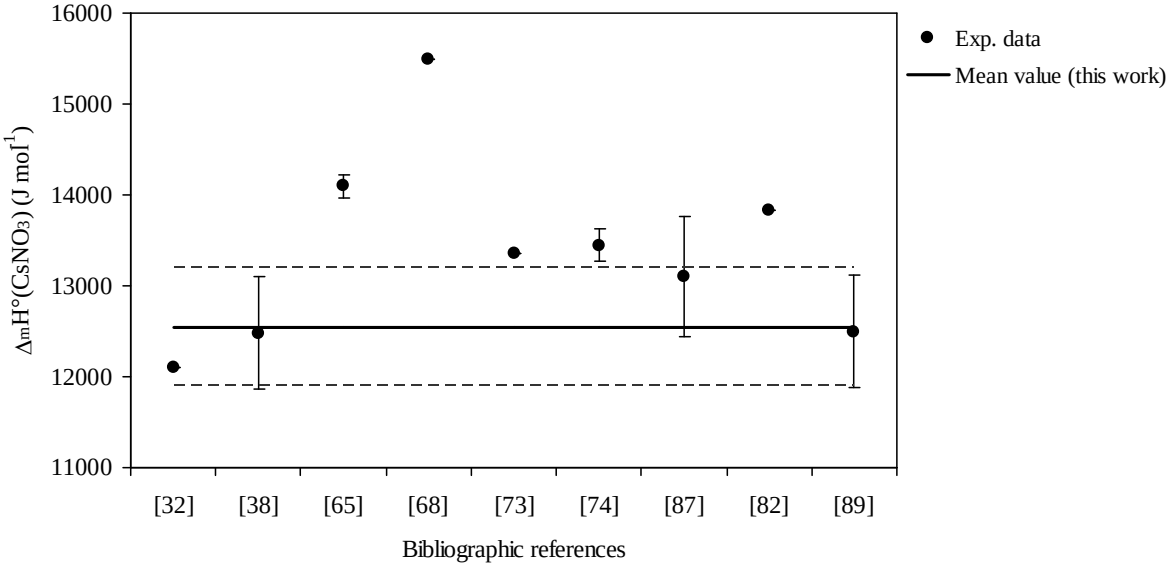

Fig. 7. Experimental melting enthalpy of $CsNO_3$ from different sources compared with the mean value (this work). Error bars represent experimental uncertainties. Acceptable values are inside dashed lines.

Considering all acceptable data, the mean value is recalculated and the recommended value for the melting enthalpy of $CsNO_3$ proposed in this work is (12545±413) J mol^{-1}.

2.2.2 Lithium nitrate ($LiNO_3$)

According to Rao et al.'s compilation [55], $LiNO_3$ crystallizes at 298 K and under atmospheric pressure in rhombohedral form (calcite type) $R\bar{3}c$ with a = 4.692 Å and c = 15.22 Å. There is no evidence for a phase transition between room temperature and the melting point. However, a study of the temperature variation of the electronic spectrum showed a discontinuity in the absorption coefficient [55]. This discontinuity was attributed to orientational disorder indicating a transformation as in $NaNO_3$ or in NH_4NO_3. Later, Wu et al. [92] confirmed the calcite type structure of $LiNO_3$ with a = 4.6920(3) Å and c = 15.2149(13) Å.

2.2.2.1 Heat capacity

• *Solid phase*

The heat capacity of $LiNO_3$ solid phase has been published by different authors [39, 53, 55, 67, 68, 93-96]. Results of different measurements are plotted in Fig. 8. The experimental techniques and relative uncertainties are showed in brackets. The constant

values of the heat capacity suggested in some publications [94-96] are ignored. These values are either smoothed or calculated.

As it can be seen, the data of Ichikawa and Matsumoto [67], Takahashi et al. [93], Maeso and Largo [68] agree satisfactorily within relative uncertainty of ±3%. The heat capacity values reported by Monia et al. [39] agree with those of Coscia et al. [54], but are lower than the other values [67, 68, 93]. Monia et al. [39] did not found a clear reason for this discrepancy, but they noticed that it could be due to the impurities. To this, one should add the hygroscopic nature of $LiNO_3$. In our opinion, the purity of salts employed is not the major source of the discrepancy between heat capacity values. Indeed, all investigations are based on samples with sufficient purity (> 99.0%). Therefore, it is the calorimeter operation that can be incriminated. For example, the heat capacity values determined by Monia et al. [39] for $RbNO_3$, under the same experimental conditions, are systematically low compared to literature data. The lower values of heat capacity [39, 54] are considered as less reliable. The data of Li et al. [53] are extremely low compared to all other values.

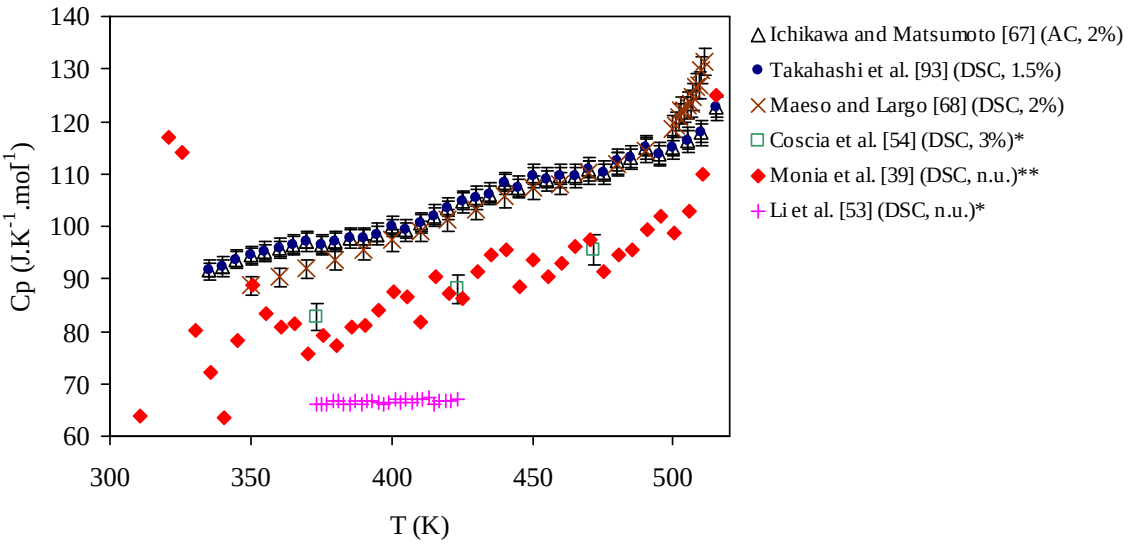

Fig. 8. Temperature dependence of the molar heat capacity of $LiNO_3$ solid phase (300 K < T < 520 K) from different sources. Error bars represent the experimental uncertainties on Cp. AC: Adiabatic Calorimetry; DSC: Differential Scanning Calorimetry; *values collected from the plot; **n.u.: no uncertainty mentioned.

• *Liquid phase*

The heat capacity of $LiNO_3$ liquid phase has been reported several times [39, 53, 54, 67, 68, 93, 97]. The temperature dependence of the molar heat capacity, according to several

authors, is presented in Fig. 9. The experimental techniques and relative uncertainties are showed in brackets.

The data of Takahashi et al. [93] and, Maeso and Largo [68] obtained by DSC are in fairly good agreement with the values of Ichikawa and Matsumoto [67] obtained by adiabatic calorimetry. As for the solid phase, the heat capacity values reported by Monia et al. [39], Li et al. [53] and, Coscia et al. [54] are low. These data are considered as unreliable.

Fig. 9 shows that the heat capacity of $LiNO_3$ liquid phase is constant. The value proposed by some authors [67, 68, 93] is (140±2%) J K^{-1} mol^{-1}. This value is in good agreement with that of Cordaro et al. [97] ((142.99±1.68) J $K^{-1}.mol^{-1}$) obtained by DSC method.

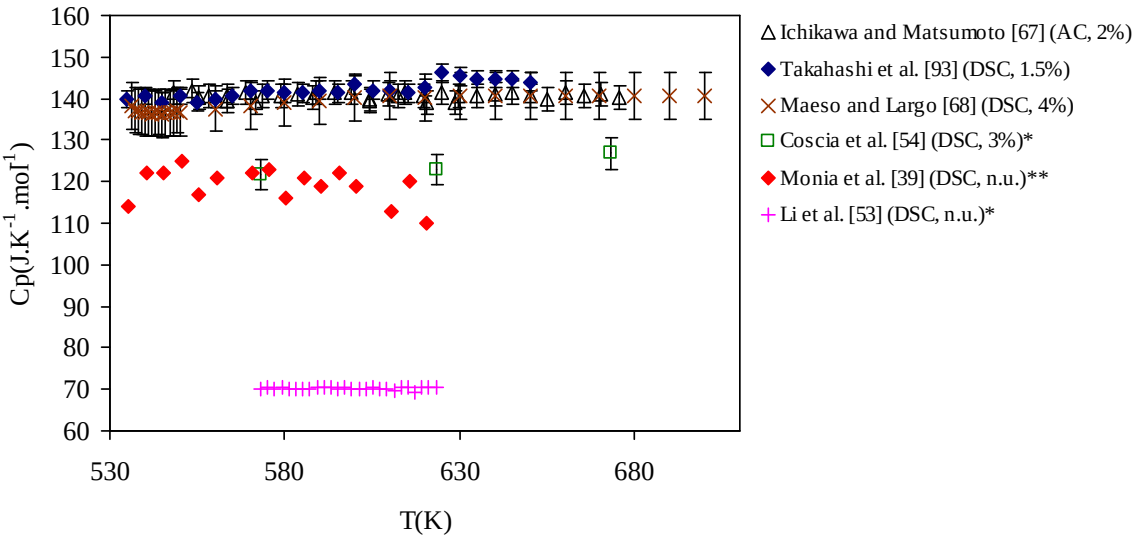

Fig. 9. Temperature dependence of the molar heat capacity of $LiNO_3$ liquid phase (530 K < T < 700 K) from different sources. Error bars represent the experimental uncertainties on Cp. AC: Adiabatic Calorimetry; DSC: Differential Scanning Calorimetry; *values collected from the plot; **n.u.: no uncertainty mentioned.

2.2.2.2 Temperature and enthalpy of melting

Temperature and enthalpy of melting of $LiNO_3$ have been reported by many authors [22, 38, 39, 52-54, 67, 68, 72, 74, 75, 80, 81, 84, 90, 93-112]. The data gathered during the present work are presented in Table 2 altogether with the experimental techniques and the sample characteristics.

• *Melting temperature*

The published melting temperatures (T_m) of $LiNO_3$ vary from 517.95 K to 543 K. These data lead to a relative uncertainty of about 5% very higher than experimental

uncertainties (< 1%). An absolute uncertainty of ± 2 K is accepted in the present analysis. This value seems reasonable considering the temperature range of experimental results.

The data from Refs. [75, 81, 99, 102, 105, 109] are rejected because of the defiency of information about purity of salt.

Mohammad et al. [101] gave the lowest temperature (517.95 K) among all those obtained by DTA method [84, 100, 102-104]. This may be related to the low sensitivity of the DTA/TGA apparatus used, as mentioned in their paper. The value of Bol'shakov et al. [72] (531 K) is a little bit high. Their experimental method is considered less accurate. Roget et al. [22] using DSC method obtained a value similar to that of Bol'shakov et al. [72]. The high value obtained by Roget et al. [22] may be due to the way that the melting temperature was determined from the DSC curve. Indeed, using the same DSC method and the same heating/cooling rate (2 K min^{-1}), Mohammad et al. [101] obtained 524.85 K, for the onset point, 529.95 K for the offset point, these temperatures have been determined from deviations from heat flow baselines, and 528.15 K for the melting temperature which seems to be the temperature corresponding to the peak top (temperature corresponding to the end of melting). All these values [22, 72, 101] are considered as unreliable and are disregarded. Thus, 25 of 34 determinations are analyzed statistically. The post-hoc test leads to 3 homogeneous subsets. The value of Goodwin and Kalmus [94] (523 K) and that of Li et al. [53] (528.05 K) are questioned. Based on the more accurate experimental method, the value of Li et al. [53] obtained by DSC is preferred. Finally, rejecting all data statistically comparable to that of Goodwin and Kalmus [94] within the experimental uncertainty, one homogeneous subset formed by 20 results is obtained. The mean value of 526.5900 K with standard deviation of 1.9243 K are obtained.

Fig. 10 compares all the melting temperatures collected from literature with the mean value. Most of the experimental melting temperatures fall within the range of acceptable values. Very few values are outside this range. The data of Roget et al. [22] ((530.85±1) K), Bol'shakov et al. [72] (531 K) and, Diogenov and Sarapulova [75] (530 K) are just above the upper limit of acceptable values. While, the value of Goodwin and Kalmus (523 K) [94] is just below the lower limit of acceptable values. The data of Ruiz et al. [99] (520.55 K), Mohammad et al. [101] ((517.95±4.9) K, DTA) and Campbell [109] ((543±0.5) K) are far from the limits of acceptable values.

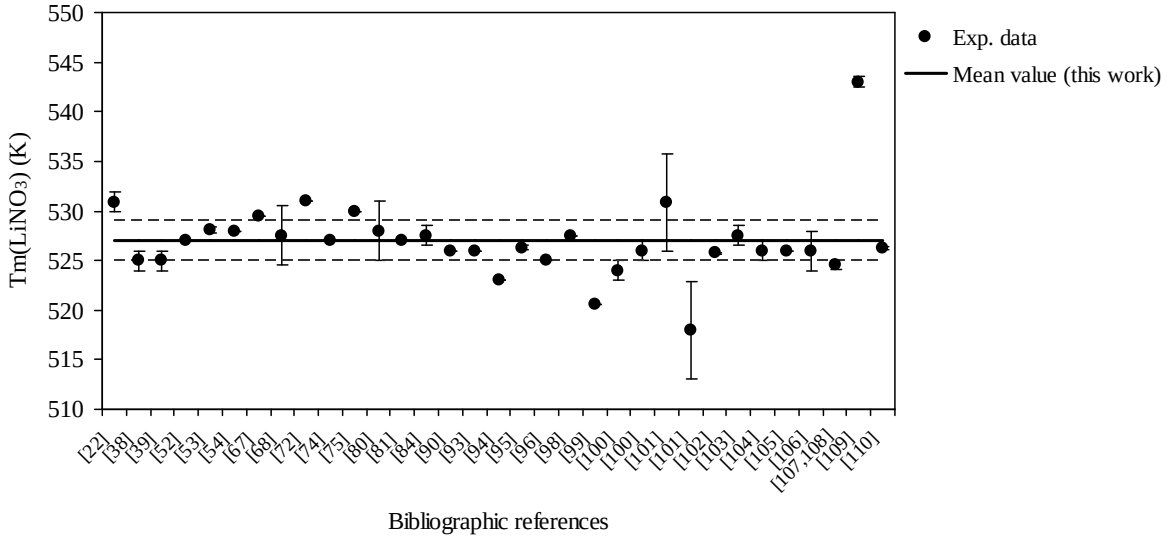

Fig. 10. Experimental melting temperature of $LiNO_3$ from different sources compared with the mean value (this work). Error bars represent experimental uncertainties. Acceptable values are inside dashed lines.

Considering all acceptable data, the mean value is recalculated and the recommended value for the melting temperature of $LiNO_3$ proposed in this work is (527±2) K.

• *Melting enthalpy*

Disregarding the very high value of Tye et al. [112] (36700 J mol^{-1}), the melting enthalpies of $LiNO_3$ ($\Delta_m H°$) compiled from literature lie between 23020 J mol^{-1} and 26924.04 J mol^{-1} which lead to a relative uncertainty of about 15% very higher than experimental uncertainties (< 6%). A maximum relative uncertainty of ± 5% is considered in the present evaluation.

Rejecting the data from Refs. [99] and [105] because of absence of salt purity information, the 17 remaining determinations lead to 2 homogeneous subsets according to the post-hoc test. The value of Cordaro et al. [97] (24320 J mol^{-1}, DSC) and that of Doucet and Vallet [110] (26924.04 J mol^{-1}, freezing) are inquired. Based on the more accurate experimental method, the value of Cordaro et al. [97] is preferred.

Finally, one homogeneous subset formed by 16 measurements lead to the mean value of 25050.4049 J mol^{-1} with standard deviation of 1268.1701 J mol^{-1} which corresponds to a relative uncertainty of 5.062 %.

Plot of experimental melting enthalpy values of $LiNO_3$ from different sources compared with the mean value is shown in Fig. 11. Apart from the experimental values of

Franzosini and Sinistri [95] ((26677.18±292.88) J mol^{-1}, DC; (26777.6±376.6) J mol^{-1}, Cry), Ruiz et al. [99] (23020 J mol^{-1}) and, Doucet and Vallet [110] (26924.04 J mol^{-1}), all other published values are acceptable within the experimental uncertainty of ±5%.

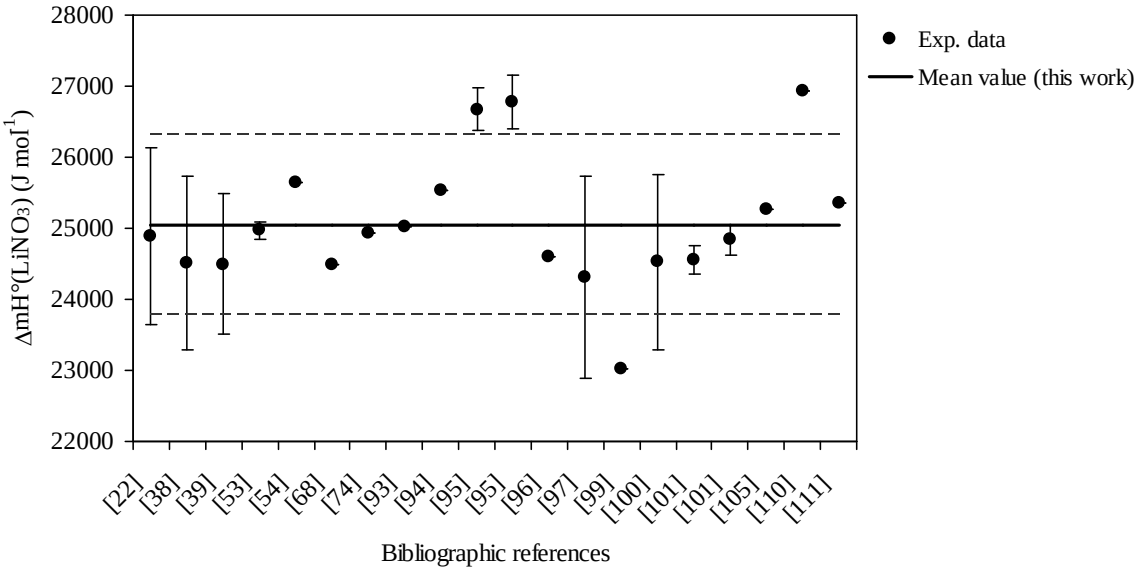

Fig. 11. Experimental enthalpy of melting of $LiNO_3$ from different sources compared with the mean value (this work). Error bars represent experimental uncertainties. Acceptable values are inside dashed lines.

Considering all acceptable data, the mean value is recalculated and the recommended value for the melting enthalpy of $LiNO_3$ proposed in this work is (25068±924) J mol^{-1}.

2.2.3 Sodium nitrate ($NaNO_3$)

As stated by Rao et al. [55], $NaNO_3$ crystallizes at 298 K and under atmospheric pressure in rhombohedral $R\bar{3}c$ with a = 5.0696 Å and c = 16.829 Å. Sodium nitrate has been found to undergo, around 548.5 K, a phase transition from phase $NaNO_3$(II), ordered rhombohedral phase (calcite type), to $NaNO_3$(I), a disordered rhombohedral phase. Numerous studies [113-121] devoted to the phase transition in $NaNO_3$ crystal, agree well with those reviewed by Rao et al. [55] and showed that the transition between low temperature form (phase-II), $R\bar{3}c$, and high temperature form (phase-I), $R\bar{3}m$, of $NaNO_3$ is a second-order transition caused by internal rotation of the NO_3^- groups in the crystal. However, Ballirano [122] pointed out that no univocal indication on the $R\bar{3}c$ (phase-II) $\rightarrow R\bar{3}m$ (phase-I) transition mechanism can be obtained, because of the relevant role played by the arbitrary

assumptions required for defining the c_0 dependence from temperature of the high temperature phase.

2.2.3.1 Heat capacity

• *Low temperature phase: $NaNO_3$ (II)*

Low temperature heat capacity of $NaNO_3$ has been determined by different authors [32, 54, 67, 93, 94, 123-143]. In Fig. 12, the heat capacity from literature is plotted as a function of temperature. The results obtained by Ping et al. [138] and by D'Aguanno et al. [143] using DSC method can not be reported in the present work, because only the plot without the experimental values is available in their papers.

As it can be seen, all experimental results agree satisfactorily within experimental uncertainties, except for the data of Dikant [132] and those of Coscia et al. [54, 140] which are too high and too low, respectively.

Dikant [132] used a pulse method which is considered to be less accurate than adiabatic calorimetry and differential scanning calorimetry. Therefore, poor reliability may be attached to his determinations. No particular reason is found for low values of Coscia et al. [54, 140] using DSC technique.

It is worthy to notice that the original paper of Kubicar [131] could not be retrieved during the present work. So the data from this paper are not reported in Fig. 12. However, the following comments can be considered. Klement [144] noticed that Kubicar's specific heat values [131] are systematically superior to the other, reasonably coherent [126-128, 130]. This is probably due to the difficulties in calibration for the pulse technique used.

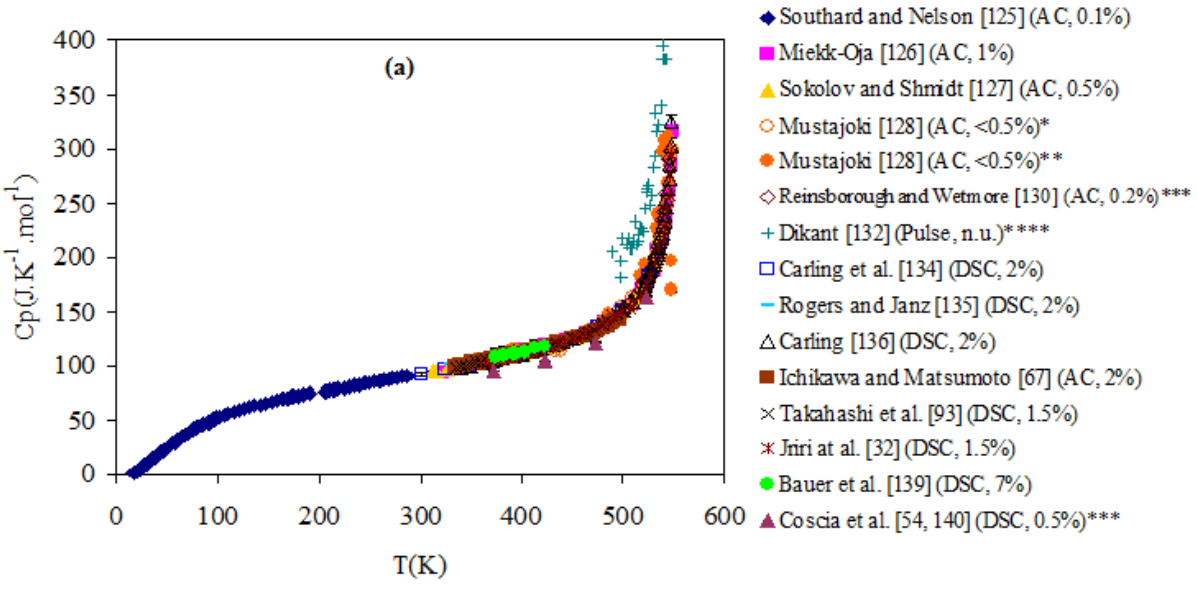

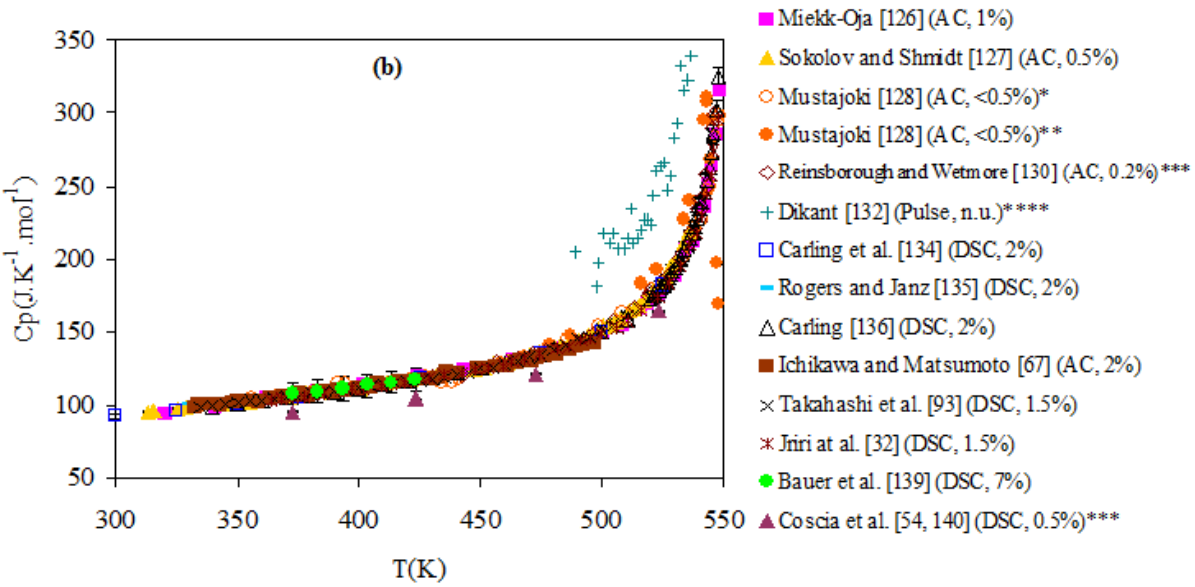

Fig. 12. Temperature dependence of the molar heat capacity of $NaNO_3$ (II) from different sources. (a) Temperature range (0 – 550) K. (b) Enlargement in the temperature range (300 – 550) K . Error bars represent the experimental uncertainties on Cp.
AC : Adiabatic Calorimetry ; Pulse : Pulse method ; DSC : Differential Scanning Calorimetry ; *Data obtained on heating ; **Data obtained on cooling ; ***Values collected from the plot ; ****n.u. : no uncertainty mentioned.

• *High temperature phase: $NaNO_3$ (I)*

Heat capacity data of $NaNO_3$ (I) are available from various authors [32, 54, 67, 93, 126, 127, 128, 129, 130, 132, 133, 135, 136, 138, 140, 143]. The results gathered from literature during the present work are plotted in Fig. 13. Not taking into account the high values obtained by Dikant [132] already considered as unreliable, the discrepancy between the experimental data is found to be more than 10%. All reported data are obtained either by differential scanning calorimetry or by adiabatic calorimetry which are the most accurate methods. Accordingly, a critical review in order to get reliable data of heat capacity of $NaNO_3$(I) is rather challenging. However, Jriri et al.'s measurements [32] and those of Miekk-Oja [126] agree within ± 3%, which is to a certain extent comparable to the experimental uncertainty in the heat capacity values.

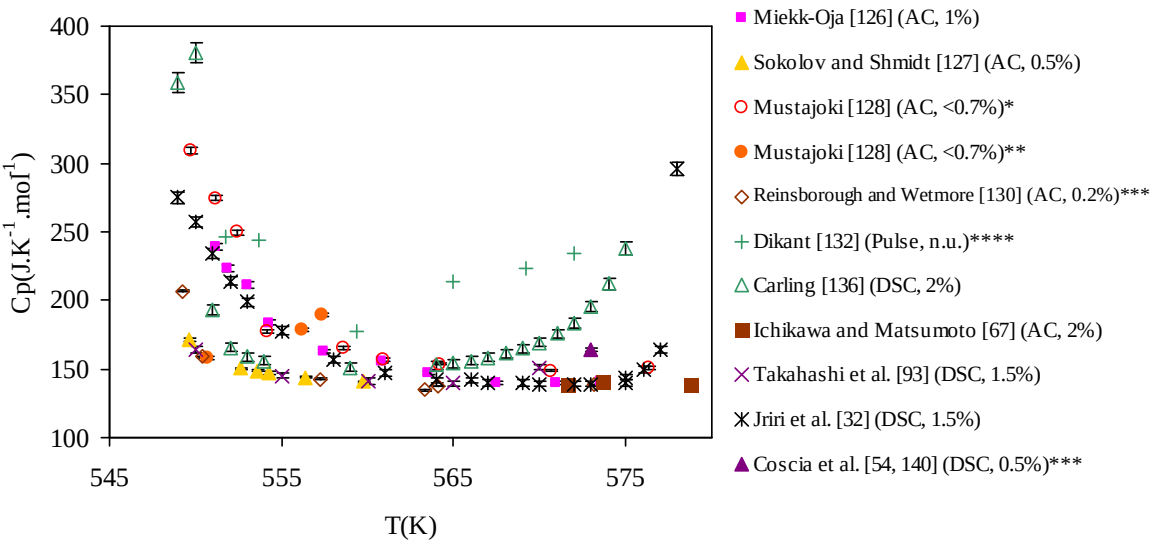

Fig. 13. Temperature dependence of the molar heat capacity of $NaNO_3$ (I) (550 K < T < 580 K) from different sources. Error bars represent the experimental uncertainties on Cp.
AC : Adiabatic Calorimetry; Pulse : Pulse method; DSC : Differential Scanning Calorimetry; *Data obtained on heating ; **Data obtained on cooling ; ***Values collected from the plot ; ****n.u. : no uncertainty mentioned.

• *Liquid phase*

The heat capacity data of $NaNO_3$ liquid phase are available in different bibliographic sources [32, 54, 65, 67, 93, 94, 97, 127, 129, 133-137, 139-143, 145-150]. The experimental data vs. temperature are shown in Fig. 14. Only the measurements of Asahina et al. [150] are not reported because we could not get their original paper. Except for the high values of Mustajoki [128], all measurements are in fairly good agreement with each other within experimental uncertainties.

From Fig. 14, it is reasonable to assume a constant heat capacity in the $NaNO_3$ liquid phase with a mean value about 140 J K^{-1} mol^{-1} [146, 150]. However, most of data obtained by drop calorimetry are higher than this mean value: Goodwin and Kalmus [94] (152.9 ± 1%) J K^{-1} mol^{-1}, Nguyen-Duy and Dancy [133] ((212 ± 32) J K^{-1} mol^{-1}) and Douglas [146] (155.7 J K^{-1} mol^{-1}). Only Janz et al. [129] (130.54 J K^{-1} mol^{-1}), and Kawakami et al. [137] ((129 ± 3) J K^{-1} mol^{-1}) showed lower values. Compared to DSC and adiabatic calorimetry, drop calorimetry is considered as less accurate.

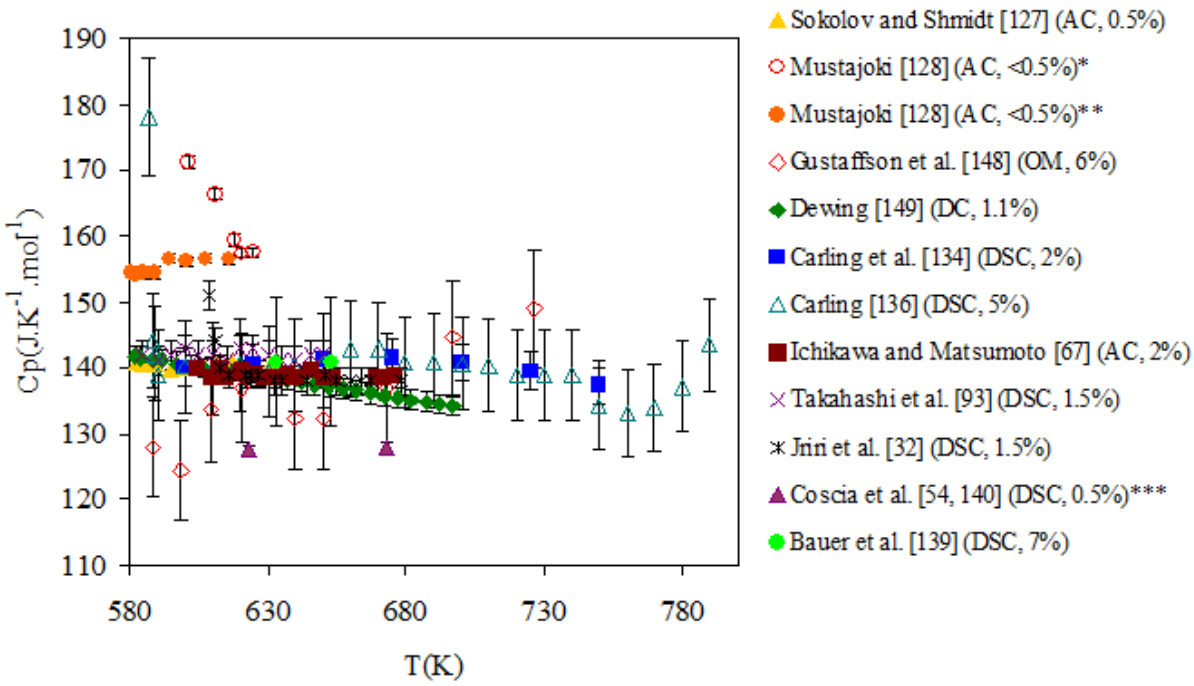

Fig. 14. Temperature dependence of the molar heat capacity of $NaNO_3$ liquid phase (580 K < T < 800 K) from different sources. Error bars represent the experimental uncertainties on Cp. AC : Adiabatic Calorimetry ; Pulse : Pulse method ; DSC : Differential Scanning Calorimetry ; *Data obtained on heating ; **Data obtained on cooling ; ***Values collected from the plot.

2.2.3.2 Temperature and enthalpy of phase changes (solid-solid transition, melting)

A wealth of experimental data exists on the thermochemical properties of $NaNO_3$. Bibliographic information as complete as possible are gathered in Table 3. However, very old papers published in 19th century especially temperatures of transition are disregarded. Most of these data were summarized by Menzies and Dutt [151].

• *Solid-solid transition temperature ($T_{II/I}$)*

The solid-solid transition temperature of $NaNO_3$ from literature is detected in the range (530 – 552.7) K [22, 32, 38, 67, 77, 83, 86, 93, 101, 105, 114-117, 119, 120, 122, 126, 128-130, 132, 133, 135, 136, 144, 153-159, 161, 162, 164, 165, 168, 169, 171-173, 175, 176, 178, 182, 183, 185-191] which leads to a relative uncertainty of about 4% very higher than experimental uncertainties (< 1%). This means that the data differ significantly from each other. Without taking into account publications in which salt purity is not defined, 42 determinations of 52 are analyzed. The post-hoc test leads to 10 homogeneous subsets. Before the critical evaluation of all considered data, an analysis of each of the following four groups of experimental techniques is first carried out.

(i) Data from DSC method

Considering the experimental uncertainties of about ± 2 K, it appears that the transition temperatures are widely scattered from 530 K to 551 K [22, 32, 38, 93, 101, 135, 136, 153-159, 161, 162, 164, 165, 168]. The post-hoc test leads to 7 homogeneous subsets. The lowest values are given by Dancy [154] (530 K) and Maeso [157, 158] (540 K). Each of these values forms one subset. The other 5 subsets can be divided into 2 groups: $T_{II/I} \leq 547$ K and $T_{II/I} > 547$ K.

(ii) Data from DTA technique

The data obtained from DTA technique vary from 532.45 K to 549 K [77, 83, 86, 101, 144, 169, 171-173, 175, 176, 178]. The post-hoc test gives 3 homogeneous subsets. The value of Mohammad et al. [101] (532.45 K) stands alone (one subset). The two major subsets lead to mean values of (547 ± 2) K and (548.5 ± 0.4) K, respectively.

(iii) Data from other calorimetric methods

Without taking into account the value of Schürmann and Nedeljkovic [105] (548 K) and that of Nguyen-Duy and Dancy [133] (535 K) (lack of salt purity), all data lie between 548 K and 549.2 K, *i.e*. $T_{II/I} > 547$ K.

(iv) Data from chemical analysis and all other methods

All considered values [114-116, 120, 122, 183, 187, 188] are in the range (548 – 552.7) K, *i.e*. superior to 547 K.

(v) Critical analysis of all data

From the preliminary analysis above, two groups of data are obtained: $T_{II/I} \leq 547$ K and $T_{II/I} > 547$ K.

The question here is which one contains the reliable value of solid-solid transition of $NaNO_3$? As stated in section *2.1*, apart from the salt purity, experimental procedures such as atmosphere, gas flow, crucible material, calibration, heating/cooling rate and the way the transition temperature is determined from the thermal analysis curve, are the basic causes of the discrepancy in the data. In the particular case of $NaNO_3$, Dancy [154] pointed out that the source of the discrepancies in the values of solid-solid transition temperature obtained from DSC measurements lies also in the difficulty in identifying the beginning of this transition. Indeed, the transition is known as a gradual phase transition (λ-type) starting at about 423 K and ending at about 549 K, just below the melting point [32, 67, 93, 130, 132, 136, 155, 199]. On the other hand, Kawashima et al. [186] noticed that the λ-transition temperature (T_λ) is the most difficult point to be controlled by the thermal control system, because the heat capacity shows anomalous temperature dependence at T_λ. From these observations and paying more

attention to the data obtained by chemical analysis and all other methods, it is worthy to consider the transition temperature higher than 547 K in agreement with the data from all other calorimetry methods.

Based on this assumption, 32 determinations of 42 are statistically analyzed. 3 homogeneous subsets are obtained. Disregarding, the three questionable values : 552 K [114], 552.3 K [116] and 552.7 K [120], one homogeneous subset is obtained leading to the mean value of 548.9993 K with standard deviation of 1.7927 K.

The comparison between the mean value and experimental data collected from literature is presented in Fig. 15. Most of the published values are acceptable within the admitted experimental uncertainty of ±2 K. The data of Poon and Salje [114] (552 K), Schmahl and Salje [116] ((552.3±0.5) K) and Antao et al. [120] ((552.7±0.5) K) are very close to the upper limit of acceptable values. While, the values of Roget et al. [22] (544.95 K), Rao and Rao [77] (545 K), Beneš et al. [162] (545.5 K) and Benages-Vilau [164, 165] (544 K), are just below the lower limit of acceptable values. Only the data of Mohammad et al. [101] ((532.45±4.9) K, DTA), Nguyen-Duy and Dancy [133] (535 K), Dancy [154] (530 K) and Maeso [157, 158] ((540.1±1) K) are far from the lower limit.

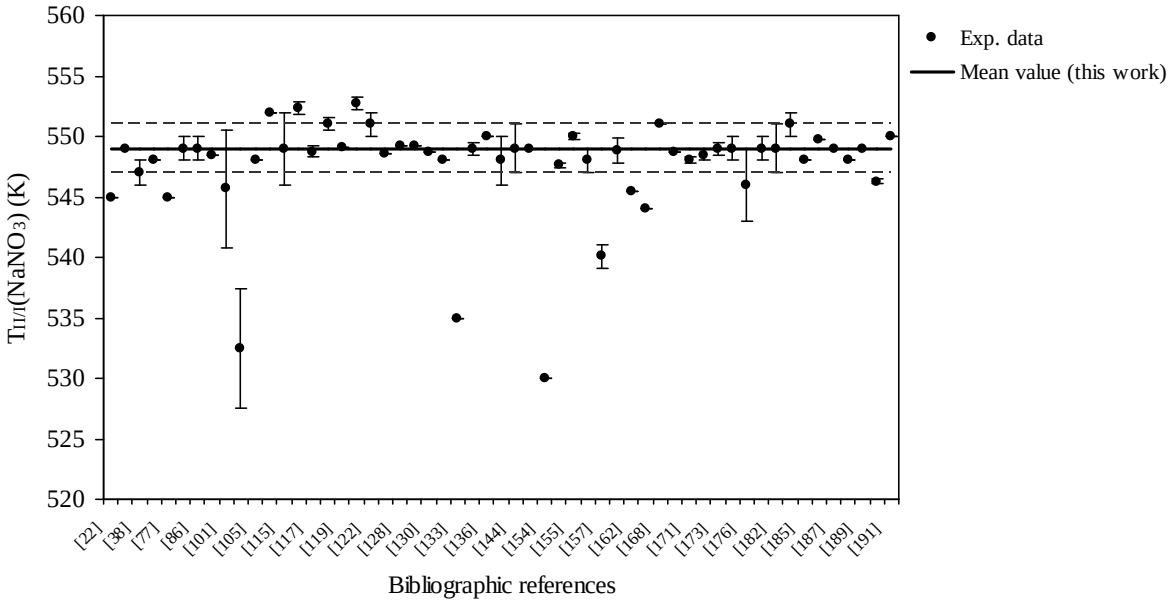

Fig. 15. Experimental solid-solid transition temperature of $NaNO_3$ from different sources compared with the mean value (this work). Error bars represent experimental uncertainties. Acceptable values are inside dashed lines. For clarity reasons, the number of categories between tick-mark labels is 2.

Considering all acceptable data, the mean value is recalculated and the recommended value for the solid-solid transition temperature of $NaNO_3$ proposed in this work is (549±2) K.

• *Melting temperature (T_m)*

The $NaNO_3$ melting point found by numerous authors, lies in the range (571.65 – 588.25) K [22, 32, 38, 47, 54, 67, 73-76, 81, 83, 86, 93-95, 101, 102, 105, 108, 115, 122, 127-130, 133, 135-137, 139, 151, 153, 154, 155-162, 164-168, 170-182, 184, 185, 192-196] which leads to a relative uncertainty of about 3% higher than experimental uncertainties (< 1%). So, the differences in data are statistically significant. Disregarding publications in which salt purity was not defined, 52 determinations of 63 are analyzed. The post-hoc test leads to at least 4 homogeneous subsets. As done above, data from each of experimental technique are firstly examined, before the critical analysis of all data.

(i) Data from DSC method

Melting temperature values of $NaNO_3$ obtained by DSC method are between 574.55 K and 583 K. The post-hoc test shows that the following values stand alone: 574.55 K [101] and 583 K [136]. For the same reasons mentioned in the case of $LiNO_3$, the lower value of Mohammad et al. [101] is regarded as unreliable. The higher value (583 K) obtained by Carling [136] also seems less reliable. Indeed, the melting temperature of KNO_3 determined by this author under the same experimental conditions is the highest value among those published except the value of Morita et al. [180] as showed in the compilation done by Jriri et al. [32].

Disregarding the data of Mohammad et al. [101] and Carling [136], all data lie between 577.5 K and 581 K.

(ii) Data from DTA technique

The data obtained from DTA technique vary from 571 K to 581 K. The post-hoc test leads to 4 homogeneous subsets which can be grouped into two sets of data (571.65 – 575.21) K [101, 176, 177] and (578 – 581) K [83, 86, 170-175, 178, 179]. The data belonging to the first group are considered as less reliable. Ballirano [122] noticed that for kinetic reasons, melting starts at 577 K and is completed at 581 K.

(iii) Data from other calorimetric methods

The data obtained from all other calorimetry methods compiled during the present work vary from 578 K to 583.2 K. The post-hoc test leads to 3 homogeneous subsets. Two values

stand alone: 578 K [182] and 583.2 K [67]. Disregarding these values, all data lie between 579.2 K and 583 K.

(iv) Data from chemical analysis and all other methods

Apart from the value of Menzies and Dutt [151] (588.25 K) obtained by freezing curve, all data (578.65 K– 581 K) agree satisfactorily within experimental uncertainties.

(v) Critical analysis of all data

From the preliminary analysis above, it is established that the melting temperature of $NaNO_3$ belongs to the range (577.5 – 581) K. Finally, 41 determinations of 52 are analyzed. These 41 determinations lead to one homogeneous subset with the mean value of 579.4488 K and standard deviation of 1.909 K.

The mean value and the experimental results are compared in Fig.16. Most of the experimental melting temperatures are acceptable within the uncertainty of ±2 K. All values outside the range of acceptable values (583.2 K [67]; 583 K [74]; 583 K [81]; 583 K [136]; (588.25±0.2) K [151]; 584 K [180]; 585 K [184]; 582 K [194]; 584 K [196]) except that of Mohammad et al. [101] ((571.65±4.9) K), are above the upper limit of acceptable values.

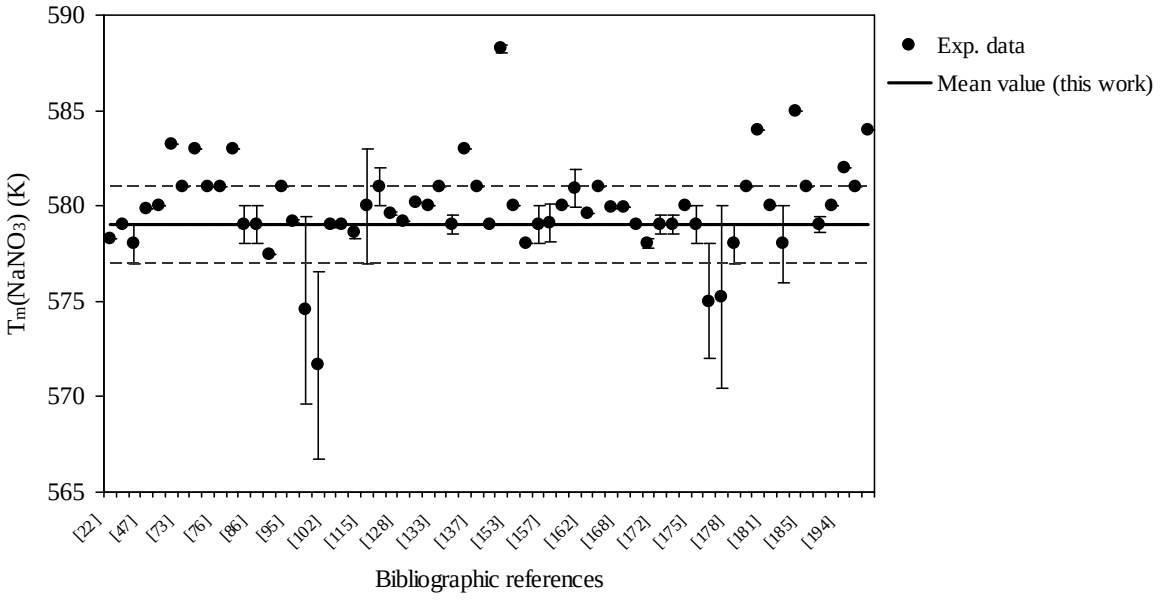

Fig. 16. Experimental melting temperature of $NaNO_3$ from different sources (all data) compared with the mean value (this work). Error bars represent experimental uncertainties. Acceptable values are inside dashed lines. For clarity reasons, the number of categories between tick-mark labels is 2.

Considering all acceptable data, the mean value is recalculated and the recommended value for the melting temperature of $NaNO_3$ proposed in this work is (579±2) K.

• *Solid-solid transition enthalpy*

Many works devoted to the solid-solid transition of $NaNO_3$ seem to substantiate the second-order transition [32, 67, 93, 130, 132, 136, 155, 186, 199] with enthalpy equal to zero. However, this transition can also be considered as a sluggish first-order transition [200] with enthalpy varying between 418 J mol^{-1} and 4686 J mol^{-1} [22, 32, 38, 77, 93, 101, 105, 126, 128, 129, 133, 135, 136, 153-155, 157-159, 161, 177]. The discrepancy in the enthalpy values is remarkable. The reasons of this discrepancy can be found in section *2.1*. Considering a maximum relative uncertainty of 5%, the post-hoc test applied to 17 of 19 determinations leads to 9 homogeneous subsets. Dancy [154] stated that, until the nature of the solid-solid transition is better understood, none of the enthalpy values can be regarded as the "best". Therefore, each value or average value of a homogeneous subset may be acceptable. However, based on the very few values that agree within the experimental uncertainties [32, 38, 93, 154, 157-159], the mean value of 3683 J mol^{-1} with an uncertainty of ± 5% can be suggested as the solid-solid transition enthalpy of $NaNO_3$.

Fig. 17 compares the mean value with experimental data from literature [22, 32, 38, 77, 93, 101, 105, 126, 128, 129, 133, 135, 136, 153-155, 157-159, 161, 177].

The range of acceptable values is very small. Less than 40% of the experimental data are in agreement within the uncertainty of ±5%. Apart from the data of Schürmann and Nedeljkovic [105] (4686.08 J mol^{-1}) and Carling [136] ((4420±130) J mol^{-1}), the published first-order solid-solid transition enthalpies of $NaNO_3$ outside the acceptable values range are distributed below the lower limit of this range. Only the value of Mustajoki [128] (3950 J mol^{-1}) is very close to the upper limit of the acceptable values. Taking into account the experimental uncertainty, this value may be considered as acceptable.

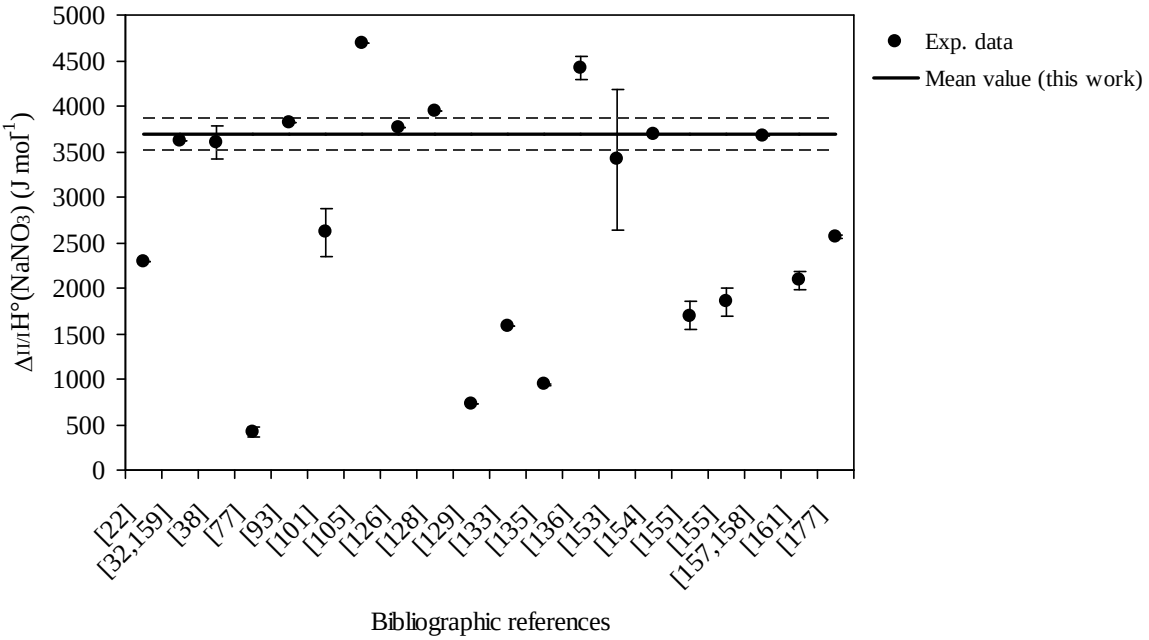

Fig. 17. Experimental solid-solid transition enthalpy of $NaNO_3$ (first-order transition) from different sources compared with the mean value (this work). Error bars represent experimental uncertainties. Acceptable values are inside dashed lines.

Considering the data belonging to the acceptable values range, the mean value is recalculated and the recommended value for the first-order solid-solid transition enthalpy of $NaNO_3$ proposed in this work is (3733±123) J mol^{-1}.

• *Melting enthalpy*

Bibliographic data of $NaNO_3$ melting enthalpy, except those published in 19th century [123, 145] are between 10030 J mol^{-1} and 16790 J mol^{-1} [22, 32, 38, 47, 54, 73, 74, 93-95, 97, 101, 105, 127-130, 133, 135, 136, 141, 152-154, 157-161, 163-166, 168, 170, 177, 179-181, 197, 198] leading to a relative uncertainty more than 40%. Disregarding publications in which salt purity was not defined, 38 determinations of 44 are analyzed. The post-hoc test leads to 4 homogeneous subsets. The lower value of Martin et al. [141] ((118±2) kJ kg^{-1} equal to (10030±170) J mol^{-1}) obtained by DSC method stands alone. Reasonable doubts exist about this value. Indeed, surprisingly Martin et al. [141] noticed that their value is in good agreement with the measurements of Rogers and Janz [135] with less than 10% deviation. Let us remind that the melting enthalpy obtained by Rogers and Janz [135] is (15439±1%) J mol^{-1} approximately equal to 181.6 kJ kg^{-1}.

The higher value of Cordaro et al. [97] ((16790±260) J mol^{-1}) obtained by DSC method is also regarded as unreliable.

Rejecting the values of Martin et al. [141] and Cordaro et al. [97], the post-hoc test leads to 2 homogeneous subsets. The value of Romero-Sanchez et al. [168] (13438.5 J mol^{-1}) obtained by DSC is questioned. This value is slightly lower than all other values obtained by the same experimental method. The reason can be found in the conditions used for the experiments.

Finally, 35 determinations of 38 forming one homogeneous subset lead to the mean value of 15159.9625 J mol^{-1} with standard deviation of 700.9186 J mol^{-1}. This standard deviation corresponds to a relative uncertainty of 4.623 %.

Plot of experimental melting enthalpy of $NaNO_3$ from different sources compared with mean value is shown in Fig. 18. Only three values ((16790±260) J mol^{-1} [97], (10030±170) J mol^{-1} [141], 13438.5 J mol^{-1} [168]) are truly outside the range of acceptable values. Taking into account the experimental uncertainty, the value of Roget et al. [22] (15980 J mol^{-1}) which is slightly higher than the upper limit of acceptable values may be acceptable.

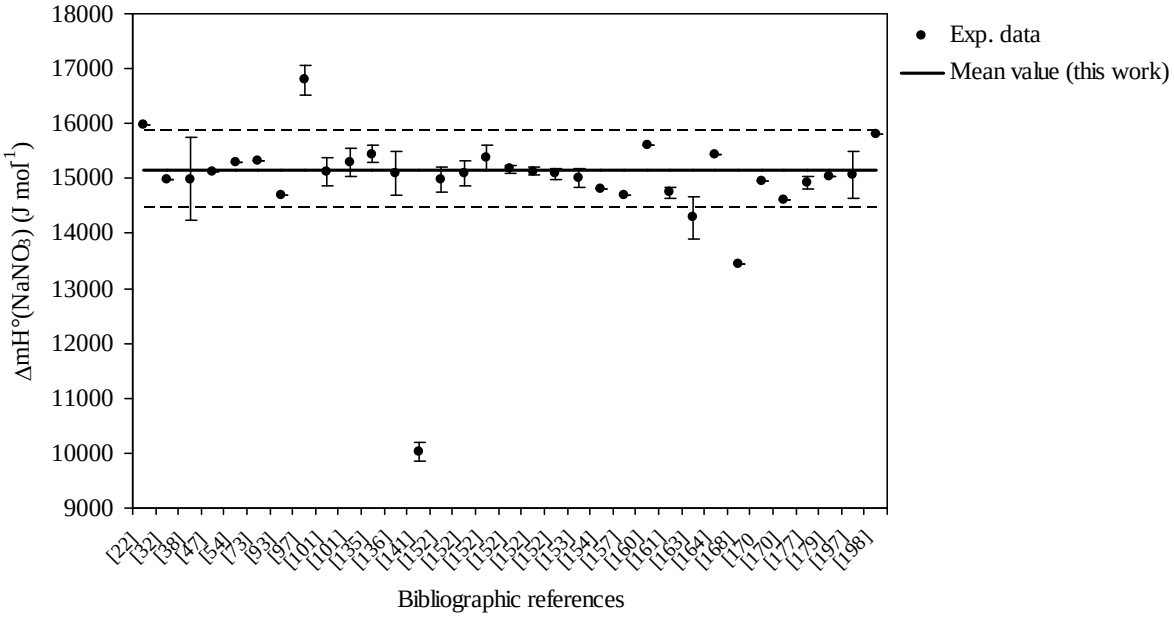

Fig. 18. Experimental melting enthalpy of $NaNO_3$ from different sources compared with the mean value (this work). Error bars represent experimental uncertainties. Acceptable values are inside dashed lines.

Considering all acceptable data, the mean value is recalculated and the recommended value for the melting enthalpy of $NaNO_3$ proposed in this work is (15129±365) J mol^{-1}.

2.3 Boundary systems

2.3.1 $CsNO_3$-$LiNO_3$ system

2.3.1.1 Phase diagram

The phase diagram data of the $CsNO_3$-$LiNO_3$ system have been determined by several researchers. These data were critically assessed by Mossarello [30] and Sangster [35], respectively. From these reviews, one can notice that the phase diagram of the system $CsNO_3$-$LiNO_3$ exhibits a congruently melting compound $Cs_{0.5}Li_{0.5}NO_3$ which forms eutectic mixtures with the end members. However, some discrepancies exist in the values of temperature and composition of eutectics. Using simultaneously direct and differential thermal analysis, Bélaïd-Drira et al. [84] reinvestigated the phase diagram of the $CsNO_3$-$LiNO_3$ system. Their data were not included in the previous assessments [30, 35]. Though, Bélaïd-Drira et al. [84] confirmed that the system has a 1:1 congruently melting compound and two eutectics, their work raised a question about the existence of the intermediate compound at ambient temperature. Indeed, by X-ray diffraction, they suggested that this compound does not exist at room temperature in contrast to the work of Bol'shakov et al. [72] who found that this coumpound exists at 273 K and has a polymorphic transition at 339 K. Unfortunately, Bélaïd-Drira et al. [84] did not present X-ray patterns as a proof. Therefore, it is necessary to re-address this issue which affects mainly the equilibria in the solid state.

The liquidus data [72, 84, 201] are in good agreement except for the $LiNO_3$-rich side where Bol'shakov et al. [72] showed very higher values.

2.3.1.2 Thermochemical data

Only the liquid mixing enthalpies of $CsNO_3$-$LiNO_3$ system are available in the literature [202, 203]. From their study, Kleppa and Hersh [202] proposed an analytical expression for the enthalpy of mixing. They used regular model solution with an interaction parameter λ = -12552 J mol^{-1}. Meschel and Kleppa [203] expressed also molar enthalpy of mixing of liquid $LiNO_3$ with (undercooled) liquid $CsNO_3$ at 623 K (Eq. 1).

$$\Delta_{mix}H^0\left(J\ mol^{-1}\right) = X_{LiNO_3}X_{CsNO_3}\left(-14351.12 - 1004.16X_{LiNO_3} - 6443.36X_{LiNO_3}X_{CsNO_3}\right) \quad (1)$$

With X_i, mole fraction of component i (i = $LiNO_3$, $CsNO_3$).

Meschel and Kleppa [203] found at 623 K, (13640±126) J mol^{-1} for the enthalpy of fusion of pure $CsNO_3$.

Though, both expressions lead to similar results, we prefer that of Meschel and Kleppa [203] because of the non-regular behaviour which is more realistic considering the presence of the intermediate compound $Cs_{0.5}Li_{0.5}NO_3$ in the binary system.

By dissolution measurements in eutectic mixture of KNO_3-$TlNO_3$-$LiNO_3$ ternary system used as bath at 373 K, Zoro et al. [204] determined the enthalpy of formation of the $Cs_{0.5}Li_{0.5}NO_3$ compound referred to the corresponding pure nitrates as -323 J mol^{-1}.

2.3.2 Phase diagrams of $CsNO_3$-$NaNO_3$ and $LiNO_3$-$NaNO_3$ systems

The phase diagrams of $CsNO_3$-$NaNO_3$ and $LiNO_3$-$NaNO_3$ systems were extensively studied. A critical analysis of the experimental data and thermodynamic evaluations were presented in the literature [23, 26, 30, 31, 35, 205, 206]. Both systems present a simple eutectic reaction with virtually no solid solubility in either of the pure components.

The calculated liquidus, eutectic temperature (T^e) and composition (X^e) obtained for $CsNO_3$-$NaNO_3$ system are comparable [26, 30, 35, 205] (T^e = 461 K – 464 K; $X^e_{NaNO_3}$ = 0.535 – 0.541). However, the calculated eutectic temperature and composition given by An et al. [206] (T^e = 455 K, $X^e_{NaNO_3}$ = 0.519) are lower than all the others. The phase diagram obtained by An et al. [206] is less consistent with available experimental data compared to other evaluations.

Four optimizations of $LiNO_3$-$NaNO_3$ were reported in literature [23, 30, 31, 205]. Except for the liquidus obtained by Beltrán et al. [205], all calculated phase diagrams are almost similar and are in agreement with experimental data. The calculated eutectic temperature of Beltrán et al. [205] (T^e = 460.98 K) is lower than all other evaluations (T^e = 467 K – 468 K). The phase diagram assessed by Hellali et al. [23] shows a better agreement with experimental data.

The calculated phase diagrams of $CsNO_3$-$NaNO_3$ and $LiNO_3$-$NaNO_3$ systems obtained by Jriri et al. [26], and Hellali et al. [23], respectively, are considered in the present work (see Figs. 19 and 20).

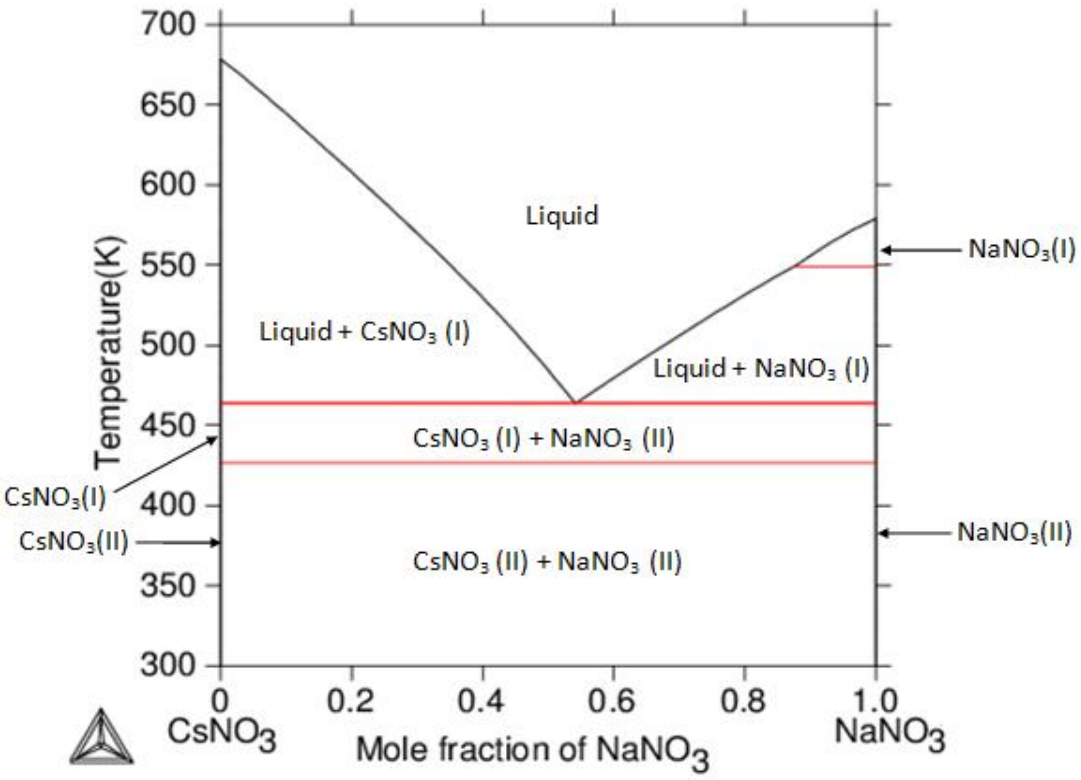

Fig. 19. Calculated phase diagram of $CsNO_3$-$NaNO_3$ system with thermodynamic parameters of Jriri et al. [26].

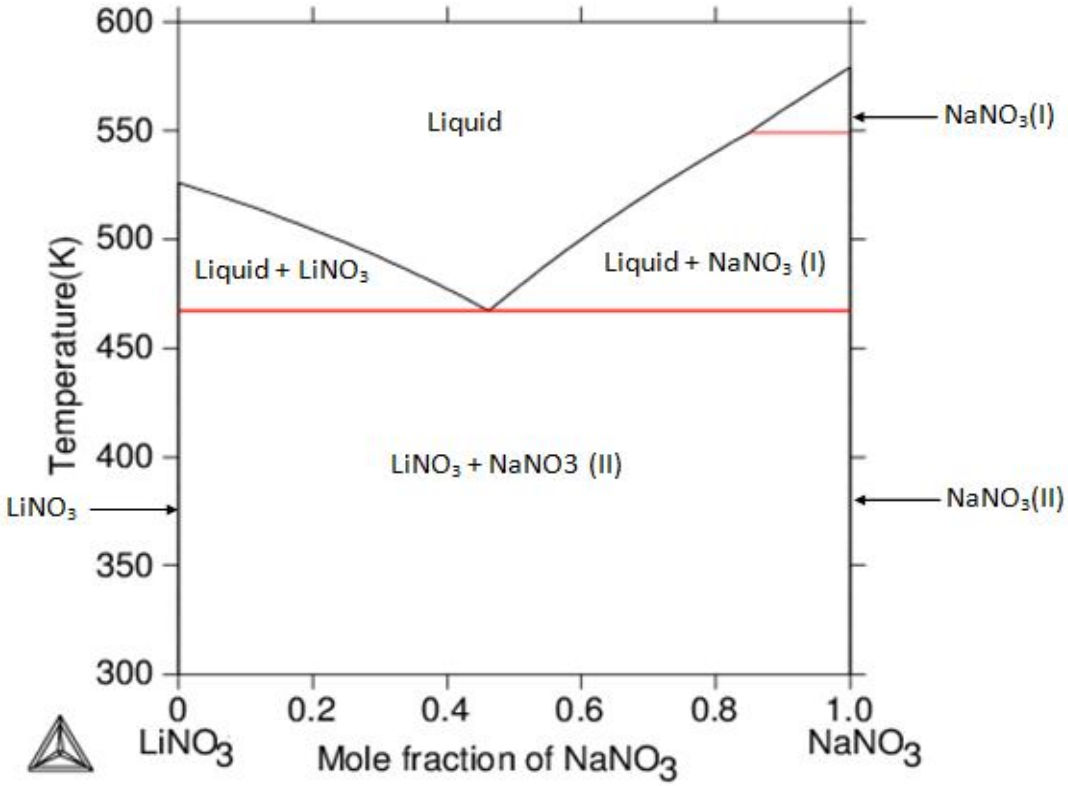

Fig. 20. Calculated phase diagram of $LiNO_3$-$NaNO_3$ system with thermodynamic parameters of Hellali et al. [23].

2.4 Phase diagram of the $CsNO_3$-$LiNO_3$-$NaNO_3$ ternary system

To the best of our knowledge, the only experimental information of phase diagram of the $CsNO_3$-$LiNO_3$-$NaNO_3$ ternary system are from Diogenov and Sarapulova [75]. By visual-thermal method, they investigated nine vertical sections and presented their results only in graphical form. They also established the crystallization surface of the ternary system. They identified two ternary eutectic reactions at 403 K (E_1) and 405 K (E_2). The equations and the molar compositions ($X_{MNO_3}^{E_i}$, M = Li, Na; i = 1, 2) corresponding to the two invariant reactions are given below:

E_1: Liq = $LiNO_3$ + $NaNO_3$ + $Cs_{0.5}Li_{0.5}NO_3$; $X_{LiNO_3}^{E_1} = 0.405$, $X_{NaNO_3}^{E_1} = 0.135$

E_2: Liq = $CsNO_3$ + $NaNO_3$ + $Cs_{0.5}Li_{0.5}NO_3$; $X_{LiNO_3}^{E_2} = 0.475$, $X_{NaNO_3}^{E_2} = 0.165$

The $NaNO_3$-$Cs_{0.5}Li_{0.5}NO_3$ section is a quasi-binary and presents a eutectic reaction (Liq = $NaNO_3$ + $Cs_{0.5}Li_{0.5}NO_3$) at 408 K.

Using the Wilson equation, Davison and Sun [207] estimated the phase equilibria of $CsNO_3$-$LiNO_3$-$NaNO_3$ system. Their work presents one major weakness: the phase diagram of $CsNO_3$-$LiNO_3$ binary system was described as a simple eutectic one.

3. Experimental investigations

Using a DTA device of great sensitivity, three samples in the $CsNO_3$-$LiNO_3$ binary system (molar compositions of $LiNO_3$, X_{LiNO_3} = 0.25; 0.50; 0.75) were analyzed. In addition, two vertical sections in the $CsNO_3$-$LiNO_3$-$NaNO_3$ ternary system were also studied: $X_{NaNO_3} = 0.2$ and $X_{CsNO_3} / X_{LiNO_3} = 1$. A detailed description of the apparatus has been given in a previous work [208]. The DTA measuring program consists in two heating/cooling cycles. The heating and cooling rates were in the range (0.3 – 0.5) K min^{-1}. Temperatures were measured using Pt/Pt10%Rh thermocouples calibrated against the invariant temperatures of high pure $AgNO_3$ (99.9 wt% purity) and KNO_3 (99.999 wt% purity). The overall uncertainty of the DTA temperature measurements was estimated at ±2 K.

The existence of the equimolar $Cs_{0.5}Li_{0.5}NO_3$ compound at ambient temperature was addressed using the X-ray diffraction technique. Samples $(Cs_X, Li_{1-X})NO_3$ with X = 1 (pure $CsNO_3$); 0 (pure $LiNO_3$) and 0.5, were analyzed at room temperature with a Siemens D5000 X-ray powder diffractometer, equipped with a copper anticathode using the Kα ray (λ = 1.5406 Å).

3.1 Reagents and samples preparation

Pure nitrates with high purity, $CsNO_3$ (Aldrich, 99.99%), $LiNO_3$ (Aldrich, 99.99%) and $NaNO_3$ (Aldrich, 99.995%) were used, for the preparation of mixtures, without further purification. All these nitrates were kept in a desiccator. Appropriate amounts of dried salts were melted several times in a platinum crucible to obtain a homogeneous substance. Then, mixtures were cooled and kept for 2 days in desiccator before analysis. For the sample ($Cs_{0.5}$, $Li_{0.5}$)NO_3, because of the likely presence of the intermediate compound $Cs_{0.5}Li_{0.5}NO_3$ at ambient temperatue, the coprecipitation method was also used.

In order to avoid any pollution of samples, all preparations were conducted in the glove box filled with argon.

3.2 Results and discussion

3.2.1 Phase diagram of the $CsNO_3$-$LiNO_3$ binary system

3.2.1.1 DTA Study

From the analysis of DTA curves, the equilibrium temperatures were determined (Table 4). Because of the pronounced tendency of supercooling, only the heating temperatures were considered. All the DTA curves show a thermal effect at about 334 K corresponding to either polymorphic transition temperature of the equimolar compound $Cs_{0.5}Li_{0.5}NO_3$ [72] or its formation temperature [84]. As an example, the DTA curves obtained for the sample with X_{LiNO_3} = 0.5 are given in Fig. 21. Whatever the method of elaboration, the thermograms have the same shape. Such an observation is a feature of an easy crystallization of the intermediate compound. The first peak observed during the heating at a mean temperature of 335 K is associated either with the formation of the intermediate compound $Cs_{0.5}Li_{0.5}NO_3$ [84] or its polymorphic transition [72]. A very weak effect (second peak) at 427.65 K appearing only in the sample obtained by repeated melting and cooling (Fig. 21a) is a signature of the II/I transition of $CsNO_3$. The thermal effect occurring at 443 K (Figs. 21a and 21b) is associated with the eutectic reaction: L = $CsNO_3$ (I) + $Cs_{0.5}Li_{0.5}NO_3$. That reveals a slight excess of $CsNO_3$ in the two samples ($Cs_{0.5}$, $Li_{0.5}$)NO_3 due certainly to weighing errors. The peak found at (456±2) K (Fig. 21a) or (463±2) K (Fig. 21b) corresponds to the fusion of the ($Cs_{0.5}$, $Li_{0.5}$)NO_3 samples.

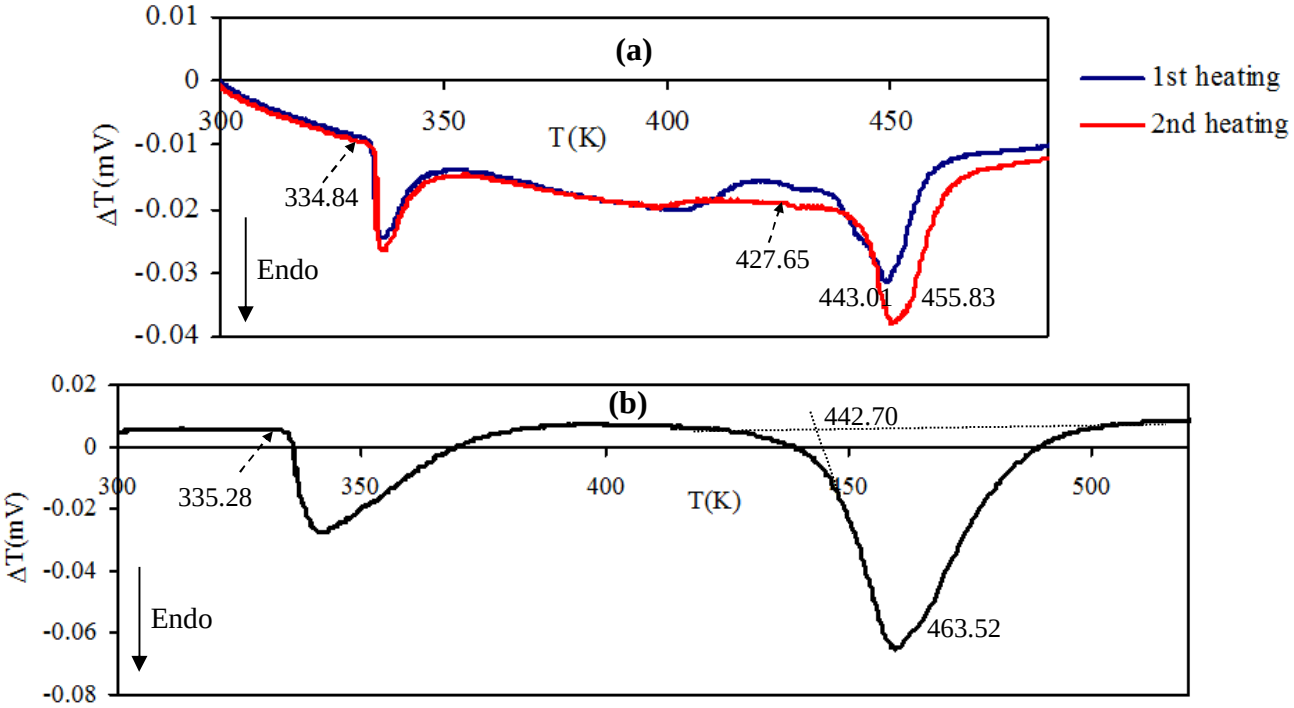

Fig. 21. DTA curves of samples $(Cs_{0.5}, Li_{0.5})NO_3$ at 0.5 K min^{-1} heating rate. (a) Sample obtained by repeated melting and cooling; (b) sample obtained by coprecipitation.

3.2.1.2 X-Ray results

The diffraction pattern at room temperature of sample $(Cs_{0.5}, Li_{0.5})NO_3$ prepared by coprecipitation is presented in Fig. 22 altogether with that of pure $LiNO_3$ (Fig. 22a) and that of pure $CsNO_3$ (Fig. 22b). As clearly showed in Fig. 22c, the XRD measurements revealed only the characteristic peaks of $CsNO_3$ and $LiNO_3$. This gives support to the presence of biphasic domain: "$CsNO_3$ + $LiNO_3$" which is in a very good agreement with Bélaïd-Drira et al.'s work [84]. Therefore, the intermediate compound $Cs_{0.5}Li_{0.5}NO_3$ does not exist at room temperature and the thermal effect observed at 335 K is obviously associated with its formation (heating) or its eutectoid decomposition (cooling).

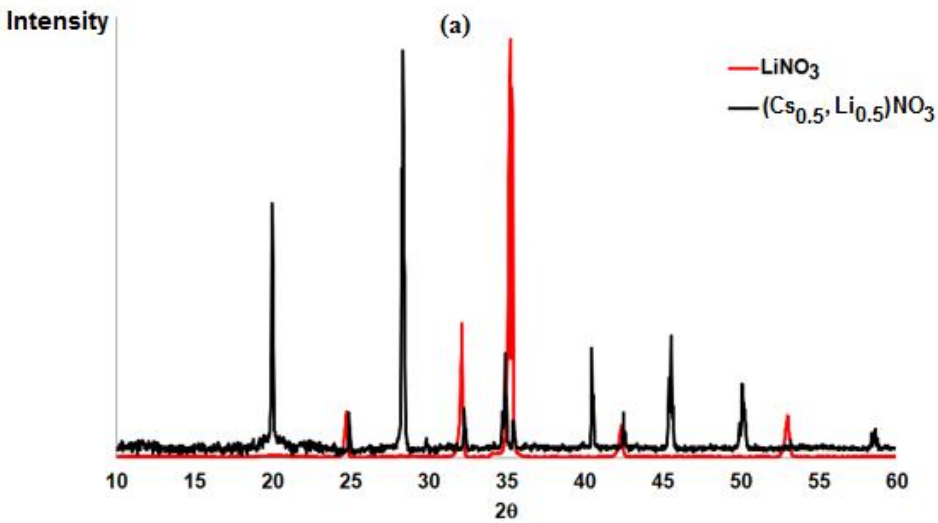

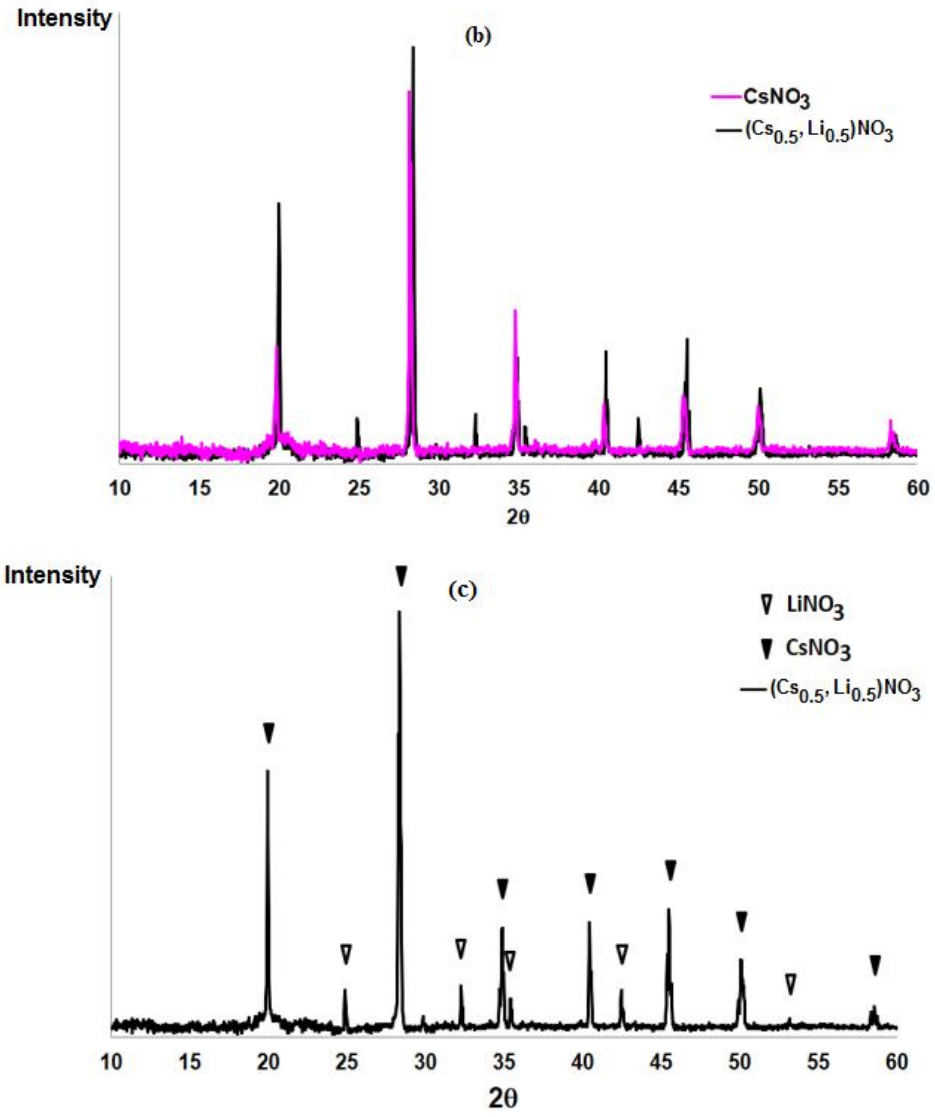

Fig. 22. X-ray diffraction patterns recorded at room temperature of samples in the $CsNO_3$-$LiNO_3$ binary system. (a) $LiNO_3$ and $(Cs_{0.5}, Li_{0.5})NO_3$; (b) $CsNO_3$ and $(Cs_{0.5}, Li_{0.5})NO_3$; (c) $(Cs_{0.5}, Li_{0.5})NO_3$.

3.2.2 $CsNO_3$-$LiNO_3$-$NaNO_3$ ternary system

As for the $CsNO_3$-$LiNO_3$ system, the interpretation of the thermal effects leads to the equilibrium temperatures in both vertical sections: $X_{NaNO_3} = 0.2$ and $X_{CsNO_3} / X_{LiNO_3} = 1$. Examples of DTA curves in these sections are shown in Figs. 23 (sample $(Cs_{0.15}, Li_{0.65}, Na_{0.2})NO_3$) and 24 (sample $(Cs_{0.25}, Li_{0.25}, Na_{0.5})NO_3$). The experimental results are listed in Tables 5 and 6. All tabulated temperatures are the mean repeatable values.

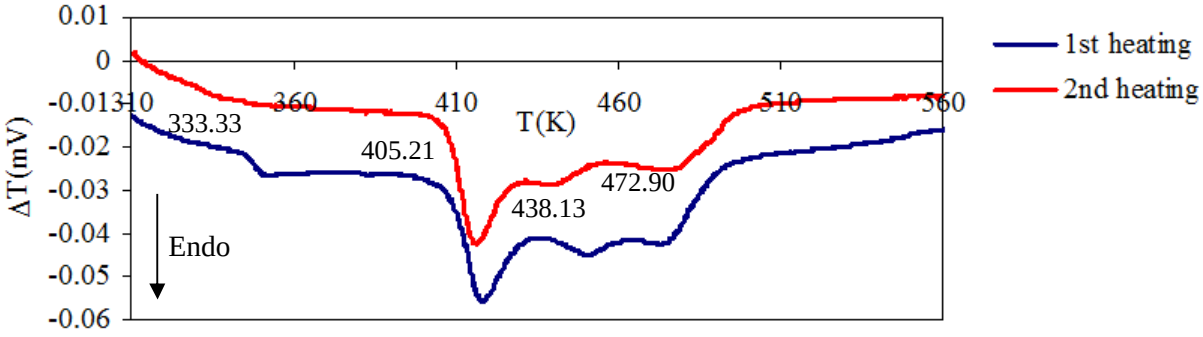

Fig. 23. DTA curves of sample ($Cs_{0.15}$, $Li_{0.65}$, $Na_{0.2}$)NO_3 at 0.5 K min^{-1} heating rate.

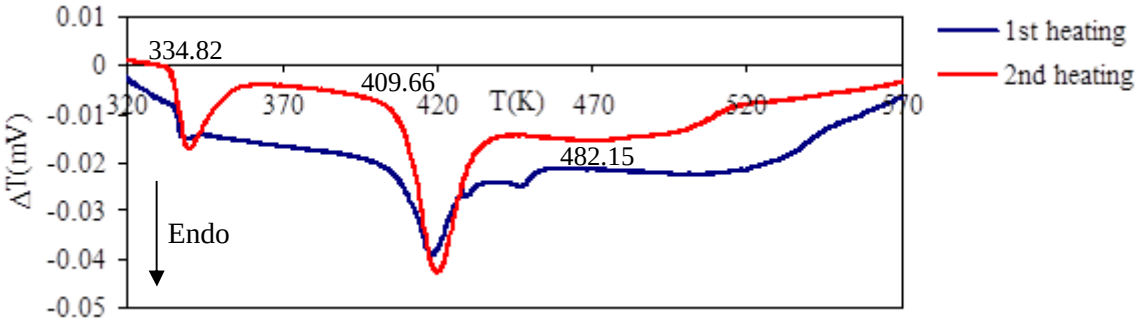

Fig. 24. DTA curves of sample ($Cs_{0.25}$, $Li_{0.25}$, $Na_{0.5}$)NO_3 at 0.5 K min^{-1} heating rate.

In order to construct the phase diagram of the $CsNO_3$-$LiNO_3$ binary system and the two vertical sections ($X_{NaNO_3} = 0.2$ and $X_{CsNO_3} / X_{LiNO_3} = 1$) of the $CsNO_3$-$LiNO_3$-$NaNO_3$ ternary system, over the entire composition range, a thermodynamic evaluation was done through the optimization procedure.

4. Thermodynamic modeling and optimization

4.1 Thermodynamic modeling

The $CsNO_3$-$LiNO_3$-$NaNO_3$ ternary system is formed by seven phases: $CsNO_3$ (II) (Hcp: Hexagonal form), $CsNO_3$ (I) (Cubic), $LiNO_3$ (Rhombo-S: Rhombohedral phase), $NaNO_3$ (II) (Rhombo-L: Rhombohedral low temperature form), $NaNO_3$ (I) (Rhombo-H: Rhombohedral high temperature form) solid phases considered as pure, intermediate compound $Cs_{0.5}Li_{0.5}NO_3$ and liquid phase. The models used to describe the Gibbs energy of the different phases are presented below. All other thermodynamic functions can be calculated directly from one or more derivatives of the Gibbs energy expression.

4.1.1 Pure components

The stable forms of the pure nitrates ($CsNO_3$, $LiNO_3$ and $NaNO_3$) are considered as single components. In Calphad-type approach, the Gibbs energy of the unary system *i* in a given physical state φ is generally expressed by Eq. (2):

$$^{0}G_i^{\varphi}(T) - {}^{0}H_i^{SER}(298.15K) = a + bT + cT\ln T + dT^2 + eT^3 + fT^4 + gT^7 + hT^{-1} + \ldots \quad (2)$$

$^{0}H_i^{SER}(298.15K)$ is the molar enthalpy of the component "*i*" in its standard reference state (SER) at 298.15 K and 10^5 Pa; *T* is the absolute temperature in Kelvin. The coefficients *a*, *b*, *c*…, are obtained from an optimization procedure.

From Eq. (2), the heat capacity of "*i*", in the state φ, can be evaluated by the following expression:

$$C_P^{i,\varphi} = -c - 2dT - 6eT^2 - 12fT^3 - 42gT^6 - 2hT^{-2} - \ldots \quad (3)$$

This expression is valid for temperatures above 298.15 K. In Calphad 2nd generation thermodynamic databases, temperatures below 298.15 K are not considered. It has to be pointed out that, in non-magnetic materials, the heat capacity at low temperature can be expressed by the following equation [209]:

$$C_P^{low} = \gamma T + AT^3 \quad (4)$$

where, γ is termed the electronic heat capacity coefficient and A is a parameter depending on the Debye temperature θ_D.

The plot C_P^{low}/T versus T^2 should therefore give a straight line.

As seen above, the transition $NaNO_3$ (II) → $NaNO_3$ (I) is assumed to be a second-order structural transition. This kind of transition is rarely represented in current thermodynamic unary databases. As stated in Ref. [210], the thermodynamic description of second-order transitions is a big challenge.

In the present work, as in the most evaluations [23, 25, 26, 35, 162, 175, 176, 205, 211, 212], the solid-solid transition in $NaNO_3$ is considered as a first-order transition. Robelin et al. [211] noticed that, this assumption has no effect on the calculated liquidus temperatures but the calculated number of phases at equilibrium at low temperatures may be incorrect. The temperature dependence of Gibbs energy for $NaNO_3$ given by Li et al. [212] is considered in the present evaluation.

4.1.2 Liquid phase

In the present evaluation, the substitutional solution model is used to describe the liquid phase. This model yields the following expression for the molar Gibbs energy:

$$G_m^L = \sum_i X_i^L \, {}^0G_i^L + RT\sum_i X_i^L \ln(x_i^L) + G^{L,xs} \quad (5)$$

Referred to the enthalpies of the components in their stable state at 298.15 K, ${}^0H_i^{SER}(298.15K)$, Eq. (5) becomes:

$$G_m^L - \sum_i X_i^L \, {}^0H_i^{SER}(298.15K) = \sum_i X_i^L \left({}^0G_i^L - {}^0H_i^{SER}(298.15K)\right) + RT\sum_i X_i^L \ln(X_i^L) + G^{L,xs} \quad (6)$$

X_i^L is the molar fraction of the component "*i*" in the liquid phase (L), ${}^0G_i^L$ is the Gibbs energy of "*i*" in the liquid state (L), *R* is the gas constant, *T* is the absolute temperature,

$G^{L,xs}$ is the excess Gibbs energy of the liquid phase (L) and can be described by the following expression:

$$G^{L,xs} = X_i^L X_j^L \sum_{\nu=0}^{\nu=n} {}^\nu L_{i,j}^L \left(X_i^L - X_j^L\right)^\nu + X_{CsNO_3}^L X_{LiNO_3}^L X_{NaNO_3}^L \left(X_{CsNO_3}^L \, {}^0L_{CsNO_3,LiNO_3,NaNO_3}^L + X_{LiNO_3}^L \, {}^1L_{CsNO_3,LiNO_3,NaNO_3}^L + X_{NaNO_3}^L \, {}^2L_{CsNO_3,LiNO_3,NaNO_3}^L\right) \quad (7)$$

where, ${}^\nu L_{i,j}^L$ $(i \neq j = CsNO_3, LiNO_3, NaNO_3)$ and ${}^\nu L_{CsNO_3,LiNO_3,NaNO_3}^L$ are the binary and the ternary interaction parameters, which are proposed by the Redlich-Kister polynomial [213] and the Redlich-Kister-Muggianu formalism [214, 215], respectively.

These parameters can be temperature dependent as follows:

$${}^\nu L^L = {}^\nu A^L + {}^\nu B^L T + {}^\nu C^L T \ln T + \ldots \quad (8)$$

The coefficients ${}^\nu A^L$, ${}^\nu B^L$, ${}^\nu C^L$, …, are constants to be optimized.

4.1.3 Stoichiometric phase

The intermediate phase $Cs_{0.5}Li_{0.5}NO_3$ named *I* in this work, is a stoichiometric compound and is modeled as $(CsNO_3)_{0.5}(LiNO_3)_{0.5}$. Its standard Gibbs energy of formation from the pure $CsNO_3$ (hexagonal form, Hcp) and $LiNO_3$ (rhombohedral form, Rhombo-S) nitrates is written as a function of temperature according to Eq. (9):

$$\Delta_f \, {}^0G_I = {}^0G_I - 0.5\,{}^0G_{CsNO_3}^{hcp} - 0.5\,{}^0G_{LiNO_3}^{rhombo-S} = C_1 + C_2T + C_3T\ln T \quad (9)$$

with constants C_1, C_2 and C_3 to be assessed.

4.2 Optimization and results

Optimization is the last step in the thermodynamic assessment task. By paraphrasing Ref. [216], optimization can be defined as a fitting process whereby the adjustable coefficients in the Gibbs energy equations are altered such that the best representation of both the experimentally measured equilibrium and thermochemical properties are obtained.

In the present work, the optimization is carried out using the Parrot module of the Thermo-Calc software [217]. The optimization procedure is based on generalized least squares (GLS) method which permits to assign each data a weight factor that reflects the uncertainty of measurements.

All recommended solid-solid transition and melting properties of $CsNO_3$, $LiNO_3$ and $NaNO_3$ from our critical analysis summarized in Table 7 are used in the present optimization.

4.2.1 Pure components

The thermodynamic descriptions for the pure nitrates (stable and metastable phases) based on our present work ($CsNO_3$ and $LiNO_3$) and from Ref. [212] ($NaNO_3$) are presented in Table 8. The limits of temperature at low temperature for $CsNO_3$ are determined from the plot C_P^{low}/T versus T^2, C_P^{low} is the heat capacity of the low temperature $CsNO_3$ form (see Fig. 25). The calculated heat capacities of the three pure nitrates compared with the selected experimental data are presented in Figs. 26, 27 and 28.

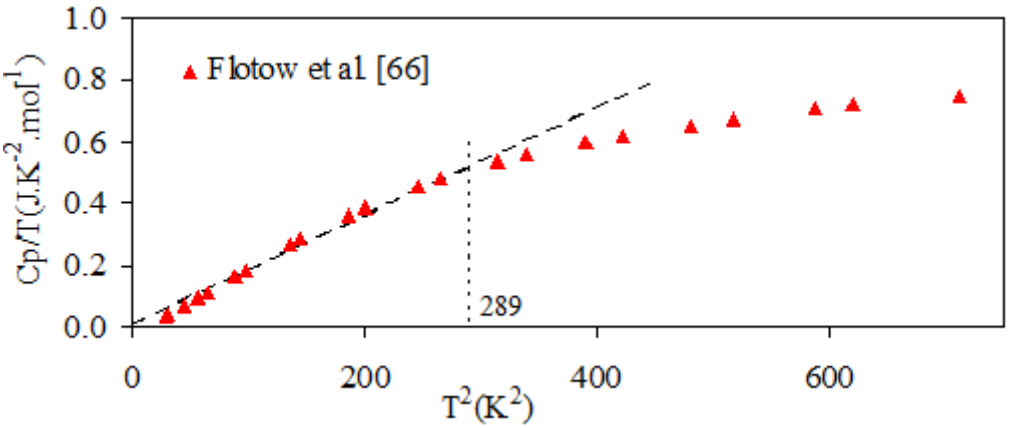

Fig. 25. Heat capacity of pure $CsNO_3$ plotted as Cp/T versus T^2.

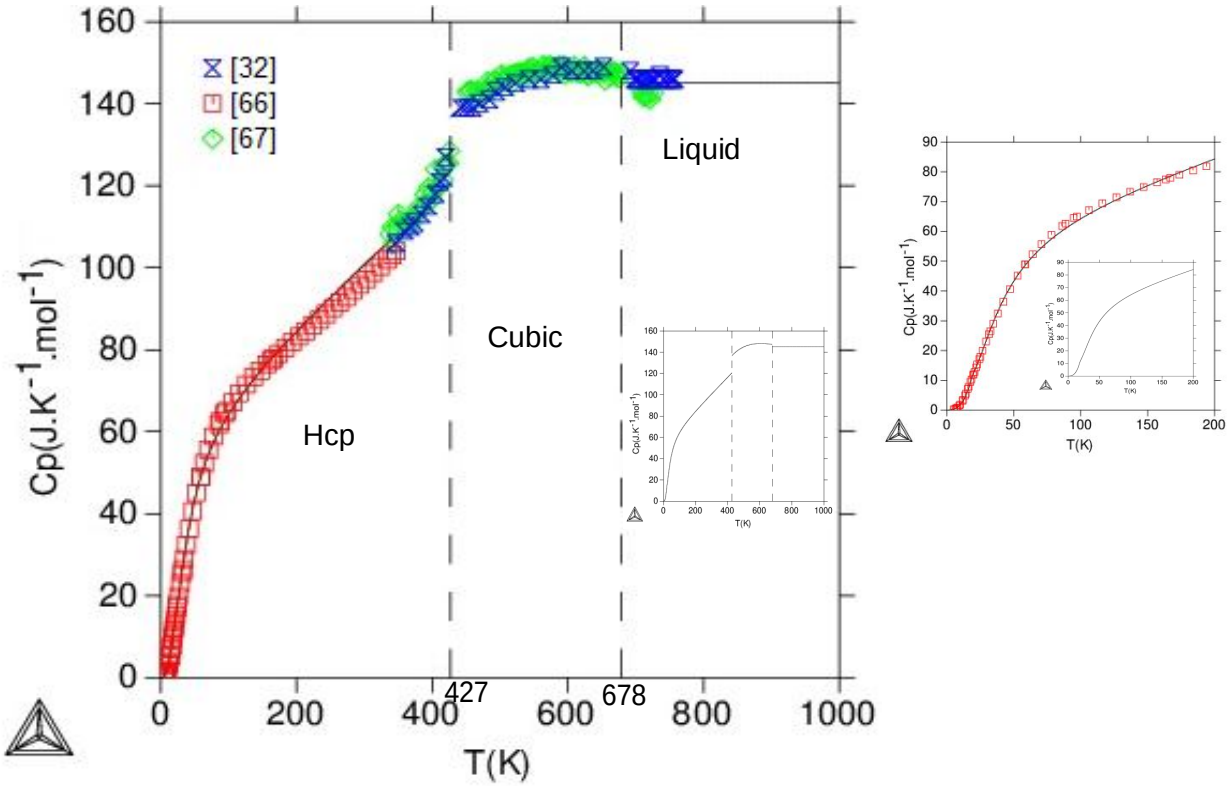

Fig. 26. Calculated heat capacity of pure $CsNO_3$ compared with experimental data.
Hcp: low temperature phase of $CsNO_3$ ($CsNO_3$ (II)); Cubic: high temperature phase of $CsNO_3$ ($CsNO_3$ (I))

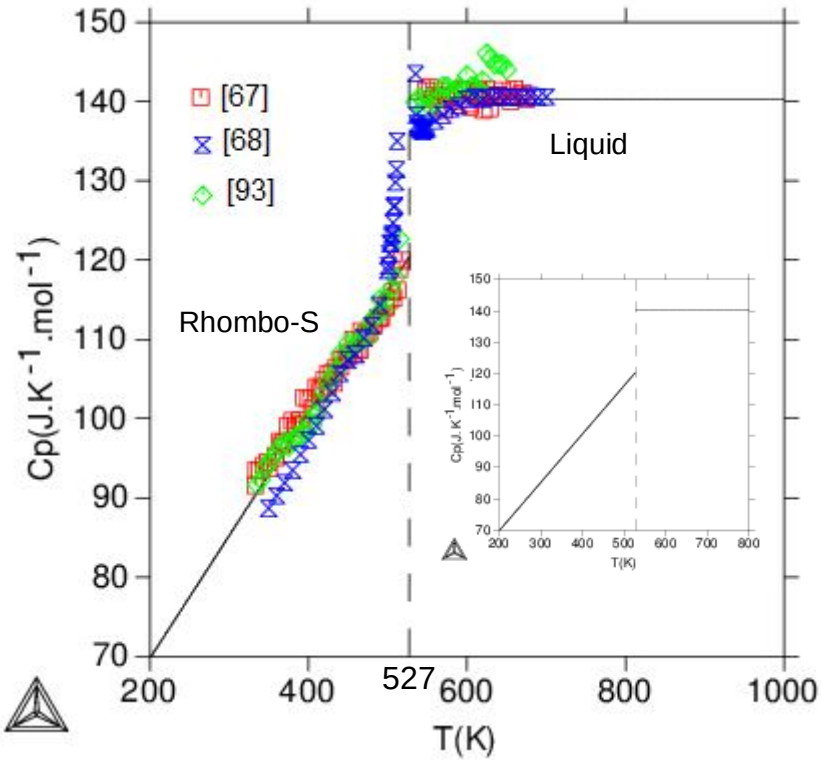

Fig. 27. Calculated heat capacity of pure $LiNO_3$ compared with experimental data.
Rhombo-S: solid phase of $LiNO_3$.

As it can be seen, the calculated heat capacities agree well with experimental data within experimental uncertainty for $CsNO_3$ and $LiNO_3$.

In assumption of first-order solid-solid transition, the agreement between calculation and experimental data for $NaNO_3$ can be considered as reasonable.

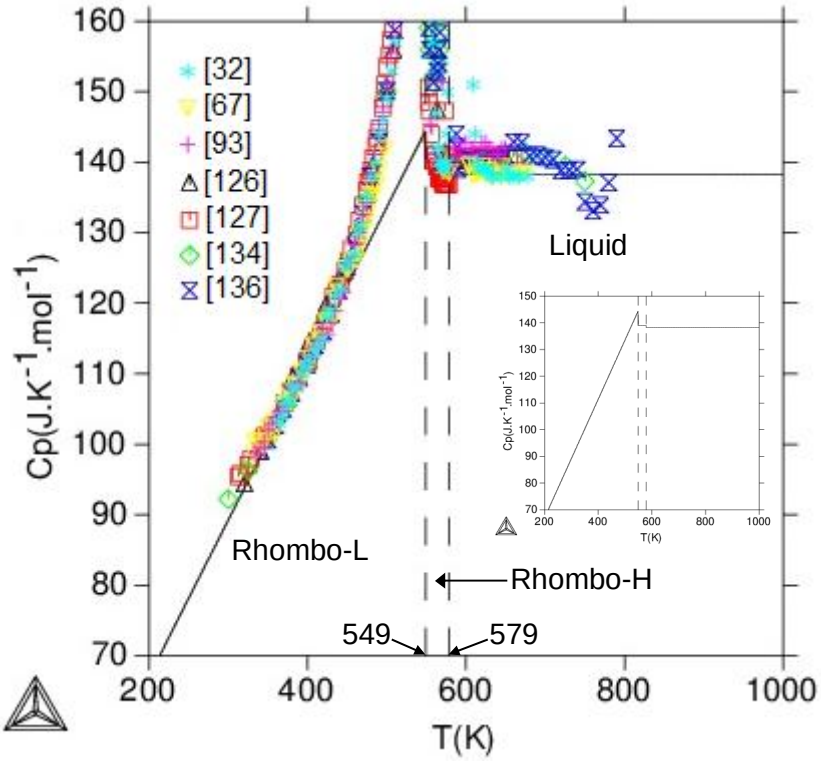

Fig. 28. Calculated heat capacity of pure $NaNO_3$ from parameters of Li et al. [212] compared with experimental data.
Rhombo-L: low temperature phase of $NaNO_3$ ($NaNO_3$ (II)); Rhombo-H: high temperature phase of $NaNO_3$ ($NaNO_3$ (I)).

4.2.2 Binary systems

4.2.2.1 $CsNO_3$-$LiNO_3$ system

Combining our present phase diagram results and those from literature [84, 201] with the enthalpies of mixing [203], the $CsNO_3$-$LiNO_3$ binary system has been optimized. Because of the very high liquidus temperatures on the $LiNO_3$-rich side, the data of Bol'shakov et al. [72] were disregarded. During the optimization procedure, the mutual solid solubilities of

$CsNO_3$ and $LiNO_3$ were neglected in agreement with the experimental results [72, 84, 201]. In addition, we have given slightly more weight to our phase diagram data taken to be more accurate. The enthalpy of formation determined by Zoro et al. [204] was also considered.

The thermodynamic parameters for liquid phase and intemediate compound $Cs_{0.5}Li_{0.5}NO_3$ (named *I*) are listed in Table 9.

Fig. 29 shows the calculated phase diagram and the selected experimental data. As can be seen, the calculation is in agreement with the experimental values.

Table 10 shows a comparison between the calculated and measured characteristics invariant equilibrium (temperature and composition) in the $CsNO_3$-$LiNO_3$ system. All invariant temperatures agree well within maximum ±4 K.

The calculated mixing enthalpy of liquid phase presented in Fig. 30 shows a good agreement with the experimental data.

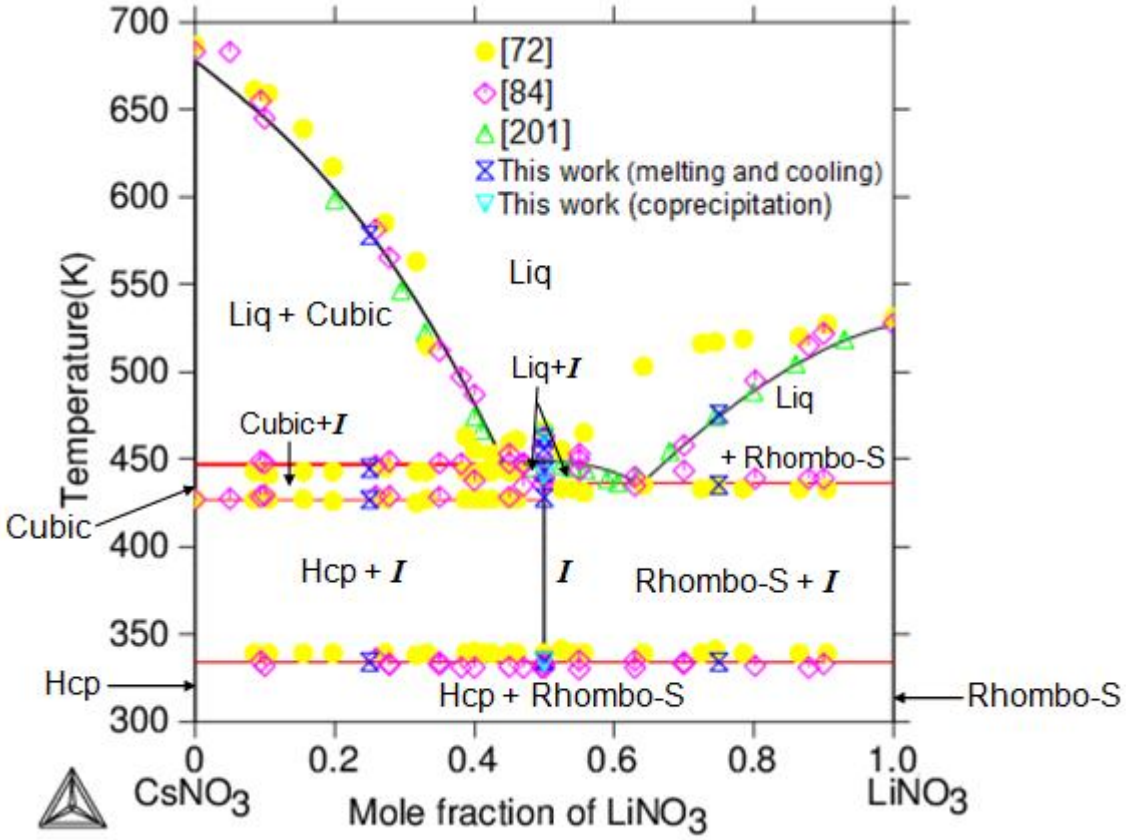

Fig. 29. Calculated phase diagram of $CsNO_3$-$LiNO_3$ system compared with experimental data. Cubic: high temperature phase of $CsNO_3$ ($CsNO_3$ (I)); Rhombo-S: solid phase of $LiNO_3$; Hcp: low temperature phase of $CsNO_3$ ($CsNO_3$ (II)); I: intermediate compound $Cs_{0.5}Li_{0.5}NO_3$.

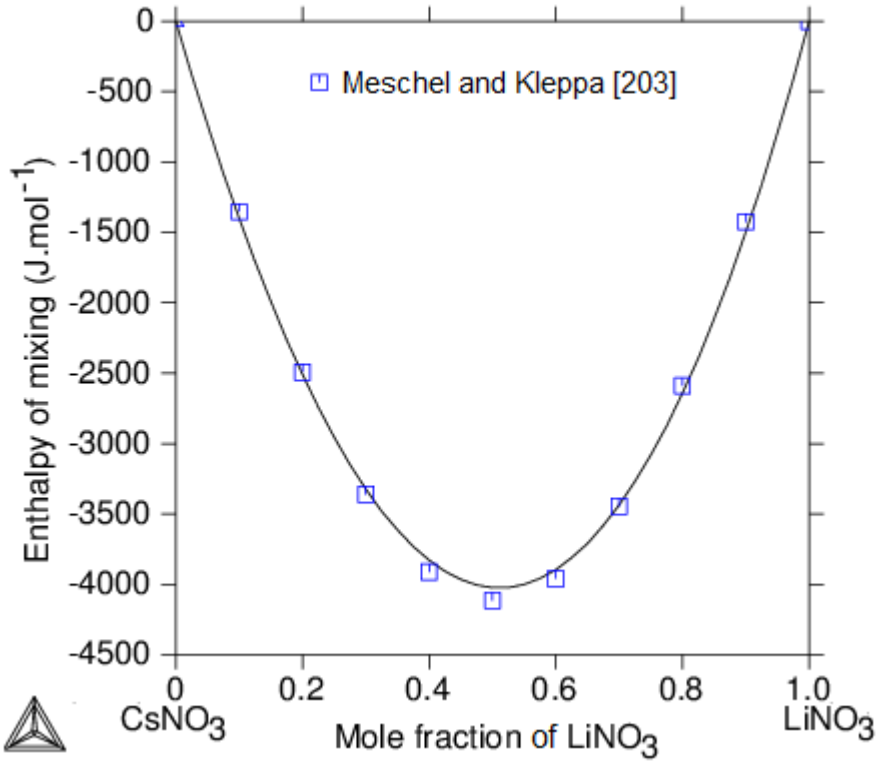

Fig. 30. Calculated enthalpy of mixing of liquid $CsNO_3$-$LiNO_3$ at 623 K, along with data from Meschel and Kleppa [203]. Reference states: liquid $CsNO_3$ and $LiNO_3$.

4.2.2.2 $CsNO_3$-$NaNO_3$ and $LiNO_3$-$NaNO_3$ systems

Because of the new lattice stabilities of pure nitrates considered in this work, the thermodynamic parameters of Jriri et al. [26] and those of Hellali et al. [23] were adjusted slightly in order to reproduce the same phase diagrams as shown in Figs. 19 and 20. The new parameters are listed in Table 9.

4.2.3 $CsNO_3$-$LiNO_3$-$NaNO_3$ ternary system

To obtain a satisfactory agreement with the phase diagram data, a ternary interaction term was necessary to represent the thermodynamic properties of the ternary liquid phase. Only the enthalpic part to the ternary interactive parameters was evaluated. Indeed, the entropic part had no significant effect on the calculation. The ternary interactive parameters obtained from the present optimization are listed in Table 9.

Figs. 31 and 32 represent the vertical sections calculated at $X_{CsNO_3} / X_{LiNO_3} = 1$ and $X_{NaNO_3} = 0.2$ compared with the experimental data. There is an overall agreement between the calculated results and the experimental data.

The calculated section for $X_{CsNO_3} / X_{LiNO_3} = 1$ is a quasi-binary and presents a eutectic reaction: Liq = $NaNO_3$ + $Cs_{0.5}Li_{0.5}NO_3$ at 411.03 K with $X^{Liq}_{LiNO_3}$ = 0.378 and $X^{Liq}_{NaNO_3}$ = 0.244. This reaction has been put in evidence experimentally in the temperature range (407 – 413) K. Diogenov and Sarapulova [75] reported a temperature at 408 K, on the basis of their investigation.

As presented in Fig. 32, the calculation confirms the two eutectic reactions (E_1 and E_2) suggested by our experimental work at (407 ± 2) K and (405 ± 2) K, respectively. Though the temperatures of both invariant reactions are in agreement within the experimental uncertainty with those of Diogenov and Sarapulova (405 K and 403 K) [75], there are differences in the compositions. Details of these invariant reactions are shown in Table 11.

The calculated monovariant lines (Fig. 33) and those obtained experimentally by Diogenov and Sarapulova [75] are almost similar. However, the polymorphic transition of $CsNO_3$ seems to be ignored in the work of Diogenov and Sarapulova [75] and may be one of reasons of discrepancy in the invariant compositions.

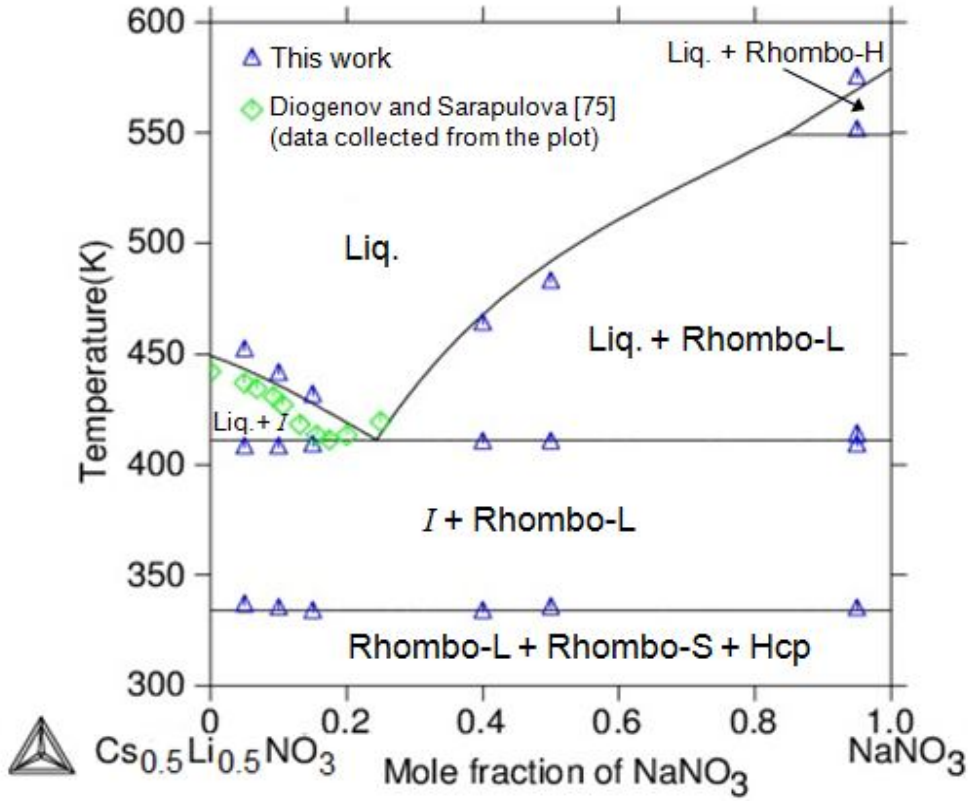

Fig. 31. Calculated vertical section at $X_{CsNO_3} / X_{LiNO_3} = 1$ compared with the experimental data. I: intermediate compound $Cs_{0.5}Li_{0.5}NO_3$; Rhombo-L: low temperature phase of $NaNO_3$ ($NaNO_3$ (II)) ; Rhombo-H: high temperature phase of $NaNO_3$ ($NaNO_3$ (I)); Rhombo-S: solid phase of $LiNO_3$; Hcp: low temperature phase of $CsNO_3$ ($CsNO_3$ (II));

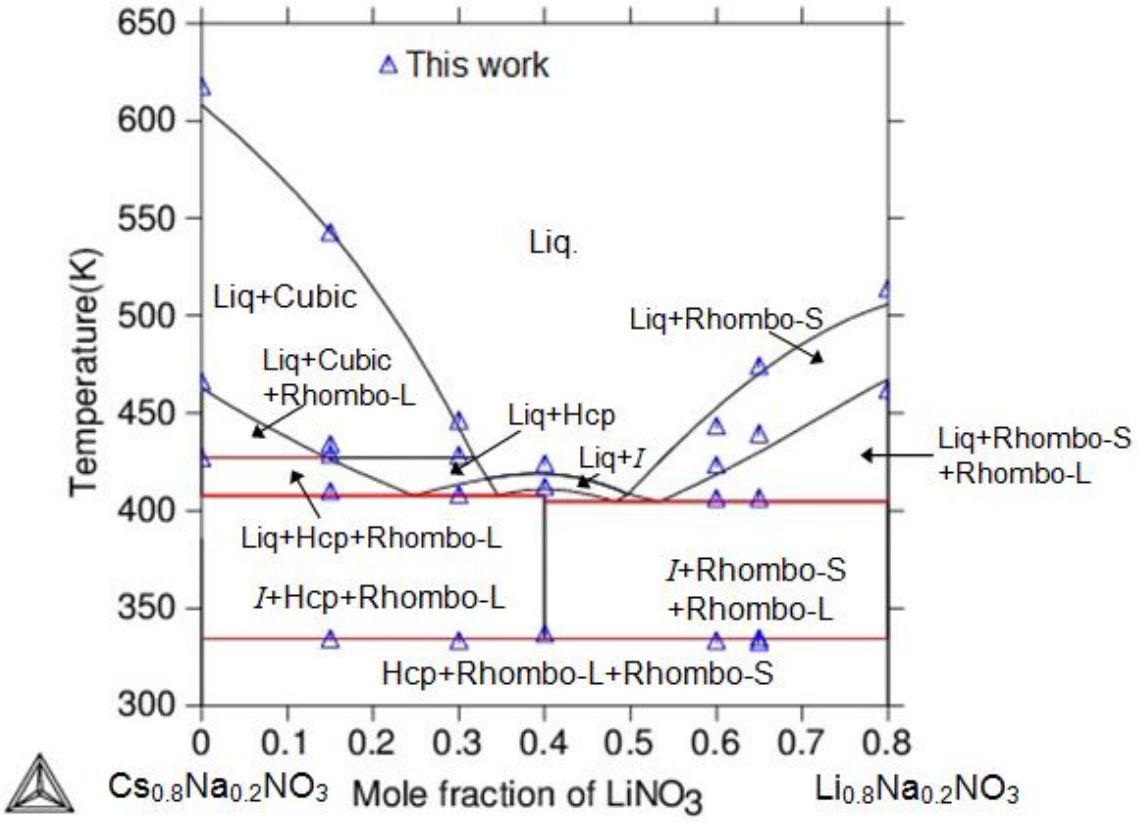

Fig. 32. Calculated vertical section at X_{NaNO_3} = 0.2 compared with the experimental data.

Cubic: high temperature phase of $CsNO_3$ ($CsNO_3$ (I)); Rhombo-S: solid phase of $LiNO_3$; Hcp: low temperature phase of $CsNO_3$ ($CsNO_3$ (II)); I: intermediate compound $Cs_{0.5}Li_{0.5}NO_3$; Rhombo-L: low temperature phase of $NaNO_3$ ($NaNO_3$ (II)).

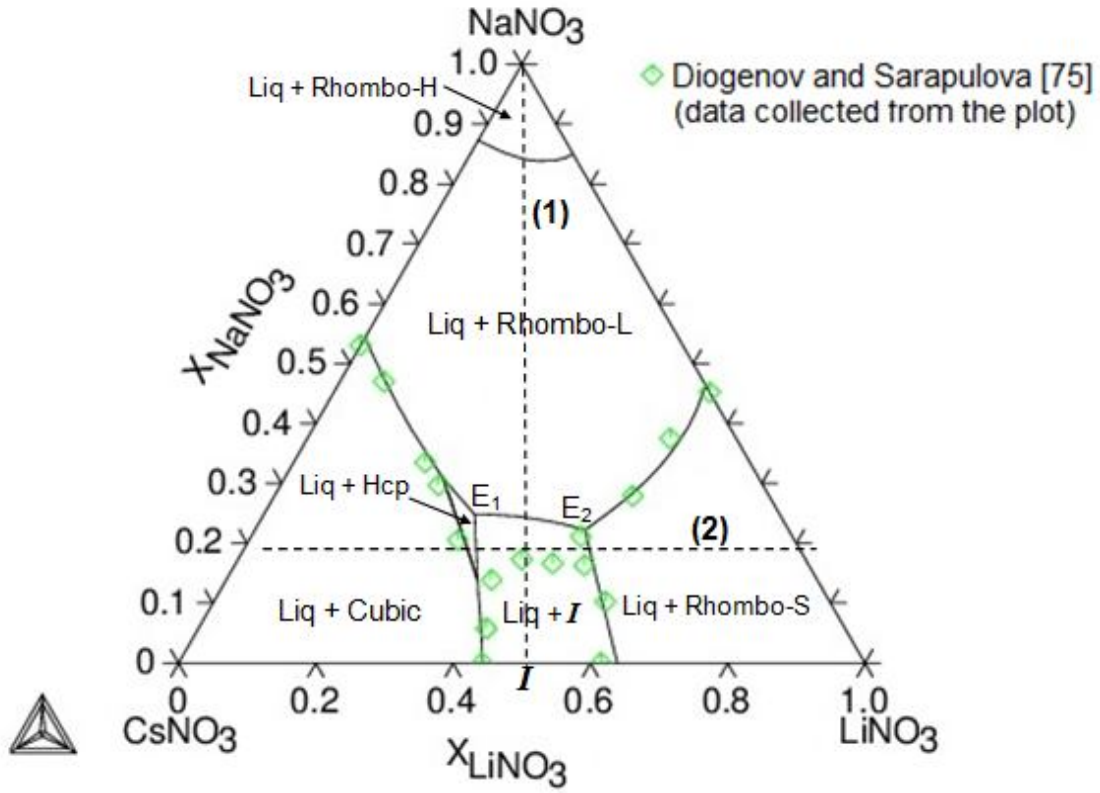

Fig. 33. Calculated monovariant lines in the $CsNO_3$-$LiNO_3$-$NaNO_3$ ternary system superimposed with data from Diogenov and Sarapulova [75]. (1) Section: $X_{CsNO_3} / X_{LiNO_3} = 1$; (2) section: $X_{NaNO_3} = 0.2$.

Rhombo-L: low temperature phase of $NaNO_3$ ($NaNO_3$ (II)); Hcp: low temperature phase of $CsNO_3$ ($CsNO_3$ (II)); I: intermediate compound $Cs_{0.5}Li_{0.5}NO_3$; Cubic: high temperature phase of $CsNO_3$ ($CsNO_3$ (I)); Rhombo-S: solid phase of $LiNO_3$.

5. Conclusions

Critical assessment of the ternary $CsNO_3$-$LiNO_3$-$NaNO_3$ system has been performed through an optimization procedure in which the experimental information based on our present work and those from literature were used. The first achievement of this work is the recommended thermochemical properties of $CsNO_3$, $LiNO_3$ and $NaNO_3$. Then, the phase equilibria in binary $CsNO_3$-$LiNO_3$ and the ternary $CsNO_3$-$LiNO_3$-$NaNO_3$ systems were studied using XRD and DTA techniques. Finally, a self consistent thermodynamic database of $CsNO_3$-$LiNO_3$-$NaNO_3$ ternary system has been constructed, which reproduced the available data within the experimental uncertainty.

The existence of the $Cs_{0.5}Li_{0.5}NO_3$ equimolar compound in $CsNO_3$-$LiNO_3$ system is confirmed with a eutectoid decomposition at 334.00 K. The phase diagram shows two eutectic reactions at 447.12 K and 436.10 K, respectively.

Two ternary eutectic reactions have been found in the ternary $CsNO_3$-$LiNO_3$-$NaNO_3$ system at 407.76 K and 404.63 K, respectively. Both are appropriate melting temperatures for medium temperature heat storage. The set of thermodynamic parameters obtained in this work could be used for the prediction of phase equilibria in multicomponent systems based on $CsNO_3$, $LiNO_3$ and $NaNO_3$.

References

[1] M. Medrano, M.O. Yilmaz, M. Nogués, I. Martorell, Joan Roca, Luisa F. Cabeza, Experimental evaluation of commercial heat exchangers for use as PCM thermal storage systems, Appl. Energy 86 (2009) 2047-2055.

[2] A. Gil, M. Medrano, I. Martorell, A. Lázaro , P. Dolado, B. Zalba, L. F. Cabeza, State of the art on high temperature thermal energy storage for power generation. Part 1-Concepts, materials and modellization, Renew. Sustain. Energy Rev. 14 (2010) 31-55.

[3] L.F. Cabeza, A. Castell, C. Barreneche, A. de Gracia, A.I. Fernández, Materials used as PCM in thermal energy storage in buildings: A review, Renew. Sustain. Energy Rev. 15 (2011) 1675-1695.

[4] S. Khare, M. Dell'Amico, C. Knight, S. McGarry, Selection of materials for high temperature latent heat energy storage, Sol. Energy Mater. Sol. Cells 107 (2012) 20-27.

[5] B. Zalba, J.M. Marín, L.F Cabeza, H. Mehling, Review on thermal energy storage with phase change: materials, heat transfer analysis and applications, Appl. Therm. Eng. 23 (2003) 251-283.

[6] M.M. Farid, A.M. Khudhair, S.A.K Razack, S. Al-Hallaj, A review on phase change energy storage: materials and applications, Energy Conver. Manag. 45 (2004) 1597-1615.

[7] S.D. Sharma, K. Sagara, Latent heat storage materials and systems: a review, Int. J. Green Energy 2(1) (2005) 1-56.

[8] F. Agyenim, N. Hewitt, P. Eames, M. Smyth, A review of materials, heat transfer and phase change problem formulation for latent heat thermal energy storage systems (LHTESS), Renew. Sustain. Energy Rev. 14 (2010) 615-628.

[9] E. Oró, A. de Gracia, A. Castell, M.M. Farid, L.F.Cabeza, Review on phase change materials (PCMs) for cold thermal energy storage applications, Appl. Energy 99 (2012) 513-533.

[10] D. Zhou, C.Y. Zhao, Y. Tian, Review on thermal energy storage with phase change materials (PCMs) in building applications, Appl. Energy 92 (2012) 593-605.

[11] B. Cárdenas, N. León, High temperature latent heat thermal energy storage: Phase change materials, design considerations and performance enhancement techniques, Renew. Sustain. Energy Rev. 27 (2013) 724-737.

[12] Z. Li, Z.-G. Wu, Numerical study on the thermal behavior of phase change materials (PCMs) embedded in porous metal matrix, Sol. Energy 99 (2014) 172-184.

[13] K. Pielichowska, K. Pielichowski, Phase change materials for thermal energy storage, Progress Mat. Sci. 65 (2014) 67-123.

[14] Z. Li, Z.-G.Wu, Analysis of HTFs, PCMs and fins effects on the thermal performance of shell-tube thermal energy storage units, Sol. Energy 122 (2015) 382-395.

[15] A. Hoshi, D.R. Mills, A. Bittar, T.S. Saitoh, Screening of high melting point phase change materials (PCM) in solar thermal concentrating technology based on CLFR, Sol. Energy 79 (2005) 332-339.
[16] S. Wang, P. Qin, X. Fang, Z. Zhang, S. Wang, X. Liu, A novel sebacic acid/expanded graphite composite phase change material for solar thermal medium-temperature applications, Sol. Energy 99 (2014) 283-290.
[17] D. Zhou, P. Eames, Thermal characterisation of binary sodium/lithium nitrate salts for latent heat storage at medium temperatures, Sol. Energy Mater. Sol. Cells 157 (2016) 1019-1025.
[18] G. Cáceres, K. Fullenkamp, M. Montané, K. Naplocha and A. Dmitruk, Encapsulated Nitrates Phase Change Material Selection for Use as Thermal Storage and Heat Transfer Materials at High Temperature in Concentrated Solar Power Plants, Energies 10 (1318) (2017) 1-21.
[19] Q. Mao, N. Liu, Li Peng, Recent investigations of Phase Change Materials use in solar thermal energy storage system, Advances Mat. Sc. Engineering ID 9410560 (2018) 1-13.
[20] Z. Li, Z.-G.Wu, Development of medium-temperature composite phase change material with high thermal stability and conductivity, Sol. Energy Mater. Sol. Cells 155 (2016) 341-347.
[21] L. Miró, J. Gasia, L.F. Cabeza, Thermal energy storage (TES) for industrial waste heat (IWH) recovery: A review, Appl. Energy 179 (2016) 284-301.
[22] F. Roget, C. Favotto, J. Rogez, Study of the KNO_3-$LiNO_3$ and KNO_3-$NaNO_3$-$LiNO_3$ eutectics as phase change materials for thermal storage in a low-temperature solar power plant, Sol. Energy 95 (2013) 155-169.
[23] D. Helali, D. Boa, H. Zamali, J. Rogez, M. Jemal, Thermodynamic assessment of the ternary $AgNO_3$-$LiNO_3$-$NaNO_3$ system, CALPHAD 35 (2011) 95-102.
[24] D. Hellali, D. Boa, H. Zamali, J. Rogez, Experimental study of phase equilibria in the ($AgNO_3$ + $LiNO_3$ + $NaNO_3$) ternary system, J. Chem. Thermodyn. 66 (2013) 102-115.
[25] M.W. Manouan, D. Boa, D. Hellali, H. Zamali, J. Rogez, Thermodynamic modeling of the $AgNO_3$-$CsNO_3$-$NaNO_3$ ternary system, CALPHAD 49 (2015)127-132.
[26] T. Jriri, J. Rogez, J.C. Mathieu, I. Ansara, Thermodynamic analysis of the $CsNO_3$-KNO_3-$NaNO_3$ system, J. Phase Equil. 20(5) (1999) 515-525.
[27] G.J. Janz, Molten Salts Handbook, Academic Press Inc., New York (1967).
[28] K.H. Stern, High Temperature Properties and Decomposition of Inorganic Salts Part 3, Nitrates and Nitrites, J. Phys. Chem. Ref. Data 1(3) (1972) 747-772.
[29] G.J. Janz, C.B. Allen, N.P. Bansal, R.M. Murphy, R.P.T. Tomkins, Physical Properties Data Compilations Relevant to Energy Storage. II. Molten Salts: Data on Single and Multi-Component Salt Systems, U.S. Department of Commerce, National Bureau of Standards (1979).
[30] N. Mossarello, Création d'une banque informatisée de données cohérentes sur les propriétés thermodynamiques des mélanges de sels fondus, Doctorat 3è cycle, Université de Provence – Aix-Marseille I, France (1986) (in French).
[31] Y. Dessureault, J. Sangster, A.D. Pelton, Evaluation critique des données thermodynamiques et des diagrammes de phases des systèmes AOH-AX, ANO_3-AX, ANO_3-BNO_3, AOH-BOH où A, B = Li, Na, K et X = Cl, F, NO_3, OH, J. Chem. Phys. 87 (1990) 407-453 (in French).
[32] T. Jriri, J. Rogez, C. Bergman, J.C. Mathieu, Thermodynamic study of the condensed phases of $NaNO_3$, KNO_3 and $CsNO_3$ and their transitions, Thermochimica Acta 266 (1995) 147-161.

[33] L.B. Pankratz, Thermodynamic Properties of Carbides, Nitrides, and Other Selected Substances, Bulletin 696: US Bureau of Mines, United States Department of the Interior (1995).
[34] Landolt-Börnstein, Thermodynamic properties of inorganic materials, Group IV, Vol. 19, Part 3, Springer-Verlag Berlin Heidelberg New York (2000) 150.
[35] J. Sangster, Thermodynamics and phase diagrams of 32 binary common-ion systems of the group Li,Na,K,Rb,Cs//F,Cl,Br,I,OH,NO_3, J. Phase Equil. 21(3) (2000) 241-268.
[36] J.F. Shackelford, W. Alexander, CRC – Materials Science and Engineering Handbook, CRC Press LLC (2001).
[37] M. Binnewies, E. Milke, Thermochemical Data of Elements and Compounds, Second, Revised and Extended Edition, Wiley-VCH Verlag GmbH, Weinheim (2002).
[38] D. Hellali, Contribution à l'étude thermodynamique des mélanges binaires et ternaires des nitrates d'argent, de césium, de lithium, de sodium et de rubidium, Habilitation universitaire en Chimie, Université El-Manar, Fac. Sc. Tunis, Tunisie (2013) (in French).
[39] H. Monia, Z. Hmida, K. Ismail, Heat capacities and enthalpies of fusion of lithium and rubidium nitrates: Heat capacities, enthalpies of fusion and enthalpies of formation of the intermediate compounds $Ag_{0.5}Rb_{0.5}NO_3$ and $Li_{0.5}Rb_{0.5}NO_3$, Thermochimica Acta 568 (2013) 204-208.
[40] M. Kamimoto, The possibility of high-temperature heat capacity measurements by Differential Scanning Calorimetry, Int. J. Thermoph. 11(2) (1990) 305-314.
[41] A. Sharma, V.V. Tyagi, C.R. Chen, D. Buddhi, Review on thermal energy storage with phase change materials and applications, Renew. Sustain. En. Reviews 13 (2009) 318-345.
[42] S. Kuravi, J. Trahan, D.Y. Goswami, M.M. Rahman, E.K. Stefanakos, Thermal energy storage technologies and systems for concentrating solar power plants, Progress En. Comb. Sc. 39 (2013) 285-319.
[43] N. Soares, J.J. Costa, A.R. Gaspar, P. Santos, Review of passive PCM latent heat thermal energy storage systems towards buildings' energy efficiency, Energy and Buildings 59 (2013) 82-103.
[44] M.M. Kenisarin, Thermophysical properties of some organic phase change materials for latent heat storage. A review, Solar Energy 107 (2014) 553-575.
[45] X. Sun, K. Ok Lee, M.A. Medina, Y. Chu, C. Li, Melting temperature and enthalpy variations of phase change materials (PCMs): a differential scanning calorimetry (DSC) analysis, Phase Transitions 91(6) (2018) 667-680.
[46] S. Drissi, A. Eddhahak, S. Caré, J. Neji. Thermal analysis by DSC of Phase Change Materials, study of the damage effect, J. Building Engineering 1 (2015) 3-19.
[47] A. Lomonaco, Stockage d'énergie thermique par matériaux à changements de phase adapté aux centrales solaires thermodynamiques, Thèse de Doctorat, Université de Pau et des Pays de l'Adour, France (2015) (in French).
[48] A. Lomonaco, D. Haillot, E. Pernot, E. Franquet, J.-P. Bédécarrats, Sodium nitrate thermal behavior in latent heat thermal energy storage: A study of the impact of sodium nitrite on melting temperature and enthalpy, Solar Ener. Mater. Solar Cells 149 (2016) 81-87.
[49] E. Charrier, E.L. Charsley, P.G. Laye, H.M. Markham, B. Berger, T.T. Griffiths, Determination of the temperature and enthalpy of the solid-solid phase transition of caesium nitrate by differential scanning calorimetry, Thermochim. Acta 445 (2006) 36-39.
[50] R. Ferro, G. Cacciamani, G. Borzone, Remarks about data reliability in experimental and computational alloy thermochemistry, Intermetallics 11 (2003) 1081-1094.

[51] J.C. Gomez, High-Temperature Phase Change Materials (PCM) Candidates for Thermal Energy Storage (TES) Applications, Milestone Report (2011) NREL/TP-5500-51446.
[52] M. Zhao, L. Zou, Y. Wu, Experimental analysis on crucible selection of thermal properties of nitrate salt, En. Procedia 143 (2017) 792-797.
[53] Y. Li, C.G. Wang, G.Y. Liu, Q.Z. Zhu, Z.Z. Qiu, Thermal property characterization of a low supercooling degree binary mixed molten salt for thermal energy storage system, Int. J. Thermophys. 41 (2019) 1-12. ttps://doi.org/10.1007/s10765-019-2501-9.
[54] K. Coscia, S. Nelle, T. Elliot, S. Mohapatra, A. Oztekin, S. Neti, Thermophysical properties of $LiNO_3$-$NaNO_3$-KNO_3 mixtures for use in concentrated solar power, J. Solar En. Engin. 135/034506 (2013) 1-5.
[55] C.N.R. Rao, B. Prakash, and M. Natarajan, Crystal Structure Transformations in Inorganic Nitrites, Nitrates, and Carbonates, National Bureau of Standards - National Standard Reference Data Series 53 (1975).
[56] J.R. Fernandes, S. Ganguly, C.N.R. Rao, Infrared spectroscopic study of the phase transitions in $CsNO_3$, $RbNO_3$ and NH_4NO_3, Spectroch. Acta 35A (1979) 1013-1020.
[57] F.J. Owens, Raman scattering study of the extrenal librational modes of the NO_3^- ion in the high temperature phase transitions of $CsNO_3$ and $RbNO_3$, Chem. Phys. Letters 64(I) (1979) 116-118.
[58] B.W. Lucas, The structure (Neutron) of phase II caesium nitrate at 298 K, $CsNO_3$, Acta Cryst. C39 (1983) 1591-1594.
[59] C. Dean, T.W. Hambley, M.R. Snow, Structures of phase IV rubidium nitrate, $RbNO_3$, and phase II caesium nitrate, $CsNO_3$, Acta Cryst. C40 (1984) 1512-1515.
[60] A.S. Chary, S.N. Reddy, T. Chiranjivi, Structural phase transition in $CsNO_3$: dielectric studies, Solid State lonics 62 (1993) 293-295.
[61] D. Pohl, T. Gross, Caesium nitrate (II) at 296 K, Acta Cryst. C49 (1993) 316-318.
[62] B. Zhou, T. Giavani, H. Bildsøe, J. Skibsted, H.J. Jakobsen, Structure refinement of $CsNO_3$(II) by coupling of ^{14}N MAS NMR experiments with WIEN2k DFT calculations, Chem. Phys. Letters 402 (2005) 133-137.
[63] N.V. Somov, F.F. Chausov, N.V. Lomova, Monoclinic low-temperature polymorph of cesium nitrate, Rus. J. Inorg. Chem. 63(11) (2018) 1443-1445.
[64] S. Satoh, The free rotation of NO_3^- ion in some nitrates, Sci. Res. Inst. Tokyo 48 (1954) 59-63.
[65] A. Mustajoki, Die spezifische Wärme des Cäsiumnitrats im Temperaturintervall 50…450°C sowie Dessen Umwandlungs und Schmelzwärme, Ann. Acad. Sci. Fenn. Series A, VI. Physica 7 (1957) 1-12 (in German).
[66] H.E. Flotow, P.A.G. O'Hare, J. Boerio-Goates, Heat capacity from 5 to 350 K and thermodynamic properties of cesium nitrate to 725 K, J. Chem. Thermodynamics 13 (1981) 477-483.
[67] K. Ichikawa, T. Matsumoto, The heat capacity of lithium, sodium, potassium, rubidium, and caesium nitrates in the solid and liquid states, Bull. Chem. Soc. Jpn. 56 (1983) 2093-2100.
[68] M.J. Maeso, J. Largo, The heat capacities of $LiNO_3$ and $CsNO_3$ from 350 to 700 K, Thermochim. Acta 222 (1993) 195-201.
[69] P.W. Bridgman, Polymorphic changes under pressure of the univalent nitrates, Proc. Am. Acad. Arts Sc. 51(12) (1916) 581-625.
[70] S. Gordon, C. Campbell, Differential thermal analysis of inorganic compounds. Nitrates and perchlorates of the alkali and alkaline earth groups and their subgroups, Anal. Chem. 27(7) (1955) 1102-1109.

[71] V.E. Plyushchev, I.B. Markina, L.P. Shklover, The diagrams of phase transformation of the binary systems obtained from rubidium and cesium nitrates with the nitrates of strontium and barium. Zh Neorg Khim. 1 (1956) 1613-1618 (in Russian).
[72] K.A. Bol'shakov, B.I. Pokrovskii and V.E. Plyushchev, Binary systems based on alkali metal nitrates, Zh. Neorgan. Khim. 6(9) (1961) 2120-2125 (in Russian).
[73] M. Bakes, J. Dupuy, J. Guion, Etude d'anomalies électroniques d'origine structural en sels fondus, C. R. Acad. Sci. Paris 256(11) (1963) 2376-2378 (in French).
[74] O.J. Kleppa, F.G. McCarty, Heats of fusion of the monovalent nitrates by high-temperature reaction calorimetry, J. Chem. Eng. Data 8(3) (1963) 331-332.
[75] G.G. Diogenov, I.F. Sarapulova, The Cs, Li, Na || NO_3 and Li, Na, Rb || NO_3 systems, Russ. J. Inorg. Chem. 10(8) (1965) 1052-1054.
[76] B.B. Owens, Melting properties of the alkali nitrates to 10000 atmospheres, J. Chem. Phys. 42(7) (1965) 2259-2262.
[77] K.J. Rao, C.N.R. Rao, Crystal structure transformations of alkali sulphates, nitrates and related substances: thermal hysteresis in reversible transformations, J. Mat. Sc. 1 (1966) 238-248.
[78] J.H. Fermor, A. Kjekshus, On the Electrical Properties of $RbNO_3$ and $CsNO_3$, Acta Chem. Scand. 26 (1972) 2645-2654.
[79] D.I. Marchidan, L. Vasu, Heat of melting for eutectics formed in binary-systems of $AgNO_3$ with KNO_3, $RbNO_3$, $CsNO_3$, AgCl and AgBr, Rev. Roum.Chim. 18 (1973) 1295.
[80] D. Sirousse-Zia, L. Denielou, J.P. Petitet, C. Tequi. Complément à l'étude thermodynamique de sels fondus à anion polyatomique, J. Phys. Lettres 38(2) (1977) 61-63 (in French).
[81] Y.S. Shenkin, Fusion diagrams for binary systems comprising alkali metal nitrates and chlorides, Zh. Fiz. Khim. 54(5) (1980) 1330-1332 (in Russian).
[82] A.S. Trunin, Designing and investigations of salt systems for solar energy utilization. In: Utilization of sun and other radiation sources in materials research. Kiev: Naukova Dumka (1983) 228-238 (in Russian).
[83] H. Zamali, M. Jemal, Diagrammes de phases des systèmes binaires KNO_3-$CsNO_3$ et KNO_3-$NaNO_3$, J. Therm. Anal. 41 (1994) 1091-1099 (in French).
[84] N. Bélaïd-Drira, H. Zamali, M. Jemal, Diagramme de phases du système binaire $CsNO_3$-$LiNO_3$. Activité des constituants du liquide, J. Therm. Anal. Calorim. 58 (1999) 607-615 (in French).
[85] D. Hellali, H. Zamali, A. Sebaoun, M. Jemal, Phase diagram of the $AgNO_3$-$CsNO_3$ system**,** J. Therm. Anal. Calorim. 57 (1999) 569-574.
[86] N. Bélaïd-Drira, H. Zamali, M. Jemal, Diagramme de phases et propriétés thermodynamiques du liquide du système binaire $CsNO_3$-$NaNO_3$, J. Soc. Chim. Tunisie 4(10) (2001) 1269-1278 (in French).
[87] E.A. Secco, R.A. Secco, Heats of solution/substitution in $TlNO_3$ and $CsNO_3$ crystals and in $RbNO_3$ and $CsNO_3$ crystals from heats of transition: the complete phase diagrams of $TlNO_3$-$CsNO_3$ and $RbNO_3$-$CsNO_3$ systems, J. Phys. Chem. Solids 63 (2002) 433-440.
[88] S. Wacharine, D. Hellali, H. Zamali, J. Rogez, M. Jemal, The phase diagram of $CsNO_3$-$RbNO_3$, J. Therm. Anal. Calorim. 107 (2012) 477-481.
[89] A. Abdessattar, D. Boa, D. Hellali, H. Zamali, Experimental study and thermodynamic analysis of ($CsNO_3$-$TlNO_3$) binary system, J. Alloys Comp. 739 (2018) 827-836.
[90] A. Cingolani, M.A. Berchiesi, G. Piantoni, D. Leonesi, The (Tl,Na,Li)NO_3, (Tl,Na,Rb)NO_3, (Tl,Na,Cs)NO_3 ternary systems, Z. Naturforsch. 27a (1972) 159-161.

[91] J.T. Nakos, Uncertainty analysis of thermocouple measurements used in normal and abnormal thermal environment experiments at Sandia's radiant heat facility and lurance canyon burn site, Sandia Report, SAND2004-1023 (2004).
[92] X. Wu, F.R. Fronczek, L.G. Butler, Structure of $LiNO_3$: point charge model and sign of the ^7Li quadrupole coupling constant, Inorg. Chem. 33 (1994) 1363-1365.
[93] Y. Takahashi, R. Sakamoto, M. Kamimoto, Heat capacities and latent heats of $LiNO_3$, $NaNO_3$, and KNO_3, International J. Thermoph. 9(6) (1988) 1081-1090.
[94] H.M. Goodwin, H.T. Kalmus, On the latent heat of fusion and the specific heat of salts in the solid and liquid state, Phys. Rev. 28(1) (1909) 1-24.
[95] P. Franzosini, C. Sinistri, Heat and entropy of fusion of lithium, sodium and potassium nitrates. Ric Sci. 3(4) (1963) 411-417.
[96] M. Kamimoto, Enthalpy measurements on $LiNO_3$ and $NaNO_2$ by twin high-temperature calorimeter, Thermochim. Acta 41 (1980) 361-369.
[97] J.G. Cordaro, A.M. Kruizenga, R. Altmaier, M. Sampson, A. Nissen, Thermodynamic properties of molten nitrate salts, in Granada (Spain), SolarPACES (2011).
[98] X. Zhang, K. Xu, Y. Gao, The phase diagram of $LiNO_3$-KNO_3, Thermoch. Acta 385 (2002) 81-84.
[99] M.L. Ruiz, I.D. Lick, M.I. Ponzi, E.R. Castellón, A. Jiménez-López, E.N. Ponzi, Thermal decomposition of supported lithium nitrate catalysts, Thermochim. Acta 499 (2010) 21-26.
[100] S. Kefi, D. Boa, D. Hellali, H. Zamali, Experimental investigation and calculation of the phase diagram of the binary system ($LiNO_3$+$TlNO_3$), J. Therm. Anal. Calorim. (2017), DOI : 10.1007/s10973-017-6645-1.
[101] M.B. Mohammad, G.A. Brooks, M.A. Rhamdhani, Premelting, Melting, and Degradation Properties of Molten Alkali Nitrates: $LiNO_3$, $NaNO_3$, KNO_3, and Binary $NaNO_3$-KNO_3, Metallurgical and Materials Transactions B (2018), https://doi.org/10.1007/s11663-018-1205-z.
[102] C. Vallet, Phase diagrams and thermodynamic properties of some molten nitrate mixtures, J. Chem. Thermodyn. 4 (1972) 105-114.
[103] M. Guizani, H. Zamali, M. Jemal, Diagramme de phases $LiNO_3$-KNO_3, C.R. Acad. Sci. Paris, t. 1, Série II c (1998) 787-789.
[104] M. Hichri, H. Zamali, M. Jemal, Système binaire $AgNO_3$-$LiNO_3$: Diagramme de phases et propriétes thermodynamiques des mélanges à l'état liquide, J. Therm. Anal. Calorim. 60 (2000) 453-461 (in French).
[105] E. Schürmann, L. Nedeljkovic, Kalorimetric und thermodynamik des systems $LiNO_3$-$NaNO_3$, Berichte der Bunsengesellschaft für Physikalische Chemie 74(5) (1970) 462-470 (in German).
[106] H.R. Carveth, Study of a three component-system, J. Phys. Chem. 2(4) (1898) 209-228.
[107] A. Lehrman, E. Adler, J. Freidus, M. Neimand, The liquidus curve and surface of the systems lithium and calcium nitrates and calcium, lithium and potassium nitrates, J. Am. Chem. Soc.59(1) (1937) 179-181.
[108] A. Lehrman, D. Breslow, The liquidus surface of the system sodium, lithium and calcium nitrates, J. Am. Chem. Soc. 60(4) (1938) 873-876.
[109] A.N. Campbell, The systems: $LiNO_3$-NH_4NO_3 and $LiNO_3$-NH_4NO_3-H_2O, J. Am. Chem. Soc. 64(11) (1942) 2680-2684.
[110] Y. Doucet, C. Vallet, Etude thermodynamique des mélanges de nitrate de potassium et nitrate de lithium fondus, C.R. Acad. Sc. Paris, t 259 (1964) 1517-1519 (in French).
[111] L.E. Gastwirt, E.F. Johnson, U.S. Atomic Energy Comm. Research and Develop. Rept., MATT-98, Plasma Physics Laboratory, Princeton University (1961).

[112] R.P. Tye, A.O Desjarlais, J.G. Bourne, in A. Cezairliyan (Ed.), Proceedings of the seventh symposium on thermophysical properties, the American Society of Mechannical Engineers (1977) 189 (cited in ref. [96]).
[113] J. Lefebvre, R. Fouret, C.M.E. Zeyen, Structure determination of sodium nitrate near the order-disorder phase transition, J. Physique 45(8) (1984) 1317-1327.
[114] W C-K Poon, E. Salje, The excess optical birefringence and phase transition in sodium nitrate, J. Phys. C: Solid State Phys. 21 (1988) 715-729.
[115] R.J. Reeder, S.A.T. Redfern, E. Salje, Spontaneous strain at the structural phase transition in $NaNO_3$, Phys. Chem. Minerals 15 (1988) 605-611.
[116] W.W. Schmahl, E. Salje, X-Ray diffraction study of the orientational order/disorder transition in $NaNO_3$: evidence for order parameter coupling, Phys. Chem. Minerals 16 (1989) 790-798.
[117] S.J. Payne, M.J. Harris, M.E. Hagen, M.T. Dove, A neutron diffraction study of the order-disorder phase transition in sodium nitrate, J. Phys.: Condens. Matter 9 (1997) 2423-2432.
[118] G. Gonschorek, H. Weitzel, G. Miehe, H. Fuess, W.W. Schmahl, The crystal structures of $NaNO_3$ at 100 K, 120 K, and 563 K, Z. Kristallogr. 215 (2000) 752-756.
[119] H. Yurtseven, S. Aslan, Temperature dependence of the Raman intensity and the Bandwidth close to the order-disorder phase transition in $NaNO_3$, Optics and Photonics Journal 2 (2012) 249-253.
[120] S.M. Antao, I. Hassan, W.H. Mulder, P.L. Lee, The $R\bar{3}c \rightarrow R\bar{3}m$ transition in nitratine, $NaNO_3$, and implications for calcite, $CaCO_3$, Phys. Chem. Minerals 35 (2008) 545-557.
[121] J.A.A. Ketelaar, B. Strijk, The atomic arrangement in solid sodium nitrate at high temperatures, Recueil Travaux Chim. Pays-Bas, 64(6) (2010), 174-182.
[122] P. Ballirano, Laboratory parallel-beam transmission X-ray powder diffraction investigation of the thermal behavior of nitratine $NaNO_3$: spontaneous strain and structure evolution, Phys. Chem. Minerals 38 (2011) 531-541.
[123] M.V. Regnault, Recherches sur la chaleur spécifique des corps simples et des corps composés, Ann. Chim. Phys. 1 (1841) 129-207 (in French).
[124] J.H. Schüller, Pogg. Ann. 136 (70) (1869) 235 (cited in book: C. Doelter, Handbuch der Mineralchemie, Band III, Erste Abteilung, Springer Science+Business Media, B.V. (1918), in German).
[125] J.C. Southard, R.A. Nelson, Low temperature specific heats. IV. The heat capacities of potassium chloride, potassium nitrate and sodium nitrate Am. Chem. Soc. 55 (1933) 4865-4869.
[126] H. Miekk-Oja, Kalorimetrische Untersuchungen ueber Umwandlungen in $NaNO_3$ und KNO_3, Ann. Acad. Sci. Fenn. Al-7 (1941) 7-65 (in German).
[127] V.A. Sokolov, H.E. Shmidt, Heat capacity and enthalpy of melting of sodium nitrate, Izv. Sekt. Fiz. Khim. Anal. Inst. Obshch. Neorg. Khim. Akad. Nauk. SSSR 26 (1955) 123-131 (in Russian).
[128] A. Mustajoki, Kalorimetrische Untersuchungen mit Bezug auf die Umwandlung in $NaNO_3$ und Dessen Sghmelzvorgang, Ann. Acad. Sci. Fenn. A6-5 (1957) 1-17 (in German).
[129] G.J. Janz, F.J. Kelly, J.L. Pérano, Melting and pre-melting phenomena in alkali metal nitrates, J. Chem. Eng. Data 9(l) (1964) 133-136.
[130] V.C. Reinsborough, F.E.W. Wetmore, Specific heat of sodium nitrate and silver nitrate by medium high temperature adiabatic calorimetry, Aust. J. Chem. 20 (1967) l-8.
[131] L. Kubicar, Fyz. Cas. 18(l) (1968) 58-63 (cited in ref. [32]).

[132] J. Dikant, Specific heat, thermal diffusivity and thermal conductivity of Ca doped $NaNO_3$ crystals near the transition point, Czech. J. Phys. B 22 (1972) 697-703.
[133] P. Nguyen-Duy, E.A. Dancy, Calorimetric determination of the thermodynamic properties of the alkali metal salts $NaNO_3$, KNO_3, $Na_2Cr_2O_7$, $K_2Cr_2O_7$ and their binary eutectic solutions, Thermochim. Acta 39 (1980) 95-102.
[134] R.W. Carling, C.M. Kramer, R.W. Bradshaw, D.A. Nissen, S.H. Goods, R.W. Mar, J.W. Munford, M.M. Karnowsky, R.N.Biefeld, N.J. Norem, Molten salt technology, Development Status Report, Sandia Laboratories, Energy Report (1981).
[135] D.J. Rogers, G.J. Janz, Melting-crystallization and premelting properties of $NaNO_3$-KNO_3. Enthalpies and heat capacities, J. Chem. Eng. Data 27(4) (1982) 424-428.
[136] R.W. Carling, Heat capacity of $NaNO_3$ and KNO_3 from 350 to 800 K, Thermochim. Acta 60 (1983) 265-275.
[137] M. Kawakami, K. Suzuki, S. Yokoyama, T. Takenaka, Heat capacity measurement of molten $NaNO_3$-$NaNO_2$-KNO_3 by drop calorimetry, VII International Conference on Molten Slags Fluxes and Salts, The South African Institute of Mining and Metallurgy (2004) 201-208.
[138] W. Ping, P. Harrowell, N. Byrne, C.A. Angell, Composition dependence of the solid state transitions in $NaNO_3$/KNO_3 mixtures, Thermochim. Acta 486 (2009) 27-31.
[139] T. Bauer, D. Laing, R. Tamme, Characterization of sodium nitrate as Phase Change Material, Int. J. Thermophys. 33 (2012) 91-104.
[140] K. Coscia, A. Oztekin, S. Mohapatra, S.Neti, S. Nelle, T. Elliot, Ternary molten salt heat transfer fluids for energy applications, Proceedings of the ASME 2012 Summer Heat Transfer Conference HT2012-58281, Rio Grande, Puerto Rico (2012).
[141] C. Martin, T. Bauer, H. Müller-Steinhagen, An experimental study of a non-eutectic mixture of KNO_3 and $NaNO_3$ with a melting range for thermal energy storage, Appl. Thermal Eng. 56 (2013) 159-166.
[142] W. Zhao, Characterization of encapsulated Phase Change Materials for thermal energy storage, Lehigh University, PhD (2013).
[143] B. D'Aguanno, M. Karthik, A.N. Grace, A. Floris, Thermostatic properties of nitrate molten salts and their solar and eutectic mixtures, Scientific Reports 8 :10485 (2018) 1-15.
[144] W. Klement Jr., A macroscopic description for the λ transition in sodium nitrate, J. Phys. Chem. 74(14) (1970) 2753-2757.
[145] C.C. Person, Recherches sur la chaleur latente de fusion, Ann. Chim. Phys. 21 (1847) 295-335 (in French).
[146] T.B. Douglas, Specific heats of liquid metals and liquid salts, Trans. ASME 79(1) (1957) 23-28.
[147] M. Bizouard, F. Pauty, Sur la mesure des chaleurs molaires de quelques sels et métaux fondus, C.R. Acad. Sci., 252 (1961) 514-515 (in French).
[148] S.E. Gustafsson, N.-O. Halling, R.A.E. Kjellander, Optical determination of thermal conductivity with a plane source technique, Z. Naturforsch. 23a (1968) 44-47.
[149] E.W. Dewing, Heat Capacities of Liquid Sodium and Potassium Nitrates, J. Chem. Eng. Data 20(3) (1975) 221-223.
[150] T. Asahina, M. Kosaka and H. Taoda, Reports of the Government Industrial Research Institute,Nagoya, 29-2 (1980) 25-30 (cited in ref. [32]).
[151] A.W.C. Menzies, N.N. Dutt, The liquidus surface of the ternary system composed of the nitrates of potassium, sodium and calcium, J. Am. Chem. Soc. 33(8) (1911) 1366-1375.

[152] M.G. Lowings, K.G McCurdy, L.G. Hepler, Heats of melting of sodium nitrate and indium by Differential Scanning Calorimetry : a suggestion for a new calibration substance, Thermochim. Acta23 (1978) 365-370.
[153] K.G. Zeeb, M.G. Lowings, K.G. McCurdy, L.G. Hepler, Heats of transition and melting of sodium nitrate by Differential Scanning Calorimetry : use of indium and sodium nitrate as calibration substances, Thermochim. Acta 40 (1980) 245-249.
[154] E.A. Dancy, Molar enthalpy of solid-solid transition in $NaNO_3$, Thermochim. Acta 59 (1982) 25l-252.
[155] B.P. Ghosh, K. Nag, Differential Scanning Calorimetric studies of several compounds showing order-disorder, J. Thermal Anal. 29 (1984) 433-437.
[156] O. Greis, K.M. Bahamdan, B.M. Uwais, The phase diagram of the system $NaNO_3$-KNO_3 studied by Differential Scanning Calorimetry, Thermochim. Acta 86 (1985) 343-350.
[157] M.J. Maeso, Tesis Doctoral, Universidad de Cantabria, Spain (1992) (cited in ref. [158]).
[158] M.J. Maeso, J. Largo, The phase diagrams of $LiNO_3$-$NaNO_3$ and LiNO3-KNO_3: the behaviour of liquid mixtures, Thermochim. Acta 223 (1993) 145-156.
[159] H. Zamali, Contribution à l'étude thermodynamique des mélanges binaires et ternaires des nitrates d'argent, de potassium et de sodium, Doctorat d'Etat ès-Sciences Physiques, D N° 194, Univ. Tunis II, Tunisie (1996) (in French).
[160] X. Zhang, J. Tian, K. Xu, Y. Gao, Thermodynamic evaluation of phase equilibria in $NaNO_3$-KNO_3system, J. Phase Equil. 24(5) (2003) 441-446.
[161] R.W. Berg, D.H. Kerridge,P.H. Larsen, $NaNO_2$+$NaNO_3$phase diagram: New data from DSC and Raman Spectroscopy, J. Chem. Eng. Data 51 (2006) 34-39.
[162] O. Beneš, R.J.M. Konings, S. Wurzer, M. Sierig, A. Dockendorf, A DSC study of the $NaNO_3$-KNO_3 system using an innovativeencapsulation technique, Thermochim. Acta 509 (2010) 62-66.
[163] B.D. Iverson, S.T. Broome, A.M. Kruizenga, J.G. Cordaro, Thermal and mechanical properties of nitrate thermal storage salts in the solid-phase, Solar Energy 86 (2012) 2897-2911.
[164] R. Benages-Vilau, Growth, morphology and solid state miscibility of alkali nitrates, PhD, Universitat de Barcelona (2013).
[165] R. Benages-Vilau, T. Calvet, M.A. Cuevas-Diarte, H.A.J. Oonk, The $NaNO_3$-KNO_3 phase diagram, Phase Transitions (2015). DOI: 10.1080/01411594.2015.1083567.
[166] K. Coscia, T. Elliott, S. Mohapatra, A. Oztekin, S. Neti, Binary and ternary nitrate solar heat transfer fluids, J. Solar En. Engin. 135/021011 (2013) 1-6.
[167] M. Chen, Y. Shen, S. Zhu, P. Li, Digital phase diagram and thermophysical properties of KNO_3-$NaNO_3$-$Ca(NO_3)_2$ ternary system for solar energy storage, Vacuum 145 (2017) 225-233.
[168] M.D. Romero-Sanchez, R.-R. Piticescu, A.M. Motoc, F. Aran-Ais,A.I. Tudor, Green chemistry solutions for sol-gel micro-encapsulation of phase change materials for high-temperature thermal energy storage, Manufacturing Rev. 5(8) (2018) 1-10.
[169] F.C. Kracek, Gradual transition in sodium nitrate. I. Physicochemical criteria of the transition, J. Am. Chem. Soc. 53(7) (1931) 2609-2624.
[170] D.M. Speros, R.L. Woodhouse, Realization of quantitative differential thermal analysis. I Heats and rates of solid-liquid transitions, J. Phys. Chem. 67(10) (1963) 2164-2168.
[171] H. Zamaly, M. Jemal, Diagramme de phases du système binaire NaNO2-NaNO3, J. Soc. Chim. Tunisie 8 (1982) 17-21 (in French).

[172] T. Jriri, J. Rogez, J.C. Mathieu, Diagramme de phases $NaNO_3$-$CsNO_3$, C.R. Acad. Sci. Paris, t. 321, Série II *b* (1995) 163-165 (in French).
[173] H. Zamali, M. Jemal, Phase diagrams of binary systems: $AgNO_3$-KNO_3 and $AgNO_3$-$NaNO_3$, J. Phase Equil. 16(3) (1995) 235-238.
[174] B.D. Babaev, System NaF-NaCl-NaNO3, Inorganic Materials 38(1) (2002) 83-84 (translated from Neorganicheskie Materialy 38(1) (2002) 96-97).
[175] A. Abdessattar, D. Hellali, D. Boa, H. Zamali, Experimental investigation and calculation of the phase diagram ofthe binary system ($NaNO_3$-$TlNO_3$), J. Alloys Comp. 651 (2015) 773-778.
[176] D. Sergeev, E.Yazhenskikh, D. Kobertz, K. Hack, M.Müller, Phase equilibria in the reciprocal NaCl-KCl-$NaNO_3$-KNO_3 system, CALPHAD 51 (2015) 111-124.
[177] C.Y. Zhao, Y. Ji, Z. Xu, Investigation of the $Ca(NO_3)_2$-$NaNO_3$ mixture for latent heat storage, Solar Ener. Mater. Solar Cells 140 (2015)281-288.
[178] N.K. Karoui, Dalila Hellali, A. Saidi, H. Zamali, The phase diagram of the isobaric binary system ($NaNO_3$ + $RbNO_3$), J. Therm. Anal. Calorim. (2016). DOI : 10.1007/s10973-015-5226-4.
[179] Y.Y. Chen, C.Y. Zhao, Thermophysical properties of $Ca(NO_3)_2$-$NaNO_3$-KNO_3 mixtures for heat transfer and thermal storage, Solar Energy 146 (2017) 172-179.
[180] T. Morita, K. Fukuda, H. Kutsuna, Kobe Shosen Daigaku Kiyo, Dai-2-rui: Shosen, Rikogakuhen 38-4 (1990) 129-137.
[181] T. Hu, H.C. Ko, L.G. Hepler, Calorimetric investigations of molten salts, J. Phys. Chem. 68(2) (1964) 387-390.
[182] D. Sergeev, E. Yazhenskikh, N. Talukder, D. Kobertz, K. Hack, M.Müller, Thermodynamics of the reciprocal NaCl-KCl-$NaNO_3$-KNO_3 system, CALPHAD 53 (2016) 97-104.
[183] J.B. Austin, R.H.H. Pierce Jr., The Linear Thermal Expansion of a single crystal of sodium nitrate,J. Am. Chem. Soc. 55(2) (1933) 661-668.
[184] G. Bruni, D. Meneghini, Bildung und Zersetzung von Mischkrystallen zwischen Alkalinitraten und -Nitriten, Z. Anorg. Chem. 64(1) (1909) 193-199 (in German).
[185] C. Vassas-Dubuisson, Effet de la température sur les raies raman de basse fréquence du nitrate de sodium. J. Phys. Radium 9(3) (1948) 91-92 (in French).
[186] R. Kawashima, K. Katsuxi, K. Suzuki, Behaviour of the fundamental absorption edge of sodium nitrate near the lambda transition, Phys. Lett. 90A(6) (1982) 297-299.
[187] M.J. Harris, E.K.H. Salje, B.K. Giittler, An infrared spectroscopic study of the internal modes of sodium nitrate: implications for the structural phase transition, J. Phys.: Condens. Matter 2 (1990) 5517-5527.
[188] J.H. Fermor, A. Kjekshus, On the electrical properties of NaNO3, Acta Chem. Scand. 22 (1968) 1628-1636.
[189] L.G. Kolomin, P.I. Protsenko, Electrical conductivity of polycrystalline alkali nitrates in stable states and at phase transitions, Izvestiya VUZ. Fizika 11(10) (1968) 119-124.
[190] Y. Takeuchi, Y. Sasaki, Elastic properties and thermal expansion of $NaNO_3$ single crystal, J. Phys. Soc. Japan 61(2) (1992) 587-595.
[191] M.O. Steinitz, D.A. Pink, J.P. Clancy, A.N. MacDonald, I. Swainson, Sodium nitrate - a difficult discontinuous phase transition, Can. J. Phys. 82 (2004) 1097-1107.
[192] J.P. Petitet, M. Fraiha, R. Tufeu, B. Le Neindre, Experimental determination of the volume change pure salts and salt mixtures at their melting point, Intern. J. Thermo. 3(2) (1982) 137-155.
[193] C.M. Kramer, Z.A. Munir,J.V. Volponi, Simultaneous Dynamic Thermogravimetry and Mass Spectrometry of the evaporation of alkali metal nitrates and nitrites, J. Thermal Anal. 27 (1983) 401-408.

[194] V.H. Schinke, F. Sauerwald, Über die Volumenänderung beim Schmelzen und den Schmelzprozeβ bei anorganischen Salzen, Z. anorg. allg. Chemie (304) (1960) 25-36 (in German).
[195] A. Kofler, Mikrothermoanalyse des Systems $NaNO_3$-KNO_3, Monatsh. Chem. 86(4) (1955) 643-652 (in German).
[196] Von G. Tammann, A. Ruppelt, Die Entmischung lückenloser Mischkristallreihen, Z. anorg. u. allg. Chem. Bd. 197 (1931) 65-89.
[197] H.C. Ko, T. Hu, J.G. Spencer, C.Y. Huang, L.G. Hepler, Cryoscopic investigations and phase equilibria, J. Chem. Eng. Data 8(3) (1963) 364-366.
[198] E.R.Van Artsdalen, Complex ions in molten salts. Ionic association and common ion effect, J. Phys.Chem. 60(2) (1956) 172-177.
[199] F. Brehat, B. Wyncke, Analysis of the temperature-dependent infrared active lattice modes in the ordered phase of sodium nitrate, J. Phys. C: Solid State Phys. 18 (1985) 4247-4259.
[200] E. Rapoport, C.W.F.T Pistorius, Polymorphism and melting of ammonium, thallous, and silver nitrates to 45 kbar, J. Chem. Phys. 44(4) (1966) 1514-1519.
[201] N.N. Nurminskii, G.G. Diogenov, Russ. J. Inorg. Chem. 5 (1960) 1011 (cited in Ref. [30]).
[202] O.J. Kleppa, L.S. Hersh, Heats of mixing in liquid alkali nitrate systems, J. Chem. Phys.34(2) (1961) 351-358.
[203] S.V. Meschel, O.J. Kleppa, Enthalpies of mixing in ternary fused nitrates, J. Chem. Phys. 48(11) (1968) 5146-5154.
[204] E. Zoro, Hellali. D. Boa, H. Zamali, J. Rogez, to be published.
[205] J.I. Beltrán, J. Wang, F. Montero-Chacón, Y. Cui, Thermodynamic modeling of nitrate materials for hybrid thermal energy storage: using latent and sensible mechanisms, Solar Energy 155 (2017) 154-166.
[206] X. An, P. Zhang, J. Cheng, S. Chen, J. Wang, Thermodynamic reevaluation and experimental validation of the $CsNO_3$-KNO_3-$NaNO_3$ system and its subsystems, Chem. Res. Chin. Univ. (2017). doi: 10.1007/s40242-017-6137-7.
[207] S.M. Davison, A.C. Sun, Thermodynamic analysis of solid-liquid phase equilibria of nitrate salts, Ind. Eng. Chem. Res. 50 (2011) 12617-12625.
[208] T. Jriri, Contribution à l'étude thermodynamique des systèmes binaires et ternaires de nitrates alcalins, Thèse de Doctorat, Université Aix-Marseille I, France (1994) (in French).
[209] M. Palumbo, B. Burton, A. Costa e Silva, B. Fultz, B. Grabowski, G. Grimvall, B. Hallstedt, O. Hellman, B. Lindahl, A. Schneider, P.E.A. Turchi, W. Xiong, Thermodynamic modeling of crystalline unary phases, Phys. Status Solidi B 251(1) (2014) 14-32.
[210] S. Stølen, Tor Grande, N.L. Allan, Chemical Thermodynamics of Materials Macroscopic and Microscopic Aspects, John Wiley & Sons Ltd, The Atrium, Southern Gate, Chichester, West Sussex PO19 8SQ, England (2004).
[211] C. Robelin, P. Chartrand, A.D. Pelton, Thermodynamic evaluation and optimization of the ($NaNO_3$ + KNO_3 + Na_2SO_4 + K_2SO_4) system, J. Chem. Thermodyn. 83 (2015) 12-26.
[212] X. Li, Z. Fei, Y. Wang, L. Xie, Experimental investigation and thermodynamic modeling of the NaCl-$NaNO_3$-Na_2SO_4 ternary system, Chem. Res. Chin. Univ. (2018). DOI: 10.1007/s40242-018-7339-3.
[213] O. Redlich, A.T. Kister, Algebraic representation of thermodynamic properties and the classification of solutions, Ind. Eng. Chem. 40(2) (1948) 345-348.

[214] Y.M. Muggianu, M. Gambino, J.P. Bros, Enthalpies de formation des alliages liquides bismuth-étain-gallium à 723 K. Choix d'une représentation analytique des grandeurs d'excès intégrales et partielles de mélange, J. Chim. Phys. 72 (1975) 83-88 (in French).
[215] M. Hillert, Empirical methods of predicting and representing thermodynamic properties of ternary solution phases, CALPHAD 4(1) (1980) 1-12.
[216] N. Saunders, A.P. Miodownik, CALPHAD (Calculation of Phase Diagrams): a Comprehensive Guide. Oxford: Pergamon, Elsevier Science (1998).
[217] J-O. Andersson, T. Helander, L. Höglund, P. Shi, Bo Sundman, THERMO-CALC & DICTRA, Computational Tools For Materials Science, CALPHAD 26(2) (2002) 273-312.

Table 1

Temperatures and enthalpies of solid-solid transition and melting of $CsNO_3$ from literature

$T_{II/I}$ (K)	T_m (K)	$\Delta_{II/I}H°$(J mol^{-1})	$\Delta_m H°$(J mol^{-1})	Method[(a)]	Sample characteristics	Ref.
429	679	5020	---	DSC	Pure salt	[79]
426.5	678.2	3800	15500	DSC	Pure-grade recrystallized (dried at 400 K under vacuum)	[68]
427	679	3325	12100	DSC	99.99% (no further purification)	[32]
428±2	683±2	3050±5%	13100±5%	DSC	>99%	[87]
427.3±0.1	---	3440±40	---	DSC	99.99% (dried at 378 K)	[49]
425±1	677±1	3413±5%	12480±5%	DSC	99.995%	[38]
427±1	680±1	3400±170	12500±625	DSC	99.99% (dried for more than 24 h at 380 K in a furnace)	[89]
434±1	677±1	---	---	DTA	Reagent grade (dried at least 2 h at 383 K)	[70]
428[(b)]	---	1464.4±15%	---	DTA	Analytical grade (dried and stored in dessicators)	[77]
424±1	677.5±1	---	---	DTA	99.99% (dried at 395 K during many days)	[83]
427±1	683±1	---	---	DTA	>99.99%	[84]
427	679	---	---	DTA	High purity (dried for more than 24 h at 380 K in an oven)	[85]
428±1	683±1	---	---	DTA	99.99% (kept at 380 K in an oven)	[86]
429±1	682±1	---	---	DTA	99.99% (dried for more than 24 h at 380 K in an oven)	[88]
429±1	681±1	---	---	DTA	99.99% (dried for more than 24 h at 380 K in a furnace)	[89]
424.5	678.5	3736.31±251.04	14100.08±125.52	AC	Analytical grade	[65]
425	679	---	---	AC	Salt for electronic applications (heated at 400 K for 70 h in a vacuum oven and then stored in a desiccator)	[66]
430.35±0.1	684.85±0.1	---	---	AC	99.9% (recrystallized)	[67]
---	690	---	13443.2±179.9	RC	99.99% (recrystallized twice from distilled water then dried at 403 K)	[74]
---	677±2	---	---	C	99%	[80]
426.85	---	3482	---	VD	Obtained by purification (dried in vacuum at 373 K for several hours)	[69]
---	683±5	---	---	VD	Optical grade (dried by heating to temperature just above the melting point under either an inert gas or a vacuum)	[76]
427	687	---	---	HC	Analytical grade	[71]
427	677	---	---	CC/VT	Analytical grade	[72]
---	680	---	---	VT	Not defined	[75]
425	679	---	13352	EMF	Not defined	[73]
423	---	---	---	EM	Analytical grade	[78]
---	690	---	---	Equil.	Not defined	[81]
427	---	---	---	DM	Not defined	[60]
---	679.65	---	---	VT	> 99.5% (carefully dried)	[90]

[(a)]DSC : Differential Scanning Calorimetry ; DTA : Differential Thermal Analysis ; AC : Adiabatic calorimetry ; RC : Reaction calorimetry ; C : Calorimetry ; VD : Volume discontinuity ; HC : Heating curve ; CC : Cooling curve ; VT : Visual-Thermal method ; EMF : Electromotive force; EM : Electrical measurements ; Equil. : Equilibrium method ; DM : Dielectric measurements. [(b)]Average value corresponding to heating and cooling.

Table 2

Temperatures and enthalpies of melting of $LiNO_3$ from literature

T_m (K)	$\Delta_m H°$(J mol^{-1})	Method[(a)]	Sample characteristics	Ref.
525.9	25025.22	DSC	99.8% (used without further purification)	[93]
527.5±3	24500	DSC	Reagent grade (kept at 380 K under vacuum for 24 h)	[68]
527.5	---	DSC	Reagent grade (recrystallized from redistilled water and dried in the oven at 378 K for 3 days)	[98]
520.55	23020	DSC	Not defined	[99]
528	25647.912	DSC	Reagent grade (dried in a separate furnace at 423 K for 24 h and stored over desiccant)	[54]
---	24320±1420	DSC	Commercial source (dried in an oven at 523 K under a flow of nitrogen gas)	[97]
525±1	24517±5%	DSC	99.99% (used without purification but care was taken to avoid moisture)	[38]
530.85±1	24889.506±5%	DSC	> 99% (kept in an oven at 353 K)	[22]
525±1	24500±4%	DSC	99.99% (used without further purification)	[39]
524±1	24526±1226	DSC	99.99% (dried in a desiccators at 380 K for more than 24 h)	[100]
527	---	DSC	> 99.0% (dried at 373 K for 48 h)	[52]
530.85±4.9	24553.90±208.35	DSC	99.99% (used without purification and deshydration)	[101]
528.05±0.3	24972±0.5%	DSC	> 99.0% (placed in powder state in a constant temperature air blast oven, 393 K, for drying 24 h)	[53]
525.75±0.1	---	DTA	Not defined	[102]
527.5±1	---	DTA	99.99% (kept at 380 K in an oven)	[103]
527.5±1	---	DTA	99.99%	[84]
526±1	---	DTA	99.99%	[104]
526±1	---	DTA	99.99% (dried in a desiccators at 380 K for more than 24 h)	[100]
517.95±4.9	24836.76±208.35	DTA	99.99% (used without purification and deshydration)	[101]
523	25522.4	DC	Great purity (purified by repeated crystallization)	[94]
526	25258.81	DC	Not defined	[105]
525	24600	DC	Pure grade (heated to about 463 K in a pyrex tube under vacuum)	[96]
526.3±0.2	26677.18±292.88	DC	Reagent grade (carefully dried under vacuum at 473 K for few days) / Spectroscopic purity (obtained by dehydration of $LiNO_3.3H_2O$)	[95]
527	24941	RC	Analytical reagent (used without purification)	[74]
528±3	---	C	99.98%	[80]
529.5	---	AC	Pure-grade recristallyzed (special grade)	[67]
526.3±0.2	26777.6±376.6	Cry	Reagent grade (carefully dried under vacuum at 473 K for few days) / Spectroscopic purity (obtained by dehydration of $LiNO_3.3H_2O$)	[95]
---	25355	DC	Not defined	[111]
526±2	---	CC	Prepared from well washed lithium carbonate (no impurity was detected by ordinary analytical tests)	[106]
524.55±0.4	---	CC	Reagent grade (recrystallized)	[107, 108]
543±0.5	---	PC	Not defined	[109]
531	---	CC	Chemically pure	[72]
526.25±0.1	26924.04	Freezing	Pure grade (deshydrated during a long time)	[110]
530	---	VT	Not defined	[75]
526	---	VT	> 99.5%	[90]
527	---	Equil.	Not defined	[81]

[(a)]DSC : Differential Scanning Calorimetry ; DTA : Differential Thermal Analysis ; DC : Drop calorimetry; RC : Reaction calorimetry ; C : calorimetry; AC : Adiabatic Calorimetry ; Cry : Cryometry ; CC : Cooling Curve ; PC : Plato method of graduated cooling ; VT : Visual-Thermal method; Equil. : Equilibrium method.

Table 3

Temperatures and enthalpies of solid-solid transition and melting of $NaNO_3$ from literature

$T_{II/I}$ (K)	T_m (K)	$\Delta_{II/I}H°$(J mol^{-1})	$\Delta_mH°$(J mol^{-1})	Method[(a)]	Sample characteristics	Ref.
---	---	---	14975±230	DSC	Reagent grade (dried at 373 K and 473 K for period ranging from 10 to 90 days)	[152]
---	---	---	15083±230	DSC	″ ″	[152]
---	---	---	15372±230	DSC	″ ″	[152]
---	---	---	15175±71	DSC	″ ″	[152]
---	---	---	15134±71	DSC	″ ″	[152]
---	---	---	15088±96	DSC	″ ″	[152]
549	580	3410±774	15004±176	DSC	Reagent grade (dried at 373 K and 473 K for period ranging from 10 to 90 days)	[153]
530	578	3683	14815	DSC	Reagent grade (dried at 383 K)	[154]
549±0.5	579±0.5	941.4±1%	15439±1%	DSC	99.999% (used without further purification)	[135]
550	583	4420±130	15100±400	DSC	Reagent grade (recrystallized from water and dried at 425 K for at least 48 h in vacuum)	[136]
(547.6 – 550) ±0.2	---	(1700 – 1850) ±150	---	DSC	Reagent grade	[155]
548±1	579±1	---	---	DSC	Chemically pure	[156]
548.5	577.5	3825	14705	DSC	99.99% (used without further purification)	[93]
540.1±1	579.1±1	3680	14700	DSC	Reagent grade (kept at 380 K under vacuum for 24 h)	[157, 158]
549	579	3620	14980	DSC	99.9% (used without further purification)	[32, 159]
---	580	---	15600	DSC	Reagent grade (recrystallized from redistilled water and dried by heating at approximately at 378 K for 3 days)	[160]
548.85±1	580.95±1	2090±100	14740±100	DSC	High purity (dried)	[161]
545.5	579.6	---	---	DSC	99.999%	[162]
---	---	---	16790±260	DSC	Commercial source (dried in an oven at 523 K under a flow of nitrogen gas)	[97]
---	579	---	----	DSC	99.99% (used without further purification)	[139]
---	---	---	14288.5±382.5	DSC	Not defined	[163]
544	581	---	15435	DSC	> 99%	[164, 165]
---	580	---	15300	DSC	Reagent grade (dried in the furnace at 423 K for 24 hours and stored over desiccant)	[54, 166]
547±1	578±1	3605±5%	14995±5%	DSC	99.995% (used without further purification)	[38]
---	---	---	10030±170	DSC	> 99.9%	[141]
544.95	578.25	2295	15980	DSC	> 99% (kept in an oven at 353 K)	[22]
---	579.85	---	15130	DSC	99.6%	[47]
---	579.95±0.1	---	---	DSC	>99.0% (dried in vacuum)	[167]
545.65±4.9	574.55±4.9	2609.5±256.7	15121.5±256.7	DSC	99.995% (kept at 378 K for 1 h)	[101]
551	579.95	---	13438.5	DSC	99.99%	[168]

[(a)]DSC : Differential Scanning Calorimetry

Table 3 (continued)

$T_{II/I}$ (K)	T_m (K)	$\Delta_{II/I}H°$(J mol^{-1})	$\Delta_mH°$(J mol^{-1})	Method[(a)]	Sample characteristics	Ref.
548.65	---	---	---	DTA	Reagent grade	[169]
---	579	---	14610 – 14958	QDTA	Reagent grade (99.98 mole%). Sample placed in Ag (99.999%) container	[170]
545	---	418.4±15%	---	DTA	Analytical grade (dried and stored in desiccator)	[77]
(548 – 549) ±2	---	---	---	DTA	Analytical reagent grade	[144]
548±0.25	578±0.25	---	---	DTA	Analytical grade (recrystallized and dried in an oven)	[171]
549±1	579±1	---	---	DTA	99.5% (kept in an oven at 395 K)	[83]
548.5±0.5	579±0.5	---	---	DTA	99.95%	[172]
549±0.5	579±0.5	---	---	DTA	99.9% (dried for more than 24 h at 394 K in an oven)	[173]
549±1	579±1	---	---	DTA	99.99% (kept in an oven at 380 K)	[86]
---	580	---	---	DTA	Reagent grade	[174]
549±1	579±1	---	---	DTA	99.995% (dried for more than 24 h at 380 K in a desiccator)	[175]
546±3	575±3	---	---	DTA	99.995%	[176]
---	575.21±4.8	2561.9±0.76%	14930.25±0.76%	STA	> 99%	[177]
549±1	578±1	---	---	DTA	99.995%	[178]
---	581	---	15045	STA	> 99%	[179]
532.45±4.9	571.65±4.9	---	15300±256.7	DTA	99.995% (kept at 378 K for 1 h)	[101]
---	579.6±0.1	---	15049±33	AC	99.99%	[127]
549.2	579.2	3950	14602±7%	AC	99.9%	[128]
548.7	580	---	15272	AC	High purity	[130]
548	583.2	---	---	AC	Special grade	[67]
---	584	---	15810	AC	Not defined	[180]
---	581	---	15439±2%	DC	Great purity (purified by repeated crystallization)	[94]
---	579.2±0.1	---	15648	DC	Reagent grade (dried in an oven at 403 K for a few hours)	[95]
---	580	---	14937	DC	Not defined	[181]
548.6	---	3770	---	DC	Analytical reagent grade	[126]
549.2	580.2	728	14728	DC	reagent grade (oven-dried at 403 K)	[129]
548	579	4686.08	15459.88	DC	Not defined	[105]
535	581	1590	14644	DC	Not defined	[133]
---	581	---	---	DC	Best grade (keptat 405 K for more than 24 hours)	[137]
549±2	578±2	---	---	DC	99.995%	[182]
---	583	---	15464±134	RC	Analytical grade (without further purification)	[74]
---	---	---	15523	Cry	Reagent grade (dried in an oven at 403 K for a few hours)	[95]

[(a)]DTA : Differential Thermal Analysis ; QDTA : Quantitative differential thermal Analysis ; STA : Simultaneous Thermal Analysis ; AC : Adiabatic calorimetry ; DC : Drop calorimetry ; RC : Reaction calorimetry ; Cry: cryometry.

Table 3 (continued)

$T_{II/I}$ (K)	T_m (K)	$\Delta_{II/I}H°$(J mol^{-1})	$\Delta_m H°$(J mol^{-1})	Method[(a)]	Sample characteristics	Ref.
551±1	---	---	---	LTE	Commercial salt (recrystallized three times)	[183]
---	585	---	---	CC	Chemically pure	[184]
---	578.65±0.4	---	---	CC	Reagent grade (recrystallized and dried)	[108]
---	579±0.1	---	---	CC	Not defined (dried salt)	[102]
---	588.25±0.2	---	---	FC	Analytical reagent (dried)	[151]
---	581	---	15315	EMF	Not defined	[73]
548	581	---	---	Raman diff.	Not defined	[185]
549.1	---	---	---	Raman diff.	Not defined	[119]
(548.74–551.02) ±(0.47–0.54)	---	---	---	Neutron diff.	Not defined	[117]
549.75	---	---	---	Absorption edge	Not defined	[186]
552	---	---	---	OM	> 99.999%	[114]
549±3	580±3	---	---	XRD	> 99.999%	[115]
552.3±0.5	---	---	---	XRD	> 99.999%	[116]
552.7±0.5	---	---	---	XRD	99.999% (held at 373 K for 10 min)	[120]
551±1	581±1	---	---	XRD	Analytical grade	[122]
549	---	---	---	IR	Analytical grade	[187]
548	---	---	---	EM	Reagent grade	[188]
549	---	---	---	EC	Not defined	[189]
548	---	---	---	Pulse method	Not defined	[132]
546.25±0.2	---	---	---	DTD	Not defined	[190]
550	---	---	---	Dilatometry	Not defined	[191]
---	579±0.4	---	---	MC	Chemically pure (melted and crystallized under vacuum)	[192]
---	581	---	---	VD	Reagent grade (dried by heating at temperature just above its melting point under either an inert gas atmosphere or a vacuum)	[76]
---	580	---	---	SDT/MS	Ultrapure (dried in air and the in vacuum at 330 K for 3 hours)	[193]
---	582	---	---	Dilatometry	Not defined	[194]
---	581	---	---	VT	Not defined	[75]
---	583	---	---	----------	Not defined	[81]
---	581	---	---	MTA	Not defined	[195]
---	584	---	---	----------	Not defined	[196]
---	---	---	15062.4±418	FPD	Reagent grade (dried by heating)	[197]
---	---	---	15815.52	FPD	Reagent grade (without purification)	[198]

[(a)]LTE : Linear Thermal Expansion measurements ; CC : Cooling curve FC: Freezing curve; EMF : Electromotive force; OM : Optical measurements ; XRD : X-Ray diffraction ; IR : Infrared spectroscopy ; EM : Electrical measurements ; EC : Electrical conductivity ; DTD : Differential Transformer Dilatometry ; MC : Melting curves ; VD : Volume discontinuity; SDT/MS: Simultaneous Dynamic Thermogravimetry and Mass Spectrometry; VT : Visual-Thermal method ; MTA : Micro-thermal Analysis ; FPD : Freezing point depression measurements.

Table 4

Experimental results of DTA measurements (heating) in the $CsNO_3$-$LiNO_3$ system

Composition X_{LiNO_3}	Experimental equilibrium temperature (K)
0.250	334.21
	427.00
	444.75
	578.04
0.500	334.84
	335.28[a]
	427.65
	442.70[a]
	443.01
	455.83
	463.52[a]
0.750	334.24
	435.49
	475.99

[a]Values obtained by coprecipitation.

Table 5

Experimental results of DTA measurements in the $CsNO_3$-$LiNO_3$-$NaNO_3$ system. Section : $X_{NaNO_3} = 0.2$

Composition		Experimental equilibrium temperature (K)
X_{LiNO_3}	X_{CsNO_3}	
0.000	0.800	425.74
		464.59
		616.22
0.150	0.650	332.92
		407.60
		427.42
		432.65
		541.41
0.300	0.500	332.00
		407.00
		427.00
		445.00
0.400	0.400	335.50
		410.84
		422.78
0.600	0.200	332.00
		405.00
		422.00
		442.00
0.650	0.150	333.33
		405.21
		438.13
		472.90
0.800	0.000	460.55
		512.56

Table 6
Experimental results of DTA measurements (heating) in the $CsNO_3$-$LiNO_3$-$NaNO_3$ system. Section : $X_{CsNO_3} / X_{LiNO_3} = 1$

Composition		Experimental equilibrium temperature (K)
X_{NaNO_3}	X_{CsNO_3}	
0.050	0.475	336.00
		407.28
		451.35
0.100	0.45	334.37
		407.35
		440.56
0.150	0.425	333.06
		408.28
		430.77
0.400	0.300	333.14
		409.55
		463.28
0.500	0.250	334.82
		409.66
		482.15
0.950	0.025	334.12
		408.24
		412.96
		550.62
		574.47

Table 7
Thermochemical properties of solid-solid transition and melting for pure nitrates and the intermediate compound $Cs_{0.5}Li_{0.5}NO_3$

Nitrates	$T_{II/I}$ (K)	T_m (K)	$\Delta_{II/I}H°$(J mol^{-1})	$\Delta_m H°$(J mol^{-1})	Ref.
$CsNO_3$	425	679	3703	14100	Pankratz [33]
	427	682	3600	13800	Landolt-Börnstein [34]
	426	680	3800	14000	Binnewies and Milke [37]
	427±2	678±1	3466±142	12545±413	Recommended values (This work)
$LiNO_3$	---	529.7	---	23806.96	Pankratz [33]
	---	526.00	---	25000.0	Landolt-Börnstein [34]
	---	526	---	25900	Binnewies and Milke [37]
	---	527±2	---	25068±924	Recommended values (This work)
$NaNO_3$	550	583	---	15104.21	Pankratz [33]
	---	579.6	---	15050.0	Landolt-Börnstein [34]
	---	580	---	15000	Binnewies and Milke [37]
	549±2	579±2	3733±123[(a)]	15129±365	Recommended values (This work)
$Cs_{0.5}Li_{0.5}NO_3$	---	463±2[(b)]	---	---	Exp. (This work)

[(a)]First-order transition. [(b)]Coprecipitation.

Table 8

Gibbs energy ${}^{0}G_{i}^{\varphi}(T) - {}^{0}H_{i}^{SER}(298.15K)$ for pure nitrates

Nitrates	Phase	Symbol	T/K	Gibbs energy (J mol^{-1})	Ref.
$CsNO_3$	$CsNO_3$(II)	Hcp	5 - 17	$-20210.0+0.7T-0.01011T^2-1.330\times10^{-4}T^4$	This work
			17 - 427	$-23576.5+264.206T-55.52T\ln(T)-0.076816T^2$ $+42984.2003T^{-1}-351803.795T^{-2}+1267294.59T^{-3}$	
			427 - 3000	$-50921.0+778.5T-136.545T\ln(T)-3.1445\times10^{-4}T^2$ $+1472528.05T^{-1}$	
	$CsNO_3$(I)	Cubic	5 - 17	$-19545.0+4.275T-0.06076T^2-1.15\times10^{-4}T^4$	This work
			17 - 427	$-22583.0+244.31T-50.9091T\ln(T)-0.10102T^2$ $+38829.4483T^{-1}-321553.964T^{-2}+1178960.83T^{-3}$	
			427 - 678	$-94736.20+1398.25964T-228.16118T\ln(T)$ $+0.043805T^2+4920826.52T^{-1}$	
			678 - 3000	$-36280.0+787.55T-141.025T\ln(T)+5.116\times10^{-4}T^2$ $-1614045.65T^{-1}$	
	Liquid	Liq	5 - 17	$-9435.0-2.175T-0.07389T^2-1.07\times10^{-4}T^4$	This work
			17 - 427	$-13260.0+275.0T-57.601T\ln(T)-0.1033T^2$ $+53870.3382T^{-1}-478775.974T^{-2}+1837388.34T^{-3}$	
			427 - 3000	$-31599.30+805.058T-145.255T\ln(T)$	
$LiNO_3$	Solid	Rhombo-S	298.15 - 527	$-18320.5096+207T-38.8286T\ln(T)$ $-0.077378T^2$	This work
			527 - 3000	$-67100+925.70T-147.4028T\ln(T)$ $+0.0014728T^2+3544600T^{-1}$	
	Liquid	Liq	298.15 - 527	$-3695.00+203.35T-37.7090T\ln(T)-0.156T^2$ $+3.7129\times10^{-5}T^3$	This work
			527 - 3000	$-25277.10+814.9266T-140.2302T\ln(T)$	
$NaNO_3$	$NaNO_3$(II)	Rhombo-L	298.15 - 549	$-484591.3+101.374T-22.62T\ln(T)-0.111T^2$	[212]
			549 - 579	$-515028.4+830.012T-139.0T\ln(T)$	
			579 - 3000	$-514565.2+824.123T-138.2T\ln(T)$	
	$NaNO_3$(I)	Rhombo-H	298.15 - 549	$-480971.3+94.78T-22.62T\ln(T)-0.111T^2$	[212]
			549 - 579	$-511408.4+823.419T-139T\ln(T)$	
			579 - 3000	$-510945.2+817.530T-138.2T\ln(T)$	
	Liquid	Liq	298.15 - 549	$-465991.3+68.908T-22.62T\ln(T)-0.111T^2$	[212]
			549 - 579	$-496428.4+797.546T-139.0T\ln(T)$	
			579 - 3000	$-495965.2+791.657T-138.2T\ln(T)$	

Table 9

Thermodynamic parameters in the $CsNO_3$-$LiNO_3$-$NaNO_3$ ternary system (in J.mol^{-1} of MNO_3)

System	Phase	Model	Parameter	Ref.
$CsNO_3$-$LiNO_3$	Liquid (L)	($CsNO_3$, $LiNO_3$)	${}^0L^L_{CsNO_3,LiNO_3} = -16096.850+2.9283T$; ${}^1L^L_{CsNO_3,LiNO_3} = 694.718+4.9574T$	This work
	I	$(CsNO_3)_{0.5}(LiNO_3)_{0.5}$	$\Delta_f {}^0G_I = \begin{cases} 5267.038 - 4.9954T - 1.8541T\ln(T) & (298\,K < T < 335\,K) \\ -322.839 - 4.6924T & (335\,K < T < 3000\,K) \end{cases}$	This work
$CsNO_3$-$NaNO_3$	Liquid (L)	($CsNO_3$, $NaNO_3$)	${}^0L^L_{CsNO_3,NaNO_3} = -5323.454+1.8446T$; ${}^1L^L_{CsNO_3,NaNO_3} = 898.371+0.2096T$	This work
			${}^2L^L_{CsNO_3,NaNO_3} = -1.6940T$	
$LiNO_3$-$NaNO_3$	Liquid (L)	($LiNO_3$, $NaNO_3$)	${}^0L^L_{LiNO_3,NaNO_3} = -1933.105+0.7814T$	This work
$CsNO_3$-$LiNO_3$-$NaNO_3$	Liquid (L)	($CsNO_3$, $LiNO_3$, $NaNO_3$)	${}^0L^L_{CsNO_3,LiNO_3,NaNO_3} = -7379.032$	This work
			${}^1L^L_{CsNO_3,LiNO_3,NaNO_3} = -28739.356$	
			${}^2L^L_{CsNO_3,LiNO_3,NaNO_3} = -5093.552$	

Table 10

Invariant reaction characteristics in the $CsNO_3$-$LiNO_3$, $CsNO_3$-$NaNO_3$ and $LiNO_3$-$NaNO_3$ binary systems

System	Invariant equilibrium	Type	T/K	Composition	Ref.
				$X^{Liq}_{LiNO_3}$	
$CsNO_3$-$LiNO_3$	Liq = *I* + Cubic	Eutectic	443	0.422	[72]
			447	0.47	[84]
			445±2	---	Exp. (this work)
			447.12	0.442	Calc. (this work)
	Liq = *I* + Rhombo-S	Eutectic	433	0.56	[72]
			433	0.63	[84]
			435±2	---	Exp. (this work)
			436.10	0.639	Calc. (this work)
	I = Hcp + Rhombo-S	Eutectoid	339[(a)]	---	[72]
			333	---	[84]
			334±2	---	Exp. (this work)
			334.00	---	Calc. (this work)
				$X^{Liq}_{NaNO_3}$	
$CsNO_3$-$NaNO_3$	Liq = Cubic + Rhombo-L	Eutectic	463.31	0.543	Calc. [26], this work
$LiNO_3$-$NaNO_3$	Liq = Cubic + Rhombo-L	Eutectic	427.20	0.464	Calc. [23], this work

[(a)]Considered as polymorphism transition of *I*.

Table 11

Ternary reaction characteristics in the $CsNO_3$-$LiNO_3$-$NaNO_3$ ternary system

Invariant equilibrium	Type	T/K	Composition		Ref.
			$X^{Liq}_{LiNO_3}$	$X^{Liq}_{NaNO_3}$	
Liq = *I* + Rhombo-L+Hcp	Eutectic (E_1)	405	0.405	0.135	[75]
		407±2	---	---	Exp. (this work)
		407.76	0.307	0.249	Calc. (this work)
Liq = *I* + Rhombo-L+Rhombo-S	Eutectic (E_2)	403	0.475	0.165	[75]
		405±2	---	---	Exp. (this work)
		404.63	0.481	0.223	Calc. (this work)
Liq = *I* + Rhombo-L	Eutectic[(a)]	408	---	---	[75]
		408±2	---	---	Exp. (this work)
		411.03	0.378	0.244	Calc. (this work)
I + Rhombo-L=Rhombo-S+Hcp	Peritectoïd	334±2	---	---	Exp. (this work)
		334.00	---	---	Calc. (this work)

[(a)]Quasi-binary eutectic